

University of Missouri, St. Louis

IRL @ UMSL

Dissertations

UMSL Graduate Works

11-10-2017

Interactions Between Amyloid-beta and Microglial Cells

Lisa Gouwens

University of Missouri-St. Louis, lkpbn7@mail.umsl.edu

Follow this and additional works at: <https://irl.umsl.edu/dissertation>



Part of the [Other Chemistry Commons](#)

Recommended Citation

Gouwens, Lisa, "Interactions Between Amyloid-beta and Microglial Cells" (2017). *Dissertations*. 710.
<https://irl.umsl.edu/dissertation/710>

This Dissertation is brought to you for free and open access by the UMSL Graduate Works at IRL @ UMSL. It has been accepted for inclusion in Dissertations by an authorized administrator of IRL @ UMSL. For more information, please contact marvinh@umsl.edu.

INTERACTIONS BETWEEN AMYLOID-BETA AND MICROGLIAL CELLS

by

Lisa K. Gouwens

MS, Biochemistry & Biotechnology, University of Missouri-St. Louis, 2011

MEd, Secondary Education, University of Arkansas-Monticello, 2001

BS, Biology, University of Arkansas-Monticello, 1998

A Dissertation

Submitted to the Graduate School

of the

University of Missouri – Saint Louis

In partial fulfillment of the requirements for the degree of

Doctor of Philosophy

in

Chemistry

with an emphasis in Biochemistry

December 2017

University of Missouri – Saint Louis

Saint Louis, Missouri

Advisory Committee

Michael R. Nichols, PhD (Chairperson)

Cynthia M. Dupureur, PhD

Wesley R. Harris, PhD

Bethany K. Zolman, PhD

for
Willis Eugene Gouwens
Robert Veld Gouwens
Donald Lee Gouwens
and their families

ACKNOWLEDGEMENTS

None of this would be possible without my advisor, Dr. Michael Nichols. I've been around UMSL for a long time, therefore I appreciate your limitless patience. Thank you for being a great teacher and mentor.

Members of the advisory committee, Drs. Dupureur, Harris, and Zolman, have all taught courses in which I was a student. In those classrooms, I grew to respect and admire you. I'm so grateful to you all for being part of my committee. In addition, I treasure the mentoring from Dr. Dupureur as we worked together in the biochemistry teaching lab. Many thanks!

What a privilege it's been to work with everyone in the Nichols Lab. Geeta, Shana, and Kelley, you were there in my first year and I thought I'd never know as much as you all about A β . Priyanka, you were a long-suffering partner in biochemistry lab and my first friend at UMSL. Sanjib, we discovered that the third decimal place is important when betting a beer on who has the best R² value on a standard curve. Ben, I'll always remember your epic skills with Photoshop. Mudar and Nathan, microvesicles are nearly invisible, and difficult to work with, but you persevered. Victoria and Fatima, I truly enjoyed our time in the Golden Age of the lab. Nyasha, together we learned that food in certain hotel restaurants can be delicious but is ridiculously overpriced. Next time, let's just order pizza.

I would also like to thank Dr. David Osborn of the Microscope Imaging and Spectroscopy Technology Lab at UMSL. Your help with imaging A β and microvesicles was invaluable and I enjoyed working with you.

Throughout my life I've been blessed with excellent science teachers, starting with Ms Gifford in 4th Grade at St. Anne Elementary. Going to school in the evening seemed like a silly idea until I saw the moon and stars through a telescope. Thank you for showing me the beauty of the universe. Science got hold of me for good when I learned about photosynthesis in high school biology class; thank you, Mr. Kelly. At UAM, Dr. Eric Sundell, Dr. Walt Godwin, and Dr. Morris Bramlett were instrumental in demonstrating both how to conduct science and how to teach.

As for my family, it would take countless pages to recount all of the joy each of you brings into my life. I love you. Your support and encouragement have sustained me during this journey. Thank you!

TABLE OF CONTENTS

ACKNOWLEDGEMENTS	iii
LIST OF TABLES	vii
LIST OF FIGURES	viii
LIST OF ABBREVIATIONS	ix
ABSTRACT	xi
CHAPTER 1: INTRODUCTION	1
1.1 Alzheimer’s disease overview	1
1.2 Amyloid beta 42 (A β 42)	2
1.3 Microglia	6
1.3.1 Inflammation and microglia	6
1.3.2 Cellular uptake of extracellular material	8
1.3.3 Internal trafficking of material in microglia	10
1.3.4 Microglial P2X ₇ receptors	10
1.4 Microvesicles	12
CHAPTER 2: METHODS	15
2.1 A β preparation	15
2.1.1 A β aliquot lyophilization	15
2.1.2 Preparation of A β monomers, protofibrils, and fibrils	16
2.1.3 Fluorescent labeling of A β	16
2.1.4 Size exclusion chromatography (SEC)	20
2.2 Characterization of fluorescently labeled A β	21
2.2.1 Fluorescence measurements	21
2.2.2 Absorbance measurements	23
2.2.3 A β concentration calculations	23
2.2.4 Electron microscopy	26
2.2.5 Dynamic light scattering	28
2.3 Cell Culture	32
2.3.1 BV-2 microglia culture	32
2.3.2 Primary microglia isolation and culture	33
2.4 Microglial AF488-A β uptake experiments	34
2.4.1 A β treatment for ELISA and confocal LSM analysis	34
2.4.2 A β treatment for fluorescence plate reader and dot blot analysis	35
2.4.3 BV-2 microglia cell binding assay	36
2.5 Fluorescence quantitation for AF488-A β -treated microglia	36
2.6 Immuno-detection of A β and confocal microscopy	39
2.6.1 Preparation of fixed cells for microscopy	39
2.6.2 Confocal microscopy	40
2.7 Immuno-dot blot	42
2.8 ELISA	43

2.9 Microvesicle generation and isolation from BV-2 and primary microglia.....	44
2.10 Fluorescence measurements of microvesicles	46
2.11 Confocal LSM imaging of microvesicles	46
2.12 Preparation of microvesicles for resin-embedded TEM.....	47
2.13 BCA Assay	48
CHAPTER 3: Aβ INTERACTIONS WITH MICROGLIAL CELL SURFACES.....	49
3.1 Binding of distinct A β conformers	49
3.2 Time-dependence of A β 42 interaction with BV-2 cell surfaces	53
3.3 Effect of temperature on A β 42 binding to BV-2 cell surfaces	55
3.4 Effect of A β 42 concentration on binding to BV-2 cell surfaces	57
3.5 Correlation of A β 42 binding and BV-2 activation	60
CHAPTER 4: SELECTIVE INTERNALIZATION OF Aβ BY MICROGLIA.....	64
4.1 Comparison of unlabeled and fluorescently-labeled A β 42 monomer, protofibril, and fibril interactions with BV-2 and primary microglia	65
4.2 Time dependent internalization of AF488-A β by primary microglia.....	67
4.3 Effect of AF488-A β concentration on primary microglial uptake	72
4.4 Non-saturable A β uptake in primary microglia.....	73
4.5 Colocalization analysis of AF488-A β with lysosomes.....	80
CHAPTER 5: MICROVESICLES.....	86
5.1 Microvesicles from BV-2 microglia	86
5.1.1. A488-Annexin V visualization of BV-2 microvesicles	87
5.1.2. Bicinchoninic acid protein assay of BV-2 microvesicles	88
5.1.3. Dynamic light scattering characterization of BV-2 microvesicles	91
5.1.4. Transmission electron microscopy of resin-embedded BV-2 microvesicles.....	93
5.1.5 Tracking microvesicles with NBD C6-HPC fluorescence	96
5.2 Characterization of microvesicles from primary microglia	99
5.3 Overall conclusion	101
BIBLIOGRAPHY.....	103
VITA.....	114

LIST OF TABLES

CHAPTER 2 METHODS	
2.1 Stoichiometry of protofibril and monomer peak fractions	27
CHAPTER 3 A β INTERACTIONS WITH MICROGLIAL CELL SURFACES	
3.1 A β internalization in BV-2 and other cell lines	58
CHAPTER 4 AF488-A β INTERNALIZATION BY PRIMARY MICROGLIA	
4.1 Primary microglia internalization of A β experiments	74
4.2 Lysosome colocalization experiments	82

LIST OF FIGURES

CHAPTER 1 INTRODUCTION

1.1 A β and APP	3
1.2 A β aggregation.....	4
1.3 Microglial activation and cytokine production	7
1.4 Mammalian cell uptake.....	9
1.5 Lysosomes.....	11
1.6 Microvesicles	13

CHAPTER 2 METHODS

2.1 Structure of Alexa Fluor® 488 tetrafluorophenyl ester	18
2.2 Labeling reaction mechanism for A β and amine-reactive AF488-TFP.....	19
2.3 Representative UV trace for SEC elution overlaid with fluorescence measurements of fractions	22
2.4 AF488 absorbs at 280 nm	24
2.5 Comparison of UV-Vis absorbance measurement methods	25
2.6 Transmission electron micrographs of unlabeled A β and AF488-A β 42.....	29
2.7 Dynamic light scattering.....	31
2.8 Plate reader fluorescence, AF488-A β	38
2.9 Confocal laser scanning microscopy	41

CHAPTER 3 A β INTERACTIONS WITH BV-2 MICROGLIAL CELL SURFACES

3.1 Binding of distinct species of A β	50
3.2 Time dependence of surface binding to BV-2 microglia.....	54
3.3 Temperature effect on surface binding to BV-2 microglia.....	56
3.4 A β 42 concentration dependence of cytokine secretion by BV-2 microglia.....	61
3.5 Correlation of A β 42 binding and BV-2 cell activation	63

CHAPTER 4 AF488-A β INTERNALIZATION BY PRIMARY MICROGLIA

4.1 AF488 fluorophore does not affect primary microglial interaction with A β	66
4.2 Internalization of AF488-A β by primary microglia	68
4.3 Primary microglia take up AF488-A β protofibrils, but not AF488-A β monomers, in a time dependent manner	71
4.4 Concentration dependent internalization of AF488-A β by primary microglia	77
4.5 Competition/saturation images and quantitation	79
4.6 Lysosome colocalization.....	85

CHAPTER 5 MICROVESICLES

5.1 AF488-Annexin V visualization of microvesicles from BV-2 cells	89
5.2 BCA assays	91
5.3 Dynamic light scattering analysis of microvesicles.....	93
5.4 TEM of resin-embedded BV-2 microvesicles	94
5.5 NBD C6-HPC fluorescence indicates the presence of microvesicles.....	97

LIST OF ABBREVIATIONS

A β 42 – amyloid beta 1-42

aCSF – artificial cerebrospinal fluid

AD – Alzheimer's disease

AF488 – Alexa Fluor® 488

AF488-A β 42 – Alexa Fluor® 488 amyloid beta 1-42

AF488-TFP – Alexa Fluor® 488 tetrafluorophenyl ester

APP – amyloid precursor protein

BCA – bicinchoninic acid

Bz-ATP – 2'(3')-O-(4-Benzoylbenzoyl)adenosine 5'-triphosphate triethylammonium salt

CSF – cerebrospinal fluid

DAMP – danger associated molecular pattern

DLS – dynamic light scattering

DMEM – Dulbecco's modified Eagle's medium

ELISA – enzyme-linked immunosorbent assay

FITC – fluorescein isothiocyanate

IL-1 β – interleukin 1 β

MALS – multi-angle light scattering

MIST – microscope imaging and spectroscopy technology

MV – microvesicle

NBD C6-HPC – 2-(6-(7-nitrobenz-2-oxa-1,3-diazol-4-yl)amino)hexanoyl-1-hexadecanoyl-sn-glycero-3-phosphocholine

PAMP – pathogen associated molecular pattern

PC – phosphatidylcholine

PRR – pattern recognition receptor

PS – phosphatidylserine

R_H – hydrodynamic radius

SEC – size exclusion chromatography

TEM – transmission electron microscopy

ThT – thioflavin T

TLR – toll-like receptor

$TNF\alpha$ – tumor necrosis factor α

UV – ultraviolet

ZEN – Zeiss Efficient Navigation

ABSTRACT

Gouwens, Lisa K. Ph.D., University of Missouri-St. Louis, December 2017. Interactions between amyloid-beta and microglial cells. Major Professor: Michael R. Nichols.

Alzheimer's disease (AD), the most common cause of dementia, is a neurodegenerative condition characterized by loss of memory and intellectual abilities. Intracellular plaques of aggregated amyloid-beta ($A\beta$) protein are a well-known pathology associated with AD. Although symptoms usually appear late in life, the accumulation of $A\beta$ begins decades earlier and causes activation of microglia, the brain's immune cells. The ensuing inflammation contributes significantly to neurodegeneration. Determination of the particular form of $A\beta$ that causes the most damage in the brain is one of the major questions in the AD field. My research focused on the interactions of microglia with monomers, protofibrils, and fibrils of $A\beta$. I found that protofibrils, not monomers or fibrils, bind to microglial surfaces, and I confirmed earlier reports that protofibrils elicit a proinflammatory response from microglia. These results were consistent regardless of changing conditions such as temperature, incubation time and $A\beta$ concentrations.

Another aspect of my research was to investigate how microglia internalize different forms of $A\beta$. The distinction between monomers and protofibrils may have

physiological significance in AD, yet there are few reports in the literature in which these two forms of A β are examined separately. Monomers and protofibrils were carefully separated by size exclusion chromatography before cell treatments, which sets apart this work from research done in other labs. Multiple conditions and strategies, including a novel quantitation method for internalized A β , demonstrated that microglia favor internalization of protofibrils over monomers. Further experiments determined that microglia are capable of internalizing protofibrils in high amounts without degradation. A significant amount of A β protofibrils remain in the cytoplasm and are not routed to lysosomes, contradicting reports in the literature.

A third research objective involves the study of microvesicles released from microglia. Microvesicles may have a role in AD by transporting A β within the brain. I conducted experiments in which microglia were stimulated to produce microvesicles, and carried out assays to both confirm the presence of and visualize microvesicles. The studies described here contribute to the understanding of the interactions between microglia and A β , potentially leading to a possible treatment or cure for AD.

CHAPTER 1: INTRODUCTION

1.1 Alzheimer's disease overview

As the number of people affected by Alzheimer's disease (AD) continues to grow, investigations into the basic biochemistry and cellular aspects of this neurodegenerative disorder continue. Ultimately fatal, AD currently afflicts over 5 million people in the United States, and this number is expected to increase to 16 million by 2050, according to the Alzheimer's Organization (March 2015 Fact Sheet). Tens of millions of people worldwide are victims of AD (World Health Organization), and this tally is expected to triple by 2050.

In most cases, AD manifests itself late in life, with loss of memory, difficulty recalling new information, and loss of intellectual abilities. These symptoms were associated with extracellular plaques of amyloid beta ($A\beta$) and intraneuronal tau tangles, first described by Dr. Alois Alzheimer in 1907 (Stelzmann, et al., 1995). Yet, the buildup of $A\beta$ and tau begins decades before the manifestation of symptoms (Selkoe, 2011). While tau is an integral component of the disease process, the aggregation of $A\beta$ between brain cells precedes the formation of tau tangles within neurons (Selkoe and Hardy, 2016). What follows is dysfunction in a variety of cell types in the brain (vascular cells, pericytes, astrocytes, oligodendrocytes, and neurons), including $A\beta$ clearance dysfunction and inflammation in microglia (discussed below), as a response to or consequence of $A\beta$ build-up in the brain (De Strooper and Karran, 2016).

1.2 Amyloid beta 42 (A β 42)

A β is a peptide that is derived from a large transmembrane protein, up to 770 amino acids in length, known as amyloid precursor protein [APP; (Wilkins and Swerdlow, 2016)]. The functions of APP include neuronal development, intracellular transport, signaling, and homeostasis (van der Kant and Goldstein, 2015). Figure 1.1A shows a schematic for APP with labels for the transmembrane domain as well as the sites of cleavage for α -, β , and γ -secretases (Selkoe, 2011). Sequential cleavage by β -secretase then γ -secretase results in the formation of the A β peptide, which can be 36-42 amino acids in length (van der Kant and Goldstein, 2015). It is the 42-residue peptide that aggregates, causing the well-known pathology of intercellular plaques in AD (Jarrett, et al., 1993).

The A β 42 monomer is a disordered peptide with a molecular weight of 4.514 kDa. The amino acid sequence, shown in Figure 1.1B, is color-coded to show residue properties. The aggregation process shown in Figure 1.2 begins during the rate-limiting nucleation phase and is followed by assembly of the aggregation nuclei via non-covalent interactions (Jarrett, et al., 1993) to form soluble dimers, trimers and so on, which results in a solution of polydisperse soluble oligomers (Bitan, et al., 2003; Kaye, et al., 2003; Mittag, et al., 2014). Nucleation dependent polymerization is characterized by a lag phase, which is then followed by rapid aggregation (Jarrett and Lansbury, 1993). Subsequent steps lead to the formation of soluble protofibrils (Harper, et al., 1999; Mittag, et al., 2014; Walsh, et al., 1997, 1999) and insoluble fibrils (Harper, et al., 1997). The protofibril-to-fibril conversion can occur via monomer addition to protofibril ends,

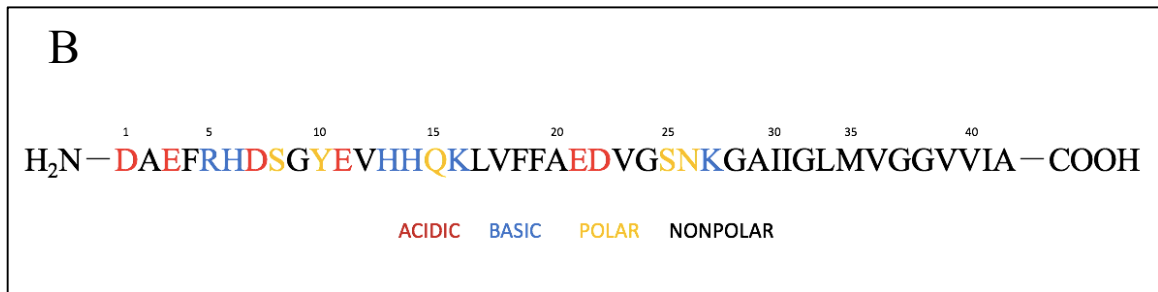
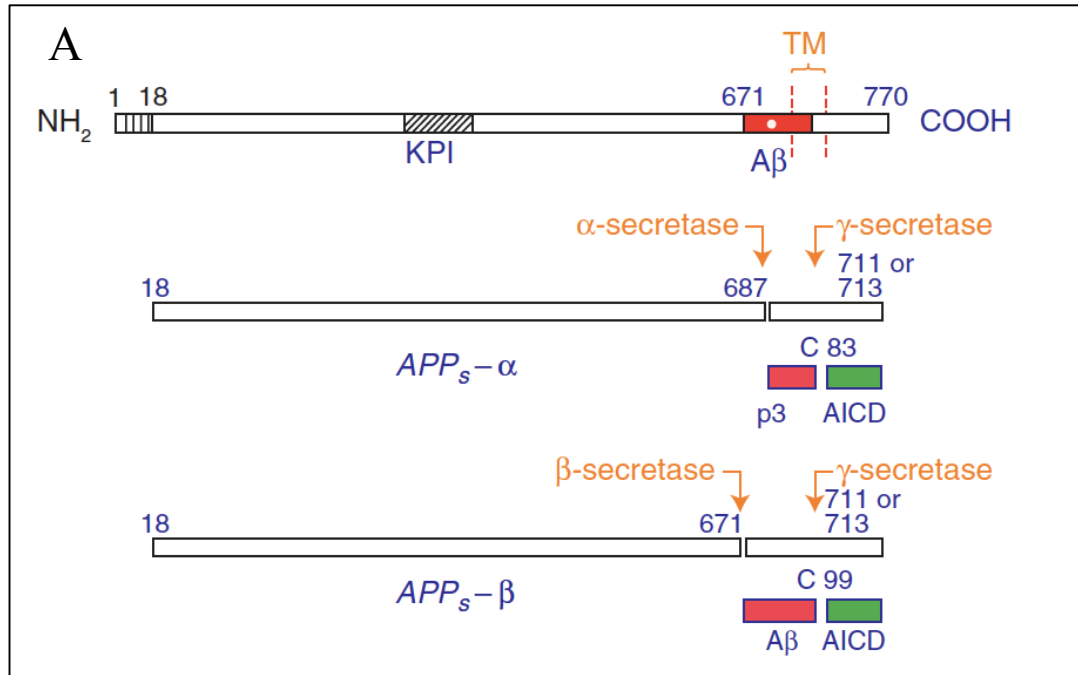


Figure 1.1. Aβ and APP. (A) APP processing (Selkoe, 2011) (B) Aβ42 schematic with one letter abbreviations for residues.

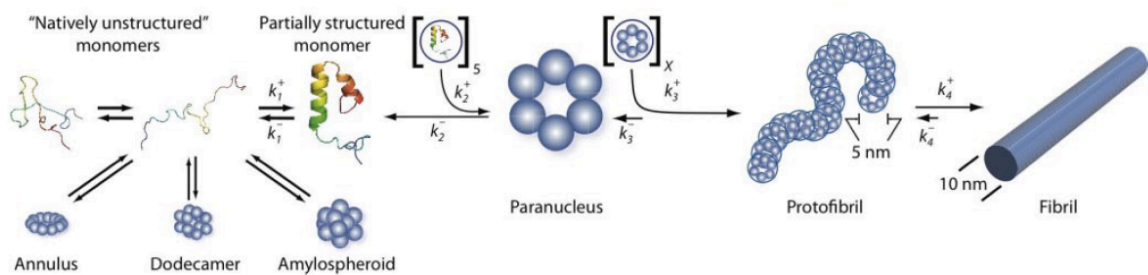


Figure 1.2 A β aggregation. Monomers are disordered peptides. The pathways which do not lead to aggregation (annulus, dodecamer, and amylospheroid) are distinct from the pathway which results in fibril aggregation via protofibrils. From Figure 1, Roychaudhuri, et al. (2009).

the joining of protofibril tips to one another, and lateral association of protofibrils (Harper, et al., 1999; Nichols, et al., 2002). A β 42 fibrils make up the dense cores of intercellular plaques (Terry, et al., 1964) with soluble A β on the periphery of the plaques (Koffie, et al., 2009).

Protofibrils are fibril precursors (Harper, et al., 1997; Walsh, et al., 1997) that have beta sheet structure (Nichols, et al., 2015; Walsh, et al., 1999). Though protofibrils are not as stable as fibrils (Kheterpal, et al., 2003; Walsh, et al., 1999), they resemble fibrils in thioflavin T (ThT) binding and circular dichroism (Walsh, et al., 1999). Protofibril lengths have been reported as <200 nm (Walsh, et al., 1997), and our measurements of protofibril lengths have been consistent with that, ranging from 50 ± 16 nm to 78 ± 35 nm (Nichols, et al., 2015; Paranjape, et al., 2012). Reported diameters for protofibrils vary from 4-6 nm (Harper, et al., 1997). The hydrodynamic radius (R_H) of protofibrils, measured by dynamic light scattering (DLS), has been reported to be 10-50 nm (Walsh, et al., 1997), and our measurements of 21 ± 6 nm (Paranjape, et al., 2012), 21.9 ± 4.0 nm (Paranjape, Terrill, and Gouwens, et al., 2013), and 23.6 ± 3.3 nm (Nichols, et al., 2015) fall into that range. Analyzed by SEC with in line multi-angle light scattering (MALS), protofibril molecular weights (M_W) ranged from 200-2600 kDa, with an average of 884 ± 302 kDa, (Nichols, et al., 2015). We are particularly interested in protofibrils because they have been shown to be toxic to neurons (Walsh, et al., 1999), disrupt ion channels (Ye, et al., 2003), and inhibit long-term potentiation in the hippocampus (O'Nuallain, et al., 2010). Additionally, results from our lab have shown that the soluble protofibrils of A β 42 are responsible for the activation of macrophages

and microglia that results in the production of cytokines (Ajit, et al., 2009; Paranjape, et al., 2012; Paranjape, Terrill, and Gouwens, 2013).

1.3 Microglia

During early embryonic development, hematopoietic stem cells give rise to microglial cells, which migrate to the central nervous system [CNS, (Ransohoff and Cardona, 2010)]. Microglia are macrophages in the CNS, shaping neural circuits during development and throughout life (Banati and Graeber, 1994; Frost and Schafer, 2016; Ji, et al., 2013); Microglia are also involved in surveillance of the intercellular space, cleaning up dead cells and debris, and responding to threats (Kettenmann, et al., 2011). Activated microglia can be found near plaques in AD brain (McGeer, et al., 1987; Meyer-Luehmann, et al., 2008), along with proinflammatory cytokines (Dickson, et al., 1993), and have been observed accumulating rapidly around new plaques (Meyer-Luehmann, et al., 2008).

1.3.1 Inflammation and microglia

The microglial inflammatory response, illustrated in Figure 1.3, is implicated in several CNS diseases (Frankola, et al., 2011). Though labeled “resting”, microglia use their many branches to actively read their surroundings (Kettenmann, et al., 2011). The exogenous signals that initiate inflammatory pathways, such as microbial infection, are pathogen-associated molecular patterns (PAMPs), which are molecular patterns not present in the host tissues (Tang, et al., 2012). Pattern recognition receptors (PRRs) such as toll like receptors (TLRs) sense and respond to PAMPs, initiating cell signaling pathways in an attempt to mitigate the problem (Tang, et al., 2012). Similarly, when they sense danger-associated molecular patterns (DAMPs), which are endogenous signals

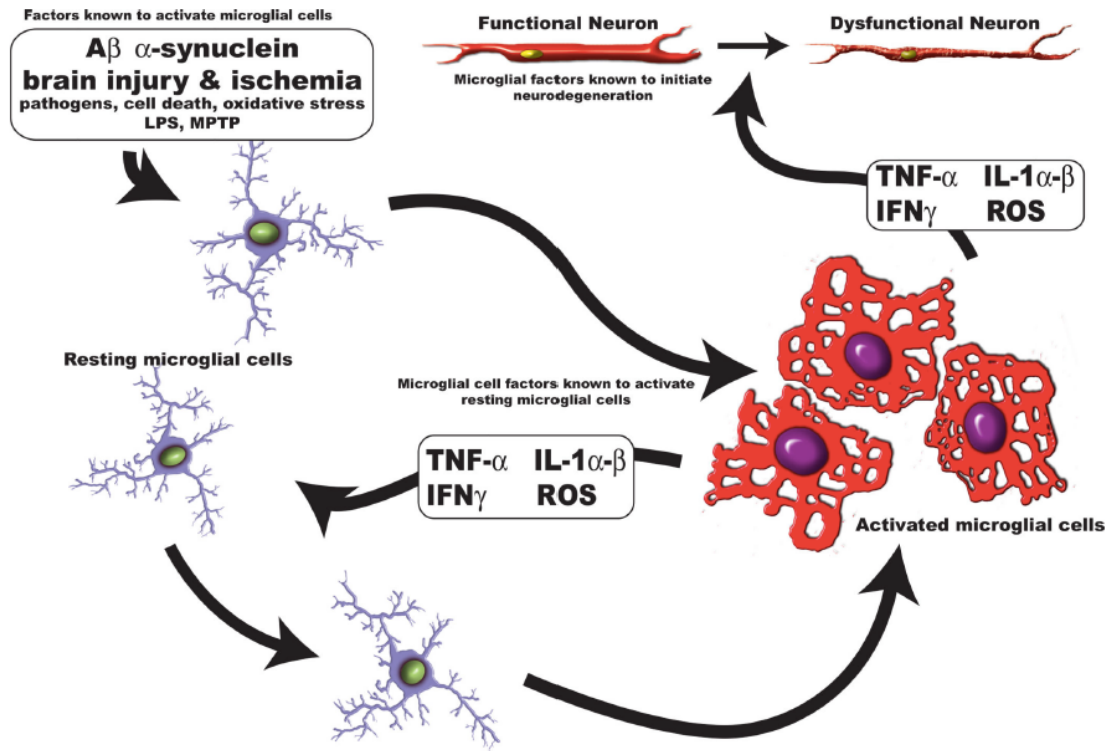


Figure 1.3 Microglial activation and $TNF\alpha$ production (Frankola, et al., 2011).

indicating injury not related to an infection (Tang, et al., 2012), such as A β , microglia become activated and produce proinflammatory cytokines, including tumor necrosis factor α (TNF α) and interleukin-1 β (IL-1 β) (Patel, et al., 2005). Chronic inflammation is thought to be partly responsible for neurodegeneration in AD, having a significant impact before symptoms appear (McGeer and McGeer, 1998). A variety of microglial receptors are involved in AD pathology. The receptors known to elicit proinflammatory responses when stimulated by fibrillar A β include a complex of CD36, $\alpha_6\beta_1$ -integrin, and integrin associated CD47 (Bamberger, et al., 2003); CD14 (Fassbender, et al., 2004); toll-like receptor (TLR) 2 and TLR4 (Reed-Geaghan, et al., 2009); CD36 (El Khoury, et al., 2003; Moore, et al., 2002); and a CD36-TLR4-TLR6 complex (Stewart, et al., 2010). Others include complement receptors, Fc receptors that bind the constant domain of immunoglobulin, formyl peptide receptors 1 and 2, receptor for advanced glycation end products, nod-like receptor protein, CD33, scavenger receptor A, and triggering receptor expressed by myeloid cells (Doens and Fernández, 2014).

1.3.2 Cellular uptake of extracellular material

Mammalian cells ingest materials by way of phagocytosis or pinocytosis. Figure 1.4 provides an illustration of general mammalian cell uptake. Only pathogens and large particles are ingested through phagocytosis, which requires receptors. Of the five forms of pinocytosis, macropinocytosis does not require receptors. In this type of internalization, cell surface membranes produce waves, or ruffles, that extend into the extracellular space and then reconnect with the plasma membrane, bringing into the cell any particles that are in the surrounding medium (Conner and Schmid, 2003).

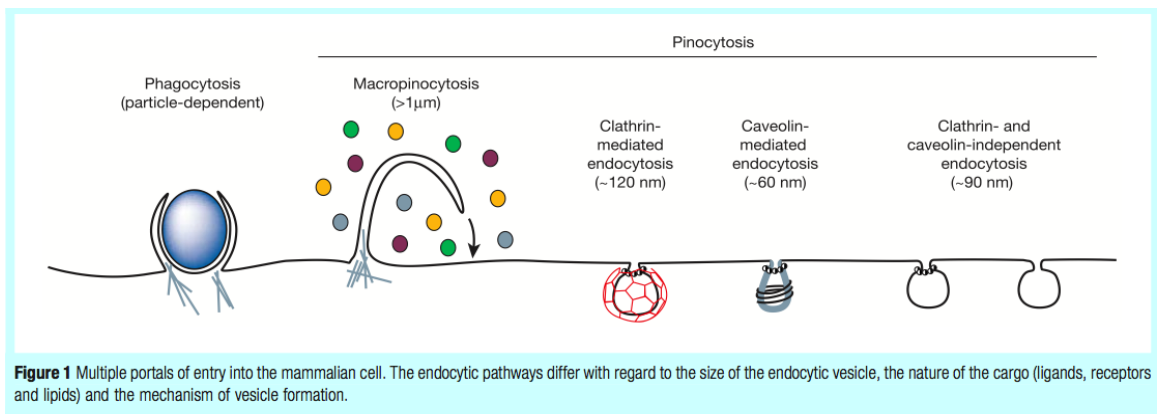


Figure 1.4 Mammalian cell uptake (Conner and Schmid, 2003).

Receptors known to be involved with A β -microglial uptake of extracellular material include scavenger receptors (Paresce, et al., 1996); a complex of CD36, $\alpha_6\beta_1$ -integrin, and CD47 (Koenigsknecht and Landreth, 2004); complement receptor 3 (CR3, Mac-1) signal regulatory protein β_1 (SIRP β_1) (Gaikwad, et al., 2009); and P2Y $_4$ (Li, et al., 2013). Surface receptors such as toll like receptors (TLRs) have been shown to be involved in the activation of microglia as they interact with A β 42 (reviewed in Su, et al., 2015). Mandrekar, et al. (2009) demonstrated that microglia take up soluble A β via fluid-phase macropinocytosis, which is not mediated by receptors.

1.3.3 Internal trafficking of material in microglia

Most cells have lysosomes, acidic organelles that break down misfolded proteins and other unwanted material. Material can be routed to lysosomes through the pathways illustrated in Figure 1.5. Once ingested substances are internalized, they become part of a vesicle known as an early endosome (EE), which develops into a late endosome (LE)/multivesicular body (MVB). An alternative is that the LE becomes a recycling endosome (RE) which moves the material out of the cell. Some material will become part of the endolysosome (EL), which is formed when the LE/MVB fuses with a lysosome. Normally, unwanted material would be degraded within the acidic lysosome. As discussed in Chapter 4, this is not always the case for microglia interacting with A β .

1.3.4 Microglial P2X $_7$ receptors

Characterized in 1996 (Surprenant, et al., 1996), P2X $_7$ receptors are found in all types of immune cells, including microglia (Burnstock and Knight, 2004; Chen and Brosnan, 2006). With regard to AD, the presence of P2X $_7$ receptors is increased in

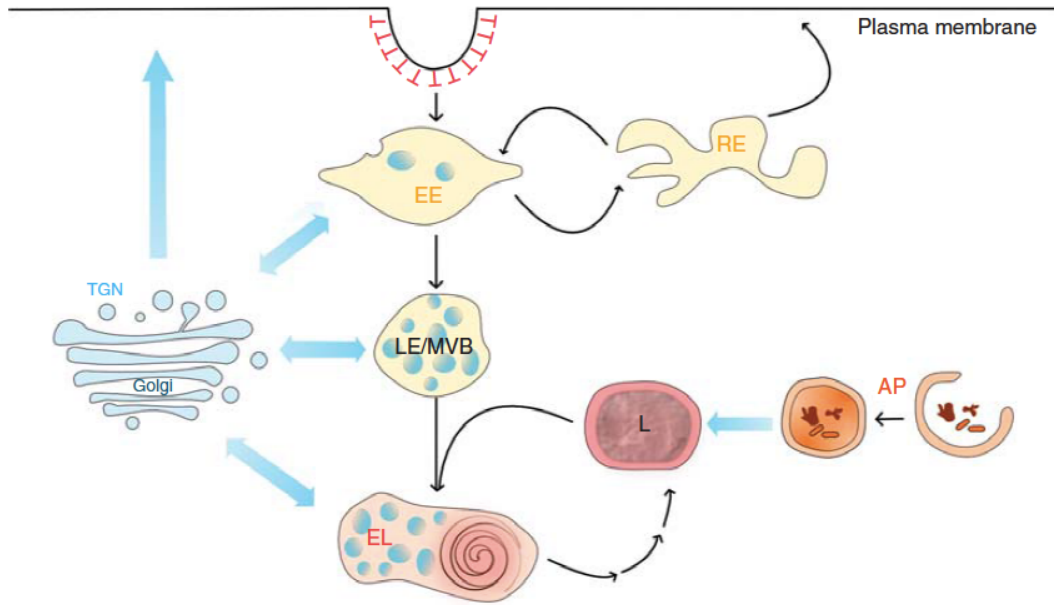


Figure 1. Delivery to lysosomes. Lysosomes (L) are terminal compartments of the endocytic and autophagic pathways (AP). Newly synthesized lysosomal proteins are delivered to them from the *trans*-Golgi network (TGN) via early endosomes (EE), recycling endosomes (RE), and late endosomes/multivesicular bodies (LE/MVB). Following lysosome fusion with late endosomes to form an endolysosome (EL), lysosomes are re-formed by a maturation process.

Figure 1.5 Lysosomes (Luzio, et al., 2014)

microglia near plaques in a mouse model of AD (Parvathenani, et al., 2003) and in human AD brains (McLarnon, et al., 2006; Takenouchi, et al., 2010). P2X₇ receptors respond to ATP at millimolar concentrations, and at even lower concentrations for the agonist 2',3'-(benzoyl-4-benzoyl)-ATP (BzATP) (Surprenant, et al., 1996). In response to ATP and/or LPS, microglia release inflammatory cytokines such as TNF α (Hide, et al., 2000) and IL-1 β (Brough, et al., 2002; Ferrari, et al., 1997; Rampe, et al., 2004). The cytokine release has been shown to occur through microvesicle production (Bianco, et al., 2005).

1.4 Microvesicles

An important aspect of intercellular communication is the release of membrane-bound packets of cytoplasm from cells (Budnik, et al., 2016). These extracellular vesicles can be categorized by size and origin into two groups: exosomes are 30-100 nm in diameter and part of larger multi-vesicular bodies, and microvesicles are 100-1000 nm in diameter and form as buds from the cell surface (Budnik, et al., 2016). As shown in Figure 1.6 (top), microvesicles are complex, having varied receptors and cargoes. The budding process is also illustrated in Figure 1.6 (bottom), and of special interest for my work is the externalization of phosphatidylserine (PS), which can be used in experiments to verify the presence of microvesicles.

Microvesicles have various roles outside of direct AD involvement. THP-1 monocytes, immune cells in the bloodstream, release IL-1 β via microvesicles (MacKenzie, et al., 2001). Microglia also release microvesicles carrying cytokines when stimulated with ATP (Bianco, et al., 2005). In 2009, Bianco and colleagues demonstrated

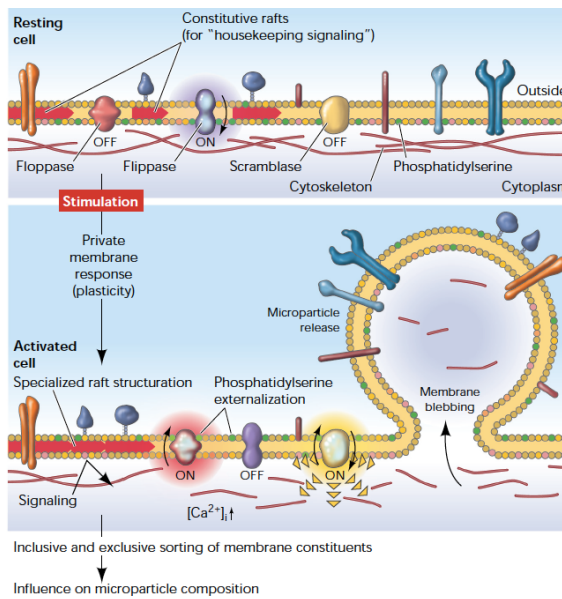
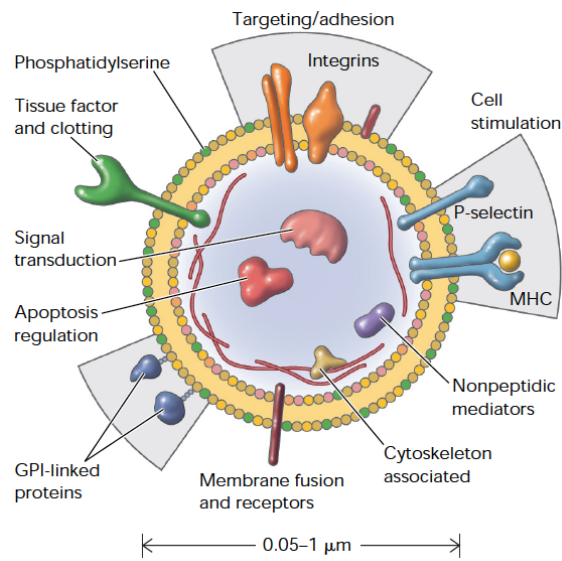


Figure 1.6 Microvesicles. Top: Structure. Bottom: formation from plasma membrane. Note the externalization of phosphatidylserine. (Hugel, et al., 2005)

the release of microvesicles from astrocytes and further showed that the mechanism proceeds through a p38 MAPK cascade and requires acid sphingomyelinase. Microglia-to-neuron signaling was demonstrated by Antonucci, et al. (2012), and microvesicle stimulation of neuronal activity was shown by Turola, et al. (2012). The usefulness of microvesicles in identifying neuroinflammation caused by multiple sclerosis and measuring reduction of neuroinflammation through treatment was reported by Verderio, et al. (2012).

With regard to microvesicles in AD, and from microglia in particular, there are interesting findings. Bianco, et al. (2005) demonstrated that microglia shed microvesicles when stimulated with ATP, and that the microvesicles contain the cytokine IL-1 β . Microvesicles from microglia can interact with fibrillar A β and convert it to a soluble and more toxic A β form (Joshi, et al., 2014). Studies of human cerebrospinal fluid revealed that the combination of microvesicles and A β 42 is toxic to human brain cells and contributes to the spread of neurodegeneration through the AD brain (Agosta, et al., 2014). The effect of microglial microvesicles on A β 42 aggregation and the role of microvesicles in A β 42 trafficking within and between cells are growing areas of research emphasis. Chapter 5 describes the work done to connect microvesicle production with A β stimulation in microglia.

CHAPTER 2: METHODS

2.1 A β preparation

The A β 42 peptide used in my experiments was supplied by the same group under two different company names. They were known as the Large Scale Peptide Synthesis Laboratory in the W.M. Keck Biotechnology Resource Laboratory, Yale School of Medicine (Yale, New Haven, CT). In June, 2013, the lab ceased operation under that name, and in May of 2014 began work as the ERI Amyloid Laboratory, LLC (ERI, Oxford, CT). The ERI Amyloid Laboratory is our current A β peptide supplier. Of the seven labeled preparations, the first three were from Yale, and the last 4 were from ERI. There were no significant differences between the peptide batches. The sequence and purity of all A β peptide shipments were confirmed by mass spectrometry at ERI.

2.1.1 A β aliquot lyophilization

A β 42 was obtained in lyophilized form and stored at -20 °C. Nucleation of amyloid proteins leads to rapid aggregation and occurs quickly in a concentrated solution (Jarrett and Lansbury, 1992), so dissociating any pre-formed A β seeds is necessary to prevent aggregation. To prepare monomeric aliquots, the peptide was dissolved in 100% hexafluoroisopropanol (HFIP) (Sigma-Aldrich, St. Louis) at 1 mM and separated into 1 mL aliquots in sterile, siliconized microcentrifuge tubes. The tubes were then left uncovered, at room temperature, overnight in a fume hood to evaporate the HFIP. On the following day, the aliquots were vacuum-centrifuged to remove any residual HFIP. A

thin film of A β was deposited on the inside walls of the microcentrifuge tubes, which were then stored in dessicant at -20 °C.

2.1.2 Preparation of A β monomers, protofibrils, and fibrils

A modified (without glucose) artificial cerebrospinal fluid (aCSF) was used to prepare A β solutions. The composition of our aCSF is 15 mM NaHCO₃, 1 mM Na₂HPO₄, 130 mM NaCl, 3 mM KCl, pH 7.8. This aCSF solution was designed to mimic the ionic strength of cerebrospinal fluid and cell culture medium while leaving out the supplements that might interfere with spectroscopy and retaining the cell compatibility of growth medium (Paranjape, Terrill, and Gouwens, et al., 2013). The solution of A β 42 monomers and protofibrils was prepared by dissolving lyophilized A β 42 (1 mg) in 50 mM NaOH to yield a 2.5 mM A β 42 solution, which was then diluted to 250 μ M A β 42 in prefiltered (0.22 μ m) artificial cerebrospinal fluid. To allow protofibril formation, the A β 42 solution was incubated at room temperature for 30 min - 4 h. The wide range of incubation times was necessary as some of the aliquots required more time to form soluble aggregates. At this point, unlabeled A β 42 was purified by size exclusion chromatography (SEC) as described in 2.1.4 below. Peptide to be fluorescently labeled underwent the procedure described in 2.1.3. Fluorescently-labeled A β 4 fibrils were prepared by leaving monomer preps at 4 °C for two or more weeks; usually fibrils form after two weeks.

2.1.3 Fluorescent labeling of A β

In some experiments with microglia, I conducted immunofluorescence assays to determine the location of A β 42 on or in treated cells (Paranjape, et al., 2012; Paranjape, Terrill, and Gouwens 2013). However, direct labeling with a fluorophore is a more

efficient method for tracking microglial interactions with A β 42. This strategy has been used by many research groups (for example, Fu, et al., 2012; Halle, et al., 2008; Li, et al., 2012; Liu, et al., 2010; Mandrekar, et al., 2009; Paresce, et al., 1997). Alexa Fluor® 488 carboxylic acid, 2,3,5,6-tetrafluorophenyl ester (AF488-TFP, Life Technologies) is an amine-reactive fluorophore that has been used to label soluble oligomers of A β 42 (Jungbauer, et al., 2009). The structure of AF488-TFP is shown in Figure 2.1. In their experiments, Jungbauer and colleagues compared oligomers labeled before aggregation to oligomers labeled after aggregation. Their work showed that allowing the peptide to aggregate before conducting the labeling experiment, rather than labeling monomers first and allowing them to aggregate, produced soluble, labeled A β oligomers that are most similar to unlabeled A β oligomers. Therefore, I used a solution containing both monomers and protofibrils, prepared as described above, for the labeling reaction.

Attaching a fluorescent label directly to the peptide had several advantages. The direct fluorescence meant that I could visualize A β 42 both on and in cells without the risk of non-specific interactions between antibodies and non-target proteins. The strength of the fluorescence allowed visualization of A β 42 even at low concentrations of 0.5, 1 and 2 μ M. Less time was required for completing experiments, and I had the option of imaging live cells.

There are three primary amine groups in the A β 42 monomer which can potentially interact with AF488-TFP: lysine-16, lysine-28, and the N-terminus. Each of these is a nucleophile that can attack the carbonyl carbon located between the tetrafluorophenyl group and the fluorophore of A488-TFP. The reaction mechanism for the A β N-terminal amine is shown in Figure 2.2.

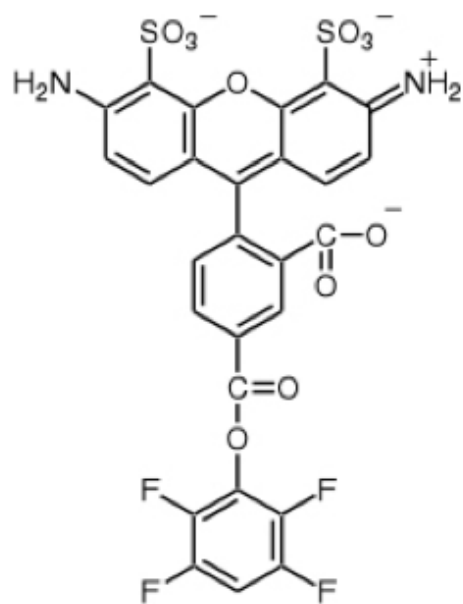


Figure 2.1 Structure of Alexa Fluor® 488 tetrafluorophenyl ester (Life Technologies).

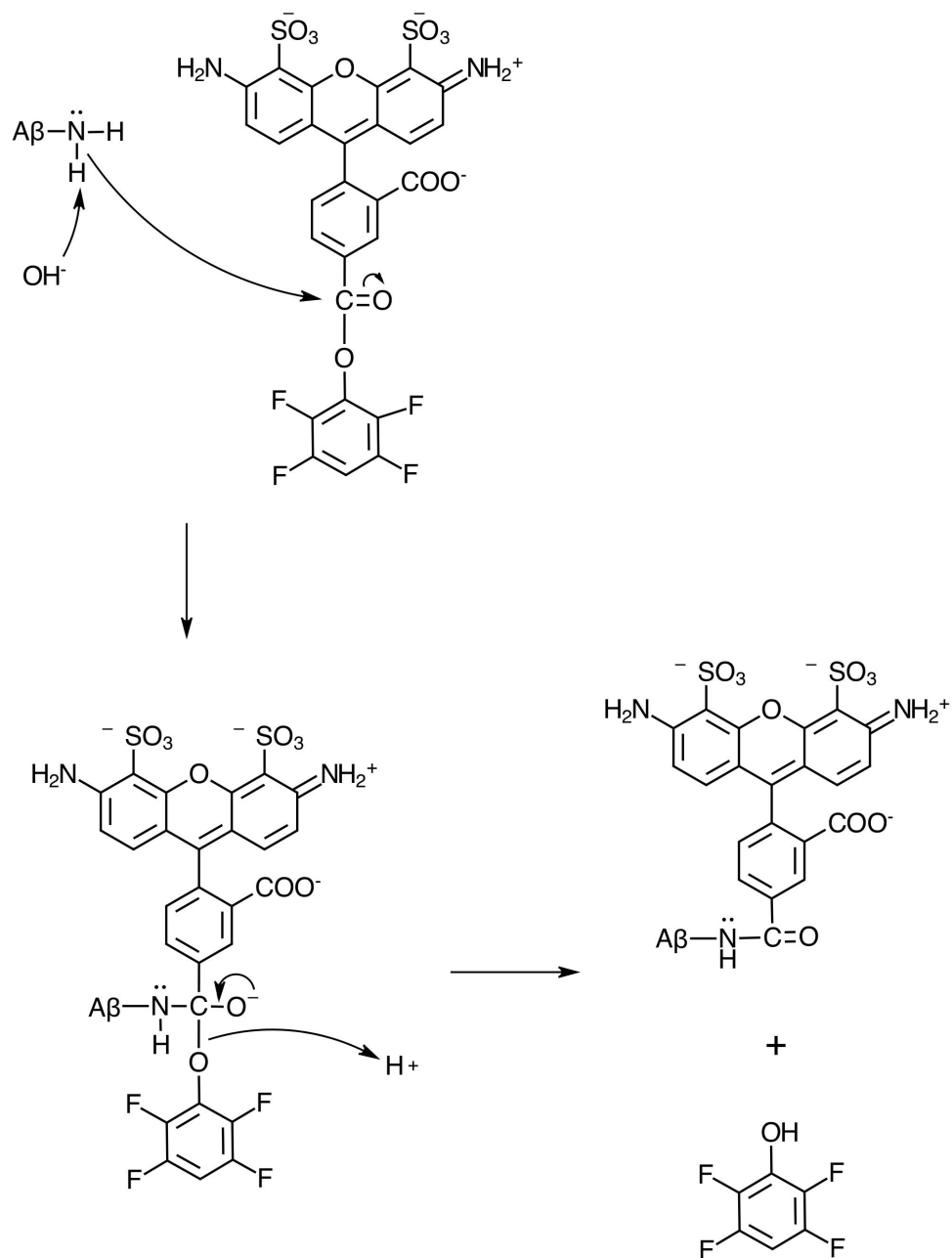


Figure 2.2 Labeling reaction mechanism for Aβ and amine-reactive AF488-TFP. I drew this mechanism using ChemDoodle® software (Version 7.0.1, iChemLabs.)

The manufacturer's protocol calls for dissolving the protein to be labeled in 1 mL of sodium bicarbonate buffer pH 8.3, dissolving the dye in dimethylsulfoxide or dimethylformamide at 10 mg/mL, and then combining the two solutions. A conversation with an Invitrogen support technician confirmed that if the pH was 8.0 or higher, the labeling reaction would proceed in our aCSF buffer. The NaOH/aCSF solution in which the peptide was prepared has a pH of 8.2.

To conduct the labeling reaction, 500 μ L of an A β 42 solution with both protofibrils and monomers was added to 100 μ g of AF488-TFP dry powder in the original tube from the manufacturer, mixed gently by pipet, and transferred to a 1.8 mL glass vial containing a 5-mm magnetic stir bar. A second 500 μ L volume of A β 42 solution was added to the original tube to capture any remaining powder, then transferred to the glass vial. The A β /AF488-TFP mixture was gently stirred for 1 h at 25°C. After stirring, the solution was transferred to a siliconized microcentrifuge tube prior to chromatographic separation.

2.1.4 Size exclusion chromatography (SEC)

Before SEC, the AF488-A β monomer+protofibril solution underwent centrifugation at 17,000 x g for 10 minutes to pellet any non-soluble fibrils that may have formed. Both unlabeled and fluorophore-labeled A β 42 centrifugation supernatants were fractionated on a Tricorn Superdex 75 10/300 GL column (GE Healthcare) using an AKTA FPLC system (GE Healthcare). Prior to injection of the A β 42, the Superdex 75 column was coated with sterile bovine serum albumin (Sigma) to prevent any non-specific binding of A β 42 to the column matrix. 1 mL of the sample was loaded, either

A β 42 or AF488-A β was eluted at 0.5 mL min⁻¹ in aCSF, and 0.5 mL fractions were collected and immediately placed on ice. Elution was monitored in-line by UV absorbance (A₂₈₀), and concentrations of unlabeled A β 42 were determined from these absorbance values. A representative UV trace, combined with fraction fluorescence measurements, for AF488-A β is shown in Figure 2.3. AF488-A β 42 concentrations were determined as described below in Section 2.2.3. Shana Terrill-Usery, Sanjib Karki, Ben Colvin, and Nyasha Makoni all assisted me with SEC.

2.2 Characterization of fluorescently labeled A β

2.2.1 Fluorescence measurements

AF488 has a maximum emission at 525 nm (Life Technologies). Measuring the fluorescence of each 0.5 mL fraction which can be used to confirm labeling success. If the fluorescence of the fractions lines up with the peaks on the inline trace then it is reasonable to assume that the labeling was successful. AF488-labeled A β 42 fluorescence in SEC fractions was determined using a Cary Eclipse fluorescence spectrophotometer. Emission scans of 500-600 nm were obtained with an excitation wavelength of 495 nm. The resulting curves were integrated from 505-550 nm to produce relative fluorescence units (RFU), shown in Figure 2.3 as red circles. The integrated fraction fluorescence values align well with the SEC trace peaks, which confirms the association of the fluorophore with the peptide.

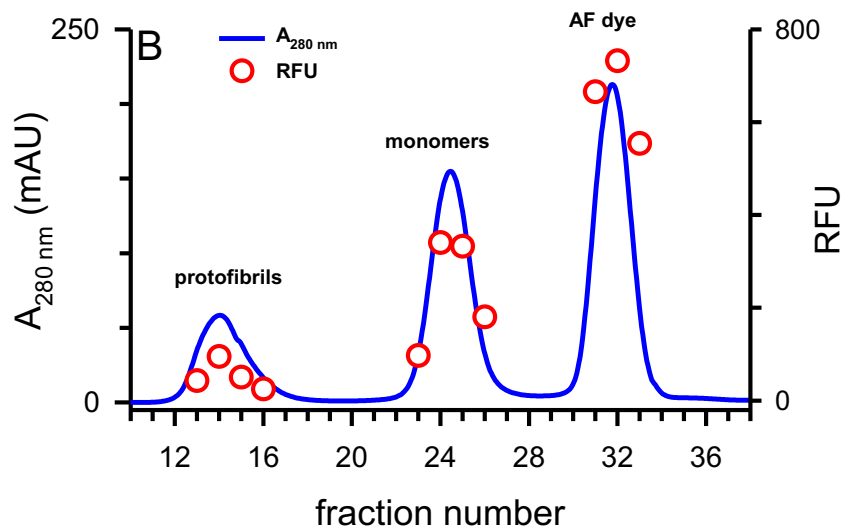


Figure 2.3 Representative UV trace for SEC elution overlaid with fluorescence measurements of fractions. SEC trace (blue line) and fraction fluorescence (red circles) showing peaks for protofibrils, monomers, and unincorporated AF488-TFP (AF dye). (Gouwens, et al., 2016)

2.2.2 Absorbance measurements

An inline UV trace identified the fractions containing A β 42. For unlabeled A β 42, this trace is used to determine the concentration of peptide in each fraction. However, the inline UV overvalued the concentrations in each fraction of AF488-A β because the AF488 fluorophore absorbs at 280 nm. Manual measurements of UV absorbance were taken to use in calculations. AF488-A β chromatography samples were scanned from 600 to 220 nm on a Cary 50 (Varian) UV/Visible spectrophotometer. Figure 2.4 contains a representative scan of a fraction containing unincorporated AF488-TFP in aCSF that is typical of the seven labeled preps. The large peak near 500 nm is due to the fluorophore, A β 42 has no absorbance at those wavelengths. A low amount of absorbance is visible at 280 nm (0.1 AU), and because of that I needed to calculate AF488-A β concentrations (see Section 2.2.3). Confirmation that using the manual absorbance measurements for calculations would be accurate came from comparing the A_{280} manual measurements to the inline UV absorbance, as is shown in Figure 2.5. Absorbance measurements of peak fractions (red circles) of protofibril, monomer, and unreacted AF488-TFP all fall on the line obtained from the inline trace (blue line). This indicates that both methods of assessing UV absorbance agree.

2.2.3 A β concentration calculations

Since A β 42 and the AF488 label both contribute to total absorbance ($A_{280, \text{tot}}$), AF488-A β 42 concentrations were obtained after subtraction of the fluorophore absorbance at 280 nm ($A_{280, \text{AF488}}$) from $A_{280, \text{tot}}$. The contribution of AF488 to $A_{280, \text{tot}}$ is described by the relationship $A_{280, \text{AF488}} = A_{494, \text{AF488}} \times 0.11$, where $A_{494, \text{AF488}}$ is the absorbance of the fluorophore at 494 nm (Life Technologies). Concentrations of AF488-

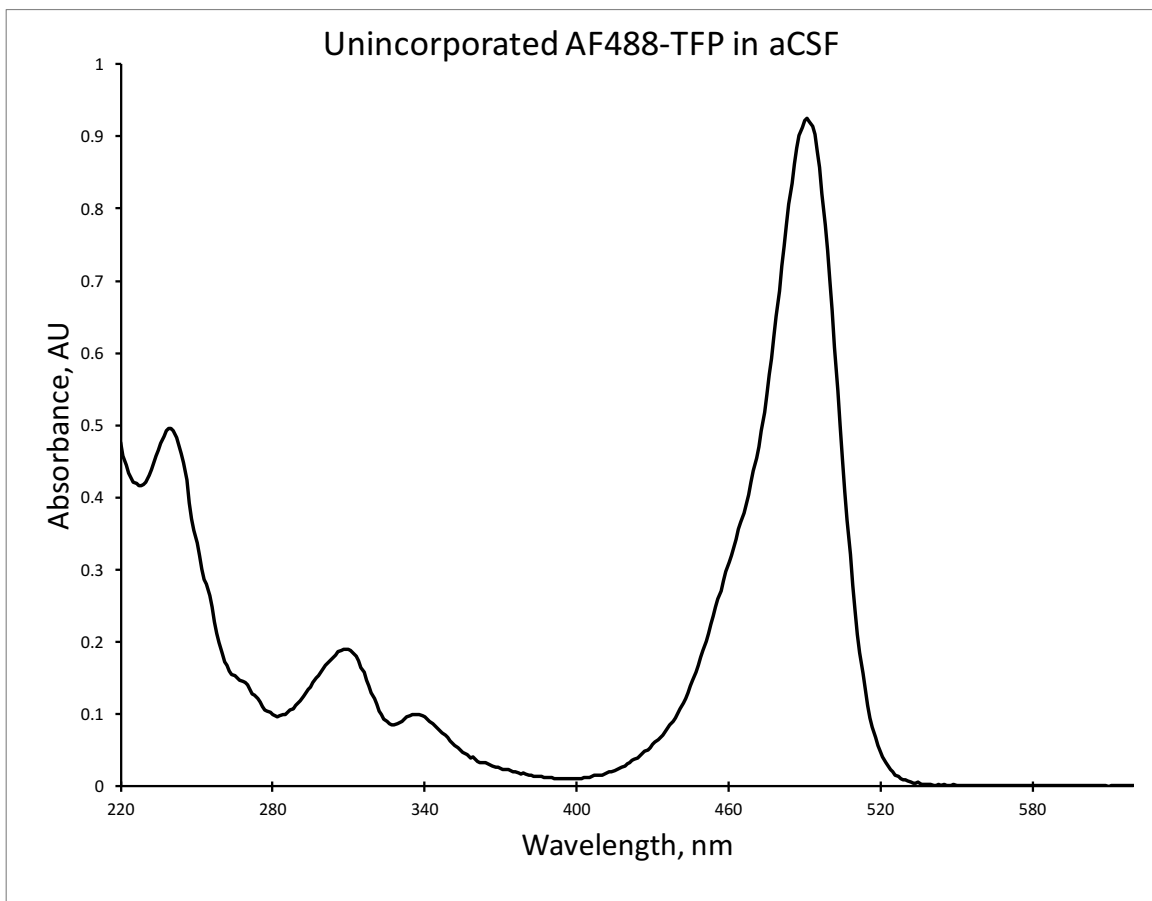


Figure 2.4 AF488 absorbs at 280 nm. The large peak at 494 nm is due to the unconjugated AF488 fluorophore. The absorbance at 280 nm is equal to 11% of the absorbance at 494 nm.

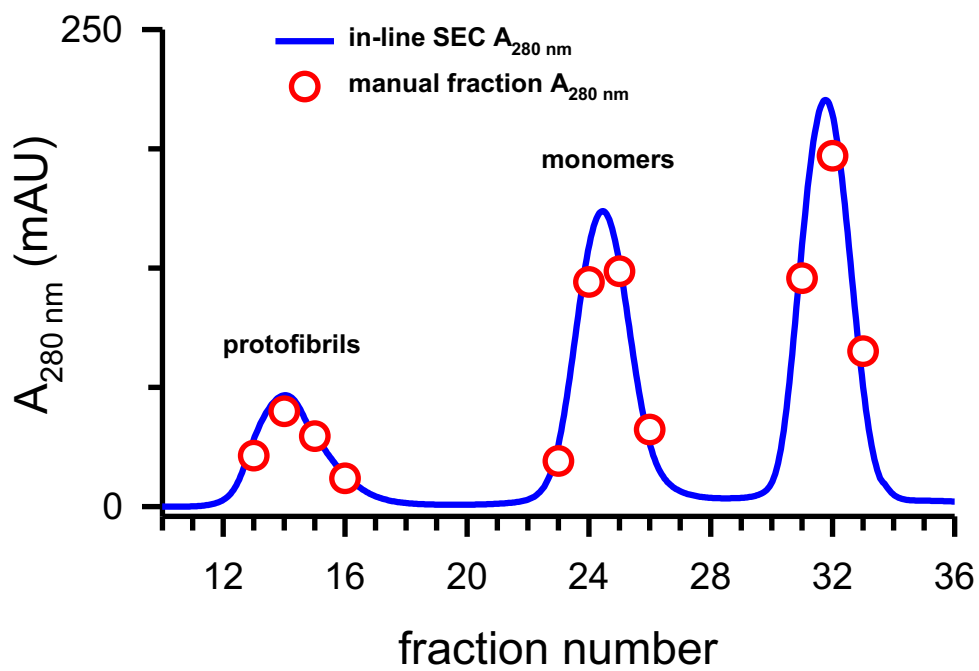


Figure 2.5 Comparison of UV-Vis absorbance measurement methods. Absorbance values at 280 nm measured by SEC inline UV (blue line) and manual UV spectrophotometry of 0.5 mL fractions (red circles). Representative data from one of the seven labeled preps.

A β in sample preparations were determined using A_{494, AF488} and A_{280, tot} from the absorbance scans and the following calculation derived from Beer's Law ($A = \epsilon l c$):

$$C_{AF488-A\beta} = [A_{280, tot} - (A_{494, AF488} \times 0.11)] \div [\epsilon_{280, A\beta} \times l] \quad (\text{Equation 1})$$

where l is the path length (1 cm) and $\epsilon_{280, A\beta}$ is the extinction coefficient at 280 nm for A β 1450 M⁻¹ cm⁻¹ (Nichols, et al., 2002). Unincorporated AF488-TFP concentrations were determined using an extinction coefficient at 494 nm of 71,000 M⁻¹ cm⁻¹ (Life Technologies). The AF488:A β 42 stoichiometry was then obtained. Table 2.1 provides a summary of the labeling stoichiometry of peak protofibril and monomer fractions. In protofibrils, lysine-16, lysine-28, and some N-termini may not be accessible to the fluorophore, so it was expected that there would be a lower labeling stoichiometry for protofibrils than monomers. For the seven AF488-A β 42 preparations used in my experiments, the average AF488:A β 42 ratio was 0.14 \pm 0.03 for protofibrils, and 0.50 \pm 0.08 for monomers. The three-fold higher stoichiometry of labeling for monomers was meaningful for data interpretation.

2.2.4 Electron microscopy

SEC-purified A β solutions, both labeled with Alexa Fluor® and unlabeled, containing protofibrils or fibrils (10 μ L) were applied to a 200-mesh Formvar-coated copper grid (Ted Pella, Inc.) Samples were allowed to adsorb for 10 min at 25 °C, followed by removal of excess sample solution. Grids were washed three times by placing the sample-containing side of the grid down on a droplet of water. Heavy metal staining was done by incubation of the grid, sample side down, on a droplet of 2% uranyl acetate (Electron Microscopy Services, Hatfield, PA) for 5-10 min, removal of excess

Table 2.1 Stoichiometry of protofibrils and monomer peak fractions. Average fluorophore:protofibril = 0.14 ± 0.03 . Average fluorophore:monomer = 0.50 ± 0.08 . Calculated as described in Methods 2.2.3.

PROTOFIBRILS				MONOMERS			
Prep	Fluor., μM	A β , μM	Fluor:A β	Prep	Fluor., μM	A β , μM	Fluor:A β
1	4.1	37	0.11	1	19	51	0.37
2	3.9	45	0.09	2	22	58	0.38
3	3.4	47	0.07	3	13	27	0.48
4	3.7	26	0.14	4	17	50	0.34
5	4.6	32	0.14	5	20	39	0.51
6	3.9	20	0.20	6	16	25	0.64
7	4.3	18	0.24	7	21	28	0.75

solution, and air drying. Affixed samples were visualized by Dr. David C. Osborn with a JEOL JEM-2000 FX transmission electron microscope operated at 200 keV.

Visualizing the AF488-A β 42 protofibrils with transmission electron microscopy allowed me to verify that they had the same length and curvilinear morphology as the unlabeled A β 42 protofibrils. Figure 2.6 shows the similarities between both labeled and unlabeled A β 42 protofibrils and fibrils. While the AF488-A β concentration (38 μ M) used for preparing the TEM grid makes for a crowded image (Panel B), the morphology of the protofibrils is unmistakable (compare Panels A and B) and was not affected by the attachment of the fluorophore. Similarly, the label did not affect aggregation, as monomers were able to aggregate into fibrils. The image shows fibrils formed from monomers after 53 days at 4 °C, but fibrils formed in other labeled monomer samples in as little as two weeks at 4 °C.

2.2.5 Dynamic light scattering

Hydrodynamic radius (R_H) measurements of A β protofibrils, and of microvesicles, were made at room temperature with a DynaPro Titan instrument (Wyatt Technology, Santa Barbara, CA). Samples (30 μ L) were placed directly into a quartz cuvette and light scattering intensity was collected at a 90° angle using a 10-s acquisition time. Particle diffusion coefficients were calculated from auto-correlated light intensity data and converted to R_H with the Stokes-Einstein equation. Average R_H values were obtained with Dynamics software (version 6.7.1). Histograms of percent intensity vs. R_H were generated by Dynamics data regularization, and intensity-weighted or mass-weighted mean R_H values were derived from regularized histograms. Figure 2.7

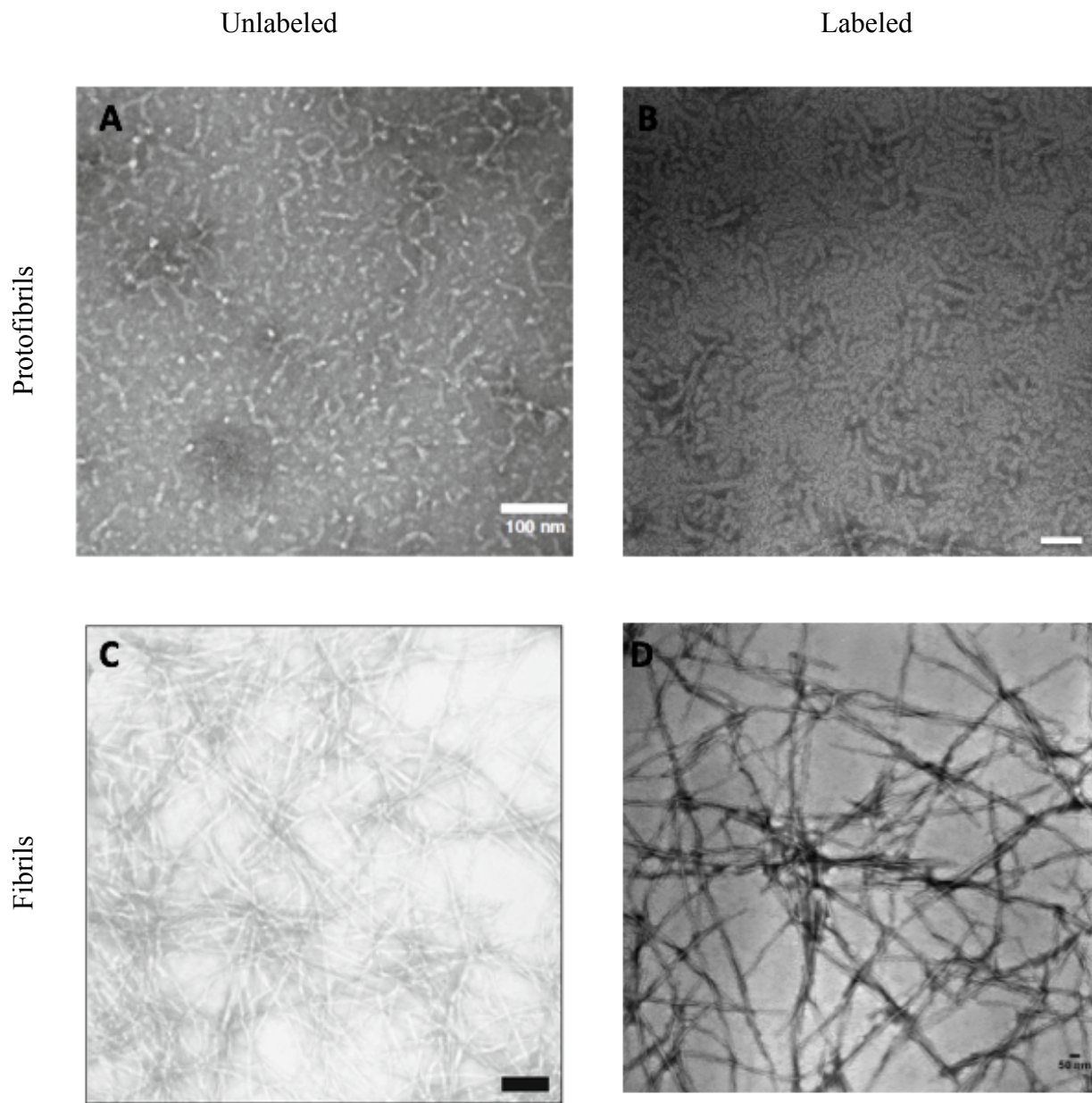


Figure 2.6 Transmission electron micrographs of unlabeled A β 42 and AF488-A β 42. (A) Unlabeled protofibrils, 10 μ M; (B) AF488-protofibrils, 38 μ M; (C) Fibrils formed from unlabeled monomers, 10 μ M; (D) Fibrils formed from AF488-monomers, 37 μ M. A and C scale bars = 100 nm (Paranjape, Terrill, and Gouwens, et al., 2013); B and D scale bars = 50 nm (Gouwens, et al., 2016).

demonstrates the similar hydrodynamic radii for both unlabeled A β and AF488-A β protofibrils. The mean R_H for unlabeled protofibrils (average of five preps) formed in aCSF was reported as 21.9 ± 4.0 nm (Paranjape, Terrill, and Gouwens, et al., 2013) and for AF488-A β protofibrils formed in aCSF the mean $R_H = 16$ nm, range = 5-50 nm (Gouwens, et al., 2016). While I have conducted DLS measurements for other investigations, the measurements of A β 42 were made by Dr. Nichols and we discussed the data.

DLS was also used to determine microvesicle size. Again, measurements were made by Dr. Nichols and there were subsequent discussions of the data. Microvesicle characterization by DLS is discussed in Section 5.1.3 of Chapter 5.

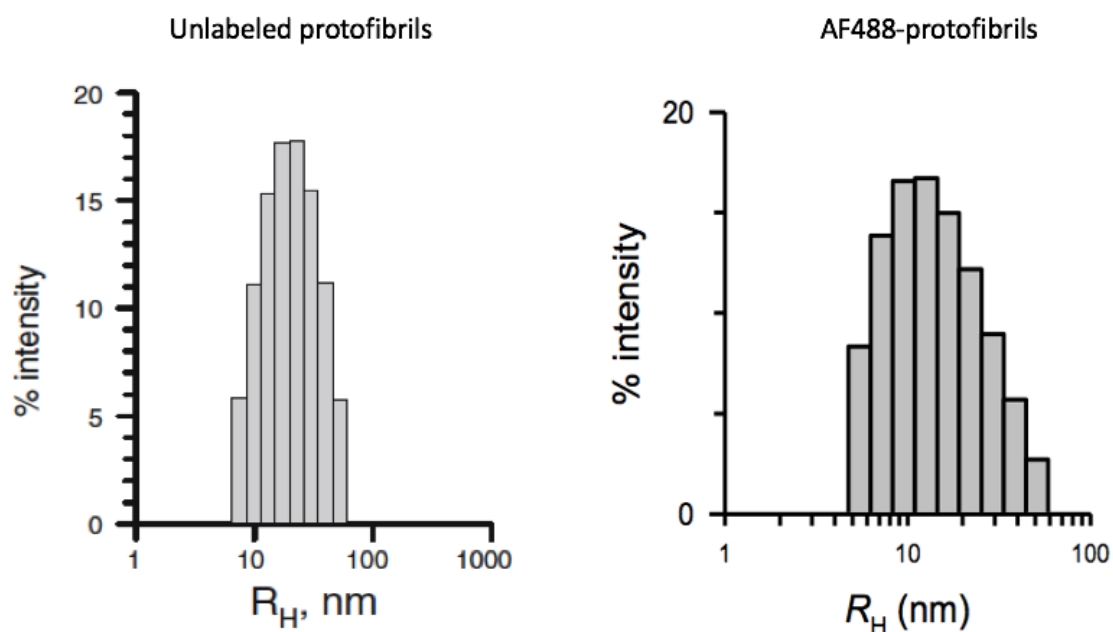


Figure 2.7 Dynamic light scattering (DLS). Protofibrils were analyzed by DLS immediately after SEC isolation. Representative regularized histograms of percent intensity vs. hydrodynamic radius are shown. *Left*: Histogram for unlabeled protofibrils prepared in aCSF, mean $R_H = 23$ nm (Paranjape, et al., 2013). *Right*: Histogram for AF488-protofibrils in aCSF, mean $R_H = 16$ nm (Gouwens, et al., 2016).

2.3 Cell Culture

2.3.1 BV-2 microglia culture

BV-2 cells are an immortalized murine microglial cell line derived from primary murine microglia by stable transfection with the J2 virus, a v-raf/v-myc oncogene-carrying retrovirus (Blasi, et al., 1990). Our BV-2 cells were provided by Dr. Gary Landreth, Case Western Reserve University, and were maintained in Dulbecco's modified Eagle's medium (DMEM, 4.5 g/L glucose, Hyclone) containing 50 U/mL penicillin, 50 µg/mL streptomycin, 50 µM β-mercaptoethanol, and 5% heat inactivated fetal bovine serum (FBS, Hyclone) in 75 cm² flasks (Corning). BV-2 cells were used for their ease of culture, to make initial observations comparing them to primary cells, and for the optimization of microglia-Aβ interactions. After thawing, 1.5 mL BV-2 cells (1e6 cells/mL) are added to 5 mL growth medium and centrifuged at 500xg for 7 min. The supernatant is removed by vacuum aspiration, then the cell pellet is resuspended in 10 mL growth medium and the cell solution is added to a T75 cell culture flask (Corning).

Cells are passaged twice weekly as follows. Growth medium is removed and, after rinsing with 1 mL sterile PBS, 1 mL 0.25% Trypsin (Sigma) is added to the flask to dislodge adherent cells from the bottom of the flask. The cells are then incubated for 7 min at 37 °C. 9 mL of growth medium is added to the flask, and from that volume 3 mL are transferred to a 15-mL conical tube, which is centrifuged at 500xg for 7 min. For the first passage after thawing, 3 mL are spun down, and for the second passage 1 mL is spun down. The amounts centrifuged will then alternate between 3 mL and 1 mL in order to keep the BV-2 concentration at an optimal level.

2.3.2 Primary microglia isolation and culture

Primary murine microglia were obtained from wild-type (WT) C57BL/6 (Harlan Laboratories). Care and breeding of the C57BL/6 parent mice were done at the University of Missouri-St. Louis Animal Facility. Isolation of microglia was conducted as described in Esen and Kielian (2007) and Paranjape et al. (2012). 3-4-day-old mouse pups were euthanized with an overdose of inhaled isoflurane (Fisher Scientific). Brains were isolated and meninges were removed under sterile conditions. Brain tissue was minced using sharp-edged forceps, resuspended in 0.5% trypsin (Hyclone), and incubated at 37 °C with shaking for 20 min to allow further dissociation of the tissue. Subsequently, the tissue was resuspended in complete DMEM containing 10% FBS, 4 mM L-glutamine, 100 U/mL penicillin, 0.1 mg/mL streptomycin and 0.25 µg/mL amphotericin-B (Fisher Scientific), OPI medium supplement (oxaloacetate, pyruvate, insulin, Sigma), and 0.5 ng/mL recombinant mouse granulocyte-macrophage colony-stimulating factor (GM-CSF, Invitrogen). The cell suspension was further triturated using a pipet and filtered through a 70 µm cell strainer to remove debris. The resulting cell suspension was centrifuged at 200g for 5 min at 25 °C, resuspended in complete medium, and seeded into 150 cm² flasks (Corning). Cells were cultured at 37 °C in 5% CO₂ until confluent (1-2 weeks), and microglia were selectively harvested from the adherent astrocyte layer by shaking at 250 rpm for 5 h in 5% CO₂ at 37 °C followed by collection of the medium. (For isolations done before 2016, the flask was shaken overnight at 37 °C in 5% CO₂.) The flasks were replenished with fresh medium and then incubated further to obtain additional microglia. Typically, this procedure was repeated 3-4 times for one flask without removal of the astrocyte layer. In the bulk of the experimentation, primary microglia were isolated by

Geeta Paranjape, Shana Terrill-Usery, Sanjib Karki, Ben Colvin, or Nyasha Makoni, and I handled the care, preparation, plating, treatment, and analysis of the cells for experiments.

2.4 Microglial AF488-A β uptake experiments

2.4.1 A β treatment for ELISA and confocal LSM analysis

For cell uptake studies, WT primary murine microglia, acquired as described above, were seeded on glass coverslips, in sterile glass-bottom Mat-Tek P35GC-1.5-14-C culture dishes (Mat-Tek Corp., Ashland, MA) or 96-well cell culture plates at a density of 5×10^5 cells/mL in complete growth medium (volumes of 0.200 mL, 0.200 mL and 0.100 mL, respectively). Prior to cell treatment, growth medium was replaced with assay medium (growth medium lacking FBS and GM-CSF). Lysosome labeling was done prior to cell treatment by adding 0.100 mL assay medium containing 0.100 μ M LysoTracker[®] Red DND-99 (Invitrogen) and incubating for 30 min at 37 °C in 5% CO₂. For treatment times >6 h, LysoTracker[®] was added to the assay medium 30 min before treatment ended. Cells were then incubated at 37 °C in 5% CO₂ with AF488-labeled A β (AF488-A β), unlabeled A β 42, aCSF control, or AF488 dye fraction. Times of incubation and concentrations of AF488-A β , unlabeled A β and AF488 dye are noted in figure legends. Following incubation, the conditioned medium was collected and stored at -20 °C for subsequent analysis by enzyme-linked immunosorbent assay (ELISA) or immuno-dot blot. Adherent microglial cells were rinsed 3X with 0.05% Tween 20 in phosphate buffered saline (PBST) and then fixed with 3.7% formaldehyde for 15 min. Fixed cells were stored overnight at room temperature in the dark before confocal microscopy

analysis. Microglia were seeded on glass coverslips by placing a 100-200 μL drop of cell suspension in the middle of the coverslip, which was in a 30 mm culture dish. A lid was placed over the culture dish to prevent evaporation during incubation. Microglia were able to adhere to the coverslip, Medium changes were accomplished by placing a pipet tip at the edge of the droplet and removing the liquid. Treatment was applied by gently adding 100 μL to the area of the coverslip occupied by the microglia. After fixing for immunofluorescence or direct fluorescence, followed by staining of the nuclei, the coverslip was placed upside-down over a 50- μL droplet of PBS or ProLong Gold Antifade Mountant (Thermo Fisher Scientific) on a microscope slide.

2.4.2 A β treatment for fluorescence plate reader and dot blot analysis

Primary WT murine microglia were plated in Nunc F96 Nunclon sterile 96-well black plates at a density of 5×10^5 cells/mL in complete growth medium (0.1 mL volume). Times of incubation and concentrations of AF488-A β , unlabeled A β are noted in figure legends. In order to remove A β from the cell surface membranes, a more thorough wash protocol was utilized for these studies. Medium was removed from treated cells and placed in clean wells in the plate. Each cell-containing well was rinsed 3X with 100 μL sterile PBS. An acid wash (100 μL) was performed using a solution of 0.5 M NaCl and 0.2 M acetic acid for 15 minutes at 4 $^{\circ}\text{C}$, then cells were rinsed 2X with PBS. All PBS and acid washes were moved to either clean wells or another plate for both fluorescence and dot blot analysis.

For intracellular extract preparation, microglia were lysed for 15 min at 25 $^{\circ}\text{C}$ with 35-50 μL radio immunoprecipitation assay (RIPA) buffer containing 150 mM NaCl,

20 mM Tris, 1 mM ethylenediaminetetraacetic acid (EDTA), 1% Triton X-100, 1% deoxycholic acid, 0.1% sodium dodecyl sulfate (SDS), and protease inhibitor cocktail (Sigma) at a 10X dilution. In some cases, multiple microglia wells were combined to yield higher concentration lysates. Microglial lysates were stored at -20 °C for further analysis.

2.4.3 BV-2 microglia cell binding assay

BV-2 microglia were removed from culture flasks with 0.25% trypsin. Cells were counted using a Cellometer® (Nexcelom Bioscience), pelleted by centrifugation at 500xg for 7 min, and resuspended at a concentration of 5×10^5 cells/mL. 0.2 mL cells were seeded in sterile glass-bottom Mat-Tek P35GC-1.5-14-C culture dishes (Mat-Tek Corp., Ashland, MA) at a density of 5×10^5 cells/mL in assay medium (growth medium lacking FBS). Prior to cell treatment, adherent cells were rinsed once with assay medium. Cells were treated with AF488-A β or unlabeled A β 42 (concentrations indicated in figure legends) and then incubated at 4 °C, room temperature, or 37 °C in 5% CO₂ for 30 min. BV-2 cells were rinsed 3X with 0.05% Tween 20 in phosphate buffered saline (PBST) and then fixed with 3.7% formaldehyde (15 min, room temperature) for confocal microscopy analysis. BV-2 microglia treated with unlabeled A β underwent the immunofluorescence assay described in Section 2.6.

2.5 Fluorescence quantitation for AF488-A β -treated microglia

To quantitate AF488-A β internalization, *in situ* cellular fluorescence measurements were carried out using a Perkin Elmer Victor 3 multi-mode plate reader.

Excitation and emission filters were 485 nm and 535 nm, respectively, with a 0.1 second signal averaging time.

The first experiments I conducted using a black plate and the plate reader employed BV-2 cells treated with AF488-A β . While the data (not shown) indicated some concentration-dependent differences in the fluorescent signal, the signal-to-noise ratio was small, and there was no way to determine if the fluorescence was from A β inside the cells, on the cells, or both. The use of an acid wash, 0.5 % NaCl and 0.2 % acetic acid, to remove antibodies on cell surfaces was reported in 2007 (Liu, et al., 2007) and I used this wash for primary cells treated with AF488-A β . First, a “proof of concept” experiment was done to assess the ability of a plate assay to measure uptake. Primary microglia were treated with 5 μ M AF488-A β monomers or protofibrils (3 wells each), 5 μ M unlabeled A β 42 monomers or protofibrils (3 wells each), 1 μ M AF488-A β protofibrils (3 wells) and aCSF control (3 wells). The plate was incubated for 30 min at 37 °C, 5% CO₂. After transferring the assay medium to clean wells, there were three washes with PBS (100 μ L per well), then the acid wash (100 μ L per well), and two more washes with PBS followed. All washes were transferred to clean wells. Because of this extensive washing including the acid wash, the fluorescence measured in the cell-containing wells reflects only internalized AF488-A β . Figure 2.8 shows the fluorescence intensity readings measured by plate reader. Negligible fluorescence intensity was measured in the cells treated with unlabeled A β 42 and the control wells. The lack of fluorescence intensity difference between AF488-A β 42 monomer and protofibril treated cells is not what I usually see. Monomer-treated cells are expected to have less fluorescence than protofibril-treated cells. The AF488-A β 42 was about two weeks post-purification,

Plate reader fluorescence comparing labeled and unlabeled Abeta

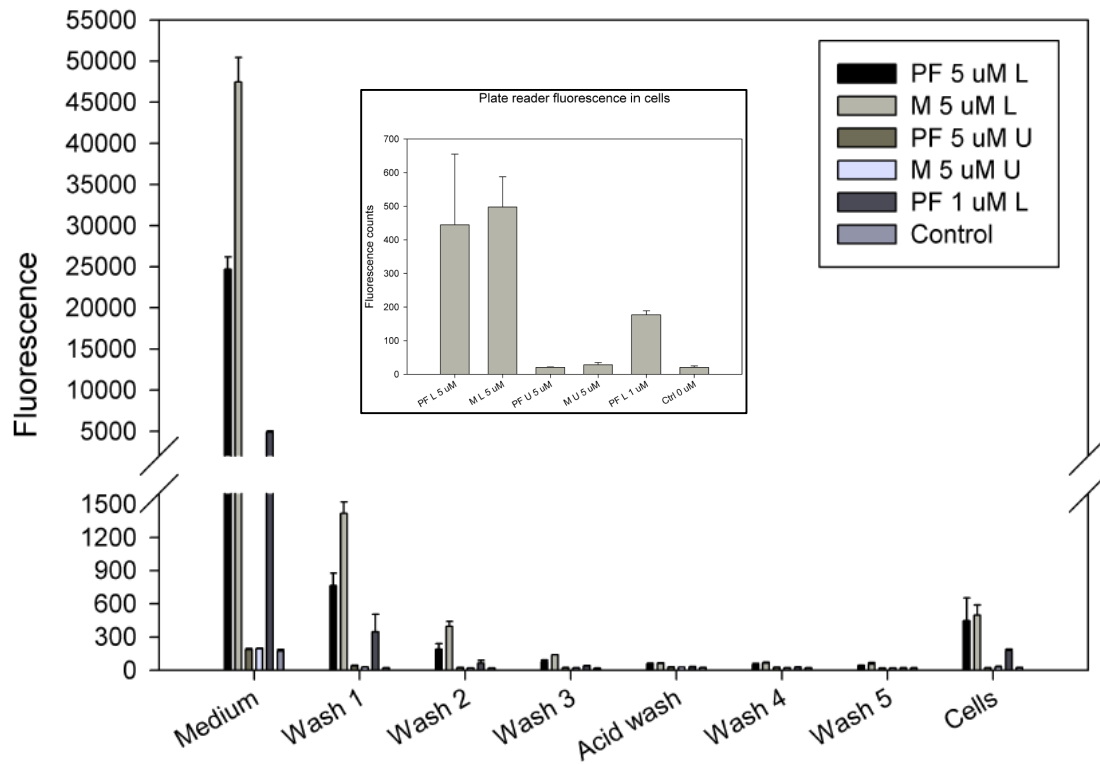


Figure 2.8 Plate reader fluorescence, AF488-A β . Representative data showing fluorescence from a microglia treatment experiment. The fluorescence in the cells is what remains after acid washing. Fluorescence in the acid wash wells represents AF488-A β removed from outer cell membrane surfaces. Inset: Fluorescence in cells after washes.

though, and so had already begun to aggregate. There is a difference between the 1 μM and 5 μM AF488-A β 42 protofibril-treated wells, so from this I knew this assay was sensitive enough to measure uptake differences in concentration and could probably be used in time dependent experiments. It was advantageous to measure uptake this way since using the 96-well plates allowed for more treatment conditions and replicates without using more reagents – especially AF488-A β – and plate reader measurements were less time-consuming and more objective than quantitating fluorescence images.

2.6 Immuno-detection of A β and confocal microscopy

2.6.1 Preparation of fixed cells for microscopy

BV-2 and primary murine microglial cells were stimulated, treated and fixed as described above (Section 2.4.1). Cell samples were then washed 3X with PBST. Cell nuclei were visualized by incubation for 5 min with 0.2 mL of 0.3 μM 4',6-diamidino-2-phenylindole dihydrochloride (DAPI). After a final wash step, 1-2 mL PBS was applied to the Mat-Tek™ dishes to avoid cellular dehydration. In some cases, ProLong Gold Antifade (Thermo Fisher Scientific) was applied, the well was covered with a glass coverslip and the antifade mountant was allowed to set overnight. Microglia treated with AF488-A β were imaged directly without further manipulation.

For microglia treated with unlabeled A β 42, fixed cells were incubated for 1 h with blocking buffer (10% w/v dried milk in PBST). Samples were washed 3X with PBST after this step and each subsequent step. All incubations were conducted with gentle shaking at 25 °C. After blocking, samples were incubated for 1 h with the anti-A β antibody Ab9 (1:5000 dilution in PBST with 5% w/v dried milk) followed by a 1 h

incubation with donkey anti-mouse IgG antibody conjugated to Northern Lights (NL) 493 (R&D Systems).

Lysosomal Lamp1 detection was done by immunostaining in a manner similar to that for unlabeled A β . After incubating for 1 h in a blocking buffer of PBS containing 1% bovine serum albumin (BSA) with gentle shaking, the cells were rinsed 3X with PBST. Next, a 1:500 dilution of anti-Lamp1 primary antibody (Novus Biologicals) into PBS containing 1% BSA and a 1:100 dilution of anti-mouse IgG-NL637 secondary antibody (R&D Systems) into PBS containing 1% BSA were each incubated for 1 h with gentle shaking and rinsed 3X with PBST. After a final wash step, cell nuclei were counterstained with DAPI and 1 mL PBS was applied to the wells to avoid cellular dehydration.

2.6.2 Confocal microscopy

The light coming from a specimen in confocal microscopy is controlled by a pinhole so that its source is limited to a single plane through the specimen. The resulting image is therefore of a slice through the cell. Any visible fluorescence is from a fluorophore within that plane of the cell, not above or below. In addition, when multiple fluorophores are used, channels can be used, as shown in Figure 2.9B, so that only particular wavelengths are collected during a scan. During the next scan of the same plane, another set of wavelengths can be collected. This prevents crosstalk resulting from the emitted light of one fluorophore exciting another fluorophore. If that happened, the recorded light emission that would be incorrectly attributed to the first fluorophore. For the work reported herein, the signal from each fluorophore was collected individually.

Both two-dimensional and Z-stack images were obtained with a Zeiss LSM 700

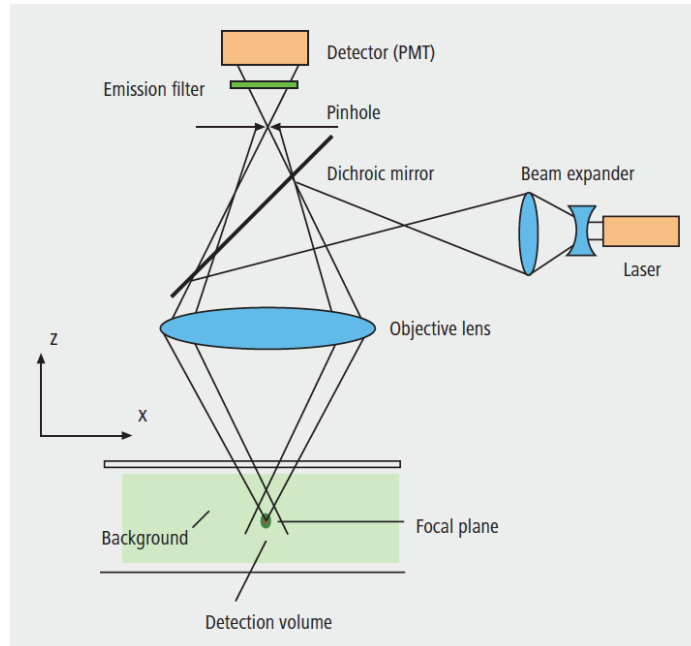


Figure 2.9 Confocal laser scanning microscopy. TOP: Light beam path. Light emission is captured point by point, and the light reaching the detector is limited by the pinhole before it reaches the detector. BOTTOM: Light collection channels. Collecting light in only one part of the spectrum at a time limits cross-talk. The setting used most often for the images in my research is the second, where each part of the spectrum is collected separately. (From Carl Zeiss LSM 700 Operating Manual, September 2011)

confocal microscope at 40X magnification using ZEN 2009 imaging and analysis software. Excitation wavelengths used were 405 nm (DAPI), 488 nm (AF488-A β 42 and anti-mouse IgG-AF488 secondary antibody), 561 nm (LysoTracker® Red, Invitrogen), and 639 nm (antimouse IgG-NL637 for Lamp1, R&D Systems). For comparison experiments, all optical and electrical settings were fixed at identical levels for each image to ensure that fluorescence intensity measurements were not influenced by different settings.

Confocal fluorescence images were quantitated with ImageJ software (NIH) using a procedure detailed by Ansari, et al. (2013). Briefly, a region of interest was drawn around each cell using a polygon drawing tool. Area and integrated density were measured for each cell using ImageJ. Background fluorescence was measured by averaging five random areas between cells in the field. The corrected total cell fluorescence (CTCF) was calculated as follows: [integrated density of total cell area – (total cell area x mean background fluorescence)].

A second method of quantitation involved selecting the channel for fluorescence produced by AF488-A β , changing the color presentation to grayscale, and measuring integrated fluorescence intensity using ImageJ. Integrated density was divided by the number of cell nuclei in the field. Excel was employed to compile the data from separate experiments and calculate error. These two methods were used for experiments in which the plate reader assay described in Section 2.5 was not used.

2.7 Immuno-dot blot

A nitrocellulose membrane was soaked in water and allowed to dry completely. Microglial cell lysates (1.7 μ L) were spotted onto the membrane and allowed to dry for

20 min. Subsequent incubation and washing steps were carried out with gentle shaking (70 rpm on a rotary platform shaker) at 25 °C. The membrane was placed in a blocking buffer of phosphate buffered saline (PBS) containing 0.1% Tween-20 and 5% dry milk and incubated for 1 h, followed by washing 3X for 5 min with PBS containing 0.2% Tween-20, pH 7.4 (0.2% PBST). Incubation for 1 h in a 1:5000 dilution of mouse anti-A β primary antibody Ab9 in PBS containing 1% dry milk and 0.1% Tween-20 was followed by incubation for 1 h in a 1:1000 dilution of anti-mouse IgG-HRP secondary antibody in the same buffer. The wash steps detailed above were done after the primary and secondary antibody incubations. The nitrocellulose membrane was then treated with ECL western blotting substrate solution (Pierce) and washed for 1 min with accelerated shaking at 120 rpm. After drying, the membrane was exposed to film for 60 secs in an autoradiography cassette. The film was developed, fixed, washed in water and dried for scan analysis. Duplicate dot blot membranes were probed for GAPDH as a control intracellular protein. The procedure differed only in the primary antibody, using mouse anti-GAPDH antibody (1:1000 dilution). Densitometry was performed on dot blot film images using ImageJ software (NIH). Victoria A. Rogers and Nyasha J. Makoni performed the immuno-dot blot analyses.

2.8 ELISA

Measurements of tumor necrosis factor α (TNF α) were done by enzyme-linked immunosorbent assay (ELISA). 96-well plates (Nunc, Fisher Scientific) were coated with 100 μ L per well of 4 μ g/mL monoclonal anti-mouse TNF α capture antibody (R&D Systems) and incubated overnight at 25 °C. 100 μ L of 4 μ g/mL monoclonal anti-mouse TNF α capture antibody (R&D Systems), washed with PBS containing 0.5% Tween-20

and blocked with PBS containing 1% bovine serum albumin (BSA), 5% sucrose and 0.05% NaN₃ followed by a wash step. Successive treatments with washing in between were done with samples or standards, biotinylated polyclonal anti-mouse TNF α detection antibody (R&D Systems in 20 mM Tris with 150 mM NaCl and 0.1% BSA, streptavidin-horseradish peroxidase (HRP) conjugate, and equal volumes of HRP substrates 3,3',5,5'-tetramethylbenzidine and hydrogen peroxide. The reaction was stopped by the addition of 1% H₂SO₄ solution. The optical density of each sample was analyzed at 450 nm with a reference reading at 630 nm using a SpectraMax 340 absorbance plate reader (Molecular Devices, Union City, CA). The concentration of TNF α in the experimental samples was calculated from a mouse TNF α standard curve of 15-2000 pg/mL. When necessary, samples were diluted to fall within the standard curve.

2.9 Microvesicle generation and isolation from BV-2 and primary microglia

BV-2 microglia seeded into a T-150 flask (Fisher) were cultured to confluence. The growth medium was then removed, and the cells were rinsed once with sterile PBS, 4 mL per flask. The PBS was removed and 4 mL aCSF was added to the control flask while 4 mL aCSF with 1 mM ATP was added to the treatment flask. Both flasks were incubated at 37 °C in 5% CO₂ for 10 minutes. The aCSF was removed and transferred to a labeled 15-mL conical tube to be centrifuged at 2000xg for 20 mins (Crescitelli, et al., 2013). Pellets formed in that spin contain apoptotic bodies or even whole cells, but the microvesicles are soluble and will remain in the supernatant. The supernatant is collected, distributed into four labeled 1.5 mL microcentrifuge tubes, 1 mL each, and 3.8 μ L 2-(6-(7-nitrobenz-2-oxa-1,3-diazol-4-yl)amino)hexanoyl-1-hexadecanoyl-sn-glycero-3-phosphocholine (NBD C6-HPC) was added to each tube (final [NBD C6-HPC] = 10

μM). Tubes were then centrifuged at 12,200 $\times g$ for 40 mins to pellet the microvesicles (Crescitelli, et al., 2013). Supernatants were removed and kept for further analysis. One of the pellets was reconstituted in 200-500 μL aCSF, then the entire volume was transferred to the second tube to reconstitute another pellet. This process was repeated for all four tubes to resuspend and concentrate the microvesicles in one volume.

The amount of primary microglial cells available was limited, and so control experiments in which cells did not receive ATP treatment were not done. Co-cultures of astrocytes and primary microglia were shaken at 250 rpm for 5 hours to dislodge microglia. The cells were then counted, centrifuged, resuspended in primary growth medium and seeded into a T-75 flask. At this point, culture times varied from overnight to one week. If the cells were cultured for more than 3 days, growth medium was changed. The primary microglia were treated with 2'(3')-O-(4-benzoylbenzoyl)adenosine 5'-triphosphate triethylammonium salt (Bz-ATP), which is a better stimulant of the P2X₇ receptors on microglia than ATP. The experimental procedure is the same as for BV-2 microglia, although the amounts of reagents are smaller since the culture flasks used were smaller in size. Microglia were rinsed with 2 mL PBS, then 2 mL growth medium with 100 μM BzATP was added. Cells were incubated 10 min at 37 °C in 5% CO₂. Supernatant was collected and centrifuged at 2000 $\times g$ for 20 min to remove apoptotic bodies. The supernatant, containing microvesicles, is collected, distributed into two labeled 1.5 mL microcentrifuge tubes, 1 mL each, and 3.8 μL 2-(6-(7-nitrobenz-2-oxa-1,3-diazol-4-yl)amino)hexanoyl-1-hexadecanoyl-sn-glycero-3-phosphocholine (NBD C6-HPC) was added to each tube (final [NBD C6-HPC] = 10 μM). Tubes were then centrifuged at 12,200 $\times g$ for 40 mins to pellet the microvesicles (Crescitelli, et al., 2013).

Supernatants were removed and kept for further analysis. One of the pellets was reconstituted in 200-500 μ L aCSF, then the entire volume was transferred to the second tube to reconstitute another pellet. This process was repeated for both tubes to resuspend and concentrate the microvesicles in one volume.

2.10 Fluorescence measurements of microvesicles

2-(6-(7-nitrobenz-2-oxa-1,3-diazol-4-yl)amino)hexanoyl-1-hexadecanoyl-sn-glycero-3-phosphocholine (NBD C6-HPC) (Life Technologies) is a fluorophore conjugate that inserts into phospholipid membranes. The presence of microvesicles in the aCSF solution described above (Methods 2.9) was determined using a Cary Eclipse fluorescence spectrophotometer. 70-100 μ L of the microvesicle-NBD C6-HPC solution was placed in a quartz cuvette. Emission scans of 500-600 nm were obtained with an excitation wavelength of 485 nm. The resulting curves were integrated from 520-580 nm to produce relative fluorescence units (RFU).

2.11 Confocal LSM imaging of microvesicles

Annexin V binding was used to make the microvesicles visible via confocal microscopy. Annexin V binds to exposed phosphatidylserine (PS) on the external leaflet of cell membranes. PS is normally located only on the inner leaflet of the plasma membrane, but is externalized upon either apoptosis or the membrane blebbing that forms microvesicles. A conjugate of Annexin V and the Alexa Fluor 488 fluorophore (Invitrogen) will bind to exposed PS and so it was used to visualize microvesicles. The microvesicle generation from microglia (Section 2.9) was followed by resuspension of the pellets in 500 μ L Annexin V binding buffer (10 mM HEPES, 140 mM NaCl, and 2.5

mM CaCl₂, pH 7.4). Then 25 μ L of -Annexin V conjugate was added, and after gentle mixing the solution sat at room temperature for 15 min. The solution was then centrifuged at 12,200xg for 40 min to pellet the microvesicles, the supernatant was removed, and the pellet was resuspended in 200 μ L binding buffer. 50 μ L of the microvesicle solution was placed on a microscope slide and a coverslip was carefully applied. Images were obtained with a Zeiss LSM 700 confocal microscope, with an excitation wavelength of 488 nm, using ZEN 2009 imaging and analysis software.

2.12 Preparation of microvesicles for resin-embedded TEM

The protocol used is based on the procedure described in Crescitelli, et al. (2013), and one of the authors, Dr. Agnes Kittel, was exceptionally helpful by offering suggestions when I requested details regarding the procedure in the published article. BV-2 supernatant samples were centrifuged at 12,200xg (or 17,000xg) for 40 mins. Supernatant was carefully removed and the pellet was rinsed once with PBS. 100 μ L of fixing buffer (4% paraformaldehyde in 10 mM PO₄ buffer, pH 7.4) was added to the pellet without disturbing it, and then incubation occurred at room temperature for one hour. After carefully removing fixing buffer, 100 μ L 1% OsO₄ in 10 mM PO₄ buffer (10 μ L OsO₄ in 990 μ L buffer) was added to the pellet and allowed to incubate 30 min at room temperature. (SAFETY PRECAUTIONS for OsO₄: gloves, coat, goggles, fume hood). OsO₄ is a secondary fixing agent that incorporates reacts with lipids and provides contrast for TEM imaging. After incubation, OsO₄ was removed and disposed of with proper safety precautions, and the pellet was washed once with 1 mL diH₂O. An ethanol series was used to dehydrate the pellet (200 μ L per tube for each step): 50% ethanol with 2% uranyl acetate 30 min; 70% ethanol for 30 min; 90% ethanol for 30 min; and 100%

ethanol for 30 min. The 100% ethanol step was repeated twice. The pellet was then embedded in 0.2 mL Low Viscosity Embedding Media (Spurr's Kit, Electron Microscopy Sciences) resin (supplied by David Osborn) and stored at RT overnight. Dr. Osborn then heated the resin to harden it, cut microtome slices 80 nm thick, and obtained TEM images.

2.13 BCA Assay

A bicinchoninic acid (BCA) assay was utilized to measure protein concentrations in microvesicle solutions. In the BCA assay, Cu^{2+} is reduced to Cu^{1+} by the presence of four protein residues (cysteine, cystine, tyrosine, and tryptophan) and the peptide backbone. First, the copper is chelated and reduced by the proteins in a basic solution. Then BCA is used to react with the reduced copper, resulting in a purple color. By measuring absorbance at 562 nm and comparing the samples to a standard curve generated with bovine serum albumin, protein concentration within the MVs can be determined. A standard curve was constructed using bovine serum albumin (BSA) diluted in aCSF, typically in the concentration range of 0 $\mu\text{g}/\text{mL}$ to 2000 $\mu\text{g}/\text{mL}$. Microvesicle samples (10 μl) were added to 100 μl of 50:1 mixture of BCA Reagent A to Reagent B (Thermo Fisher Scientific) and mixed thoroughly in individual wells of a 96-well plate. The plate was covered and incubated for 30 min at 37 °C followed by cooling for an additional 15 min. Absorbance was determined for each well at a wavelength of 562 nm using a SpectraMax 340 absorbance plate reader (Molecular Devices, Union City, CA). Mudar Ismail and Natan Zeller conducted the assays and I constructed the graphs.

CHAPTER 3: A β INTERACTIONS WITH MICROGLIAL CELL SURFACES

A β 42 is known to interact with microglial surface receptors, leading to uptake and activation (Section 1.3.1). Previous studies in our lab and had shown that protofibrils can activate a proinflammatory response in THP-1 macrophages and in microglia, while monomers and fibrils do not. Being aware of the difference in response to A β conformers, we wanted to know if it was related to a difference in surface interaction. Therefore, my goal was the visualization of A β 42 on outer cell membrane surfaces using immunofluorescence. I examined the differences in surface binding among monomers, protofibrils and fibrils of A β 42. I also conducted studies investigating the effects of time, temperature, and A β 42 concentration on microglial surface interactions. Further, I investigated the correlation between A β 42 binding to microglia and the subsequent microglial activation. One distinguishing feature of my work was the use of SEC purified monomers and protofibrils, as well as fibrils isolated by centrifugation. This differed from most of the studies in the literature reporting the use of “soluble” A β , which usually includes a mix of monomers and multiple aggregated forms.

3.1 Binding of distinct A β conformers

When BV-2 microglia were incubated with different forms of A β 42 – monomers, protofibrils and fibrils –immunofluorescence revealed that membrane binding was occurring only with protofibrils, as shown in Figure 3.1. BV-2 microglial cells were added at a concentration of 5×10^4 cells/mL in the wells of Mat-Tek dishes (Methods

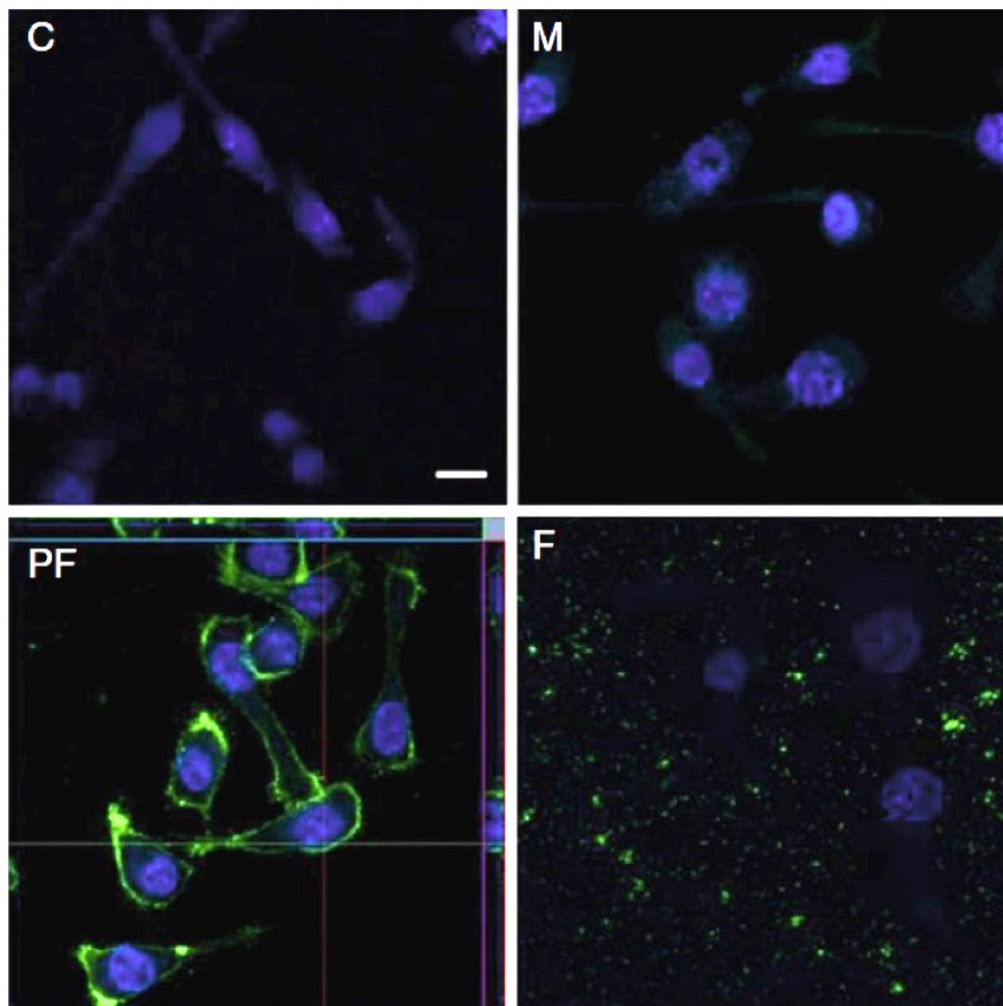


Figure 3.1 Binding of distinct species of A β . BV-2 microglia were incubated for 30 min at 4 °C with 15 μ M A β 42 monomers, protofibrils, or fibrils. Control cells were incubated with assay medium. A β (green) was visualized via immunofluorescence with anti-A β antibody Ab9 (primary) and anti-mouse IgG-NL493 conjugate (secondary). Nuclei were stained with DAPI (blue). C = control; M = monomer-treated cells; PF = protofibril-treated cells; F = fibril-treated cells. Images were acquired at 40X magnification on a Zeiss LSM 700 confocal microscope. Scale bar is 16 μ m and applies to all four images (Paranjape, Terrill, and Gouwens, et al., 2013).

2.4.3). The Mat-Tek dishes have wells with optical glass bottoms to facilitate sample visualization with an inverted microscope. BV-2 cells were incubated on ice with 15 μM $\text{A}\beta$ monomers, protofibrils or fibrils in assay medium, while the control cells were incubated in assay medium alone. After incubation, cells were fixed and underwent the confocal assay described in Methods 2.4.3, with Ab9 primary antibody and NL493-IgG secondary antibody. DAPI chemical staining was used to show cell nuclei. Images were obtained on the Zeiss LSM 700 located in the Microscope Imaging and Spectroscopy Technology (MIST) Laboratory in the UMSL Center for Nanoscience.

The reason for holding the temperature at 4 $^{\circ}\text{C}$ was to slow the activity of the cells and prevent phagocytosis, allowing visualization of cell surface interactions. In Figure 3.1, monomer-treated cells (M) look like the control cells (C), with no visible green fluorescence that would indicate the presence of $\text{A}\beta$ inside or on the cells, while the cell nuclei (blue) are clearly visible. It is not likely that monomers were taken up and degraded by the microglia since the low temperature would have interfered with uptake and metabolic activities. The image of cells incubated with fibrils (F) shows green fluorescence scattered between the cells, rather than outlining cells, which indicates that fibrils adhered to the well but not to cell membranes. Only protofibrils (PF) could be seen on cell surfaces, and they were not readily visible within cells.

One advantage of using the confocal microscope is the ability to acquire a “z-stack” in which a number of images are made at successive depths within the field of view. These slices can then be rendered by Zeiss Efficient Navigation (ZEN) software to create cross-section images. The PF panel of Figure 3.1 shows this type of imaging. The thin rectangular section at the top of the image corresponds to a slice through the z-stack

made at the horizontal green line near the center of the image. Similarly, the rectangular region to the right corresponds to a slice through the z-stack at the location of the red vertical line on the image. In all three views of this field, A β protofibrils are concentrated on the surface membranes of BV-2 cells. Similar results were seen in replicate experiments, leading to the conclusion that BV-2 cell membranes interact with protofibrils of A β , but not monomers or fibrils.

Binding of A β to the cell surface membranes of monocytes was assessed previously by Bamberger, et al. (2003), and they identified a receptor complex consisting of SR-B receptor CD36, $\alpha_6\beta_1$ -integrin, and integrin associated protein CD47 which was responsible for the interaction. In their binding assays, they used A β fibrils adhered to glass slides, applied monocytes to the slides, and counted the number of cells adhering to the pre-treated slides after a 5-minute incubation. This group was able to show cells binding to fibrils, but the quantity of A β used was large enough that the fibrils were visible to the unaided eye on the slides. It's possible that the amount of A β enhanced the binding and accounts for the difference between our results and theirs. Additionally, fibril binding may be different for monocytes and microglia.

We did not address the binding of oligomeric A β to microglia, but this was investigated by Liu, et al. (2012). They were able to show images of oligomers bound to microglial surfaces and colocalized with toll-like receptor 2 (TLR2), but the binding was limited and punctate, while the binding of protofibrils shown here almost completely covers the cells. The difference could be due to the nature of protofibrils and oligomers since they are different types of A β aggregates.

It is likely that the hydrophobic nature of protofibrils allows them to bind to the cell membrane indiscriminately even as they trigger receptor-mediated responses in microglia. Some microglial surface receptors are activated by protofibrils (Section 1.3.1), resulting in the production of proinflammatory cytokines, and we have confirmed the secretion of TNF α by BV-2 microglia as a result of protofibril, but not monomer or fibril, treatment (Paranjape, et al., 2012; Paranjape, Terrill, Gouwens, et al., 2013). Several microglial receptors are known to interact with A β , and they can be categorized into three types: scavenger receptors, G protein-coupled receptors, and toll-like receptors (reviewed in Yu and Ye, 2014). When distinguishing the A β species involved in the interactions, most researchers identify “soluble” or “fibrillar” A β , without further description. However, after centrifugation to remove pre-formed fibrils, we carefully separate monomers from protofibrils using SEC. To my knowledge, there are no published images that differentiate between these three forms of A β in binding to microglia.

3.2 Time-dependence of A β 42 interaction with BV-2 cell surfaces

The investigation of membrane interactions between BV-2 microglia and different conformers of A β 42 revealed that BV-2 cells most readily attract protofibrils, so the next set of experiments was conducted using this A β species. A time-dependent measure of plasma membrane interaction was done by first incubating microglia at 4 °C for 30 min to allow surface binding while preventing internalization, then varying the times of incubation at 37 °C. Representative results from these experiments are shown in Figure 3.2. Immunofluorescence revealed the location of A β mainly on the exterior surfaces of the BV-2 cells at all time points measured. To rule out the possibility that cell membranes

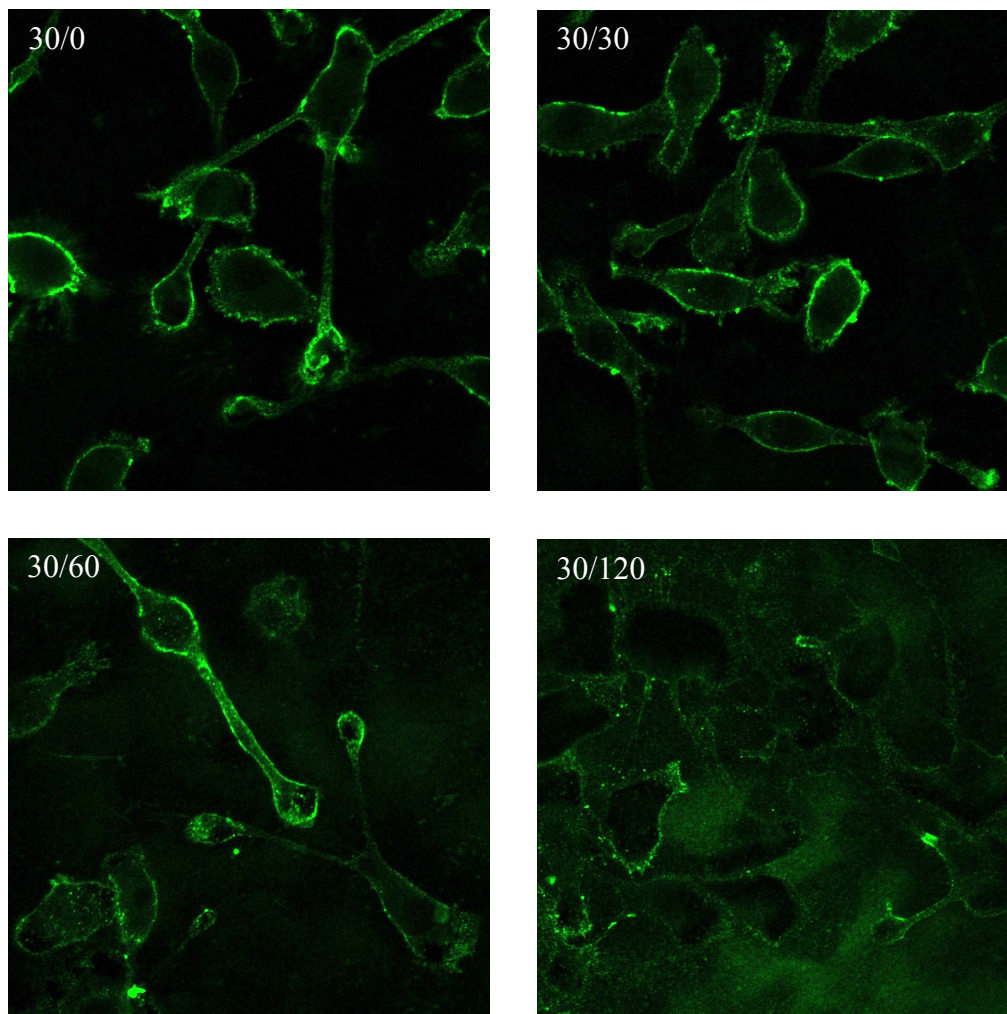


Figure 3.2 Time dependence of surface binding to BV-2 microglia. BV-2 microglia were plated in Mat-Tek dishes at a density of 5×10^4 cells/mL in cell assay medium. On the following day, cells were treated with $15 \mu\text{M}$ A β 42 protofibrils in cell assay medium. All plates were incubated on ice for 30 min, then incubated for 0 (30/0), 30 (30/30), 60 (30/60), or 120 (30/120) min at 37 °C. Immunofluorescence assay was conducted using anti-A β Ab9 primary antibody and anti-mouse IgG-NL493 secondary antibody. Confocal images were acquired at 40X magnification with a Zeiss LSM confocal microscope.

were not permeable to the antibodies used in the immunofluorescence assay, an assay was conducted in which Triton-X 100 was applied to fixed cells before the antibodies were added. Images acquired after the immunofluorescence assay were nearly identical to those obtained without the permeabilizing reagent, confirming that the lack of fluorescence was not due to the inability of antibodies to reach internalized A β (data not shown). From the results in Figure 3.2, it was apparent that BV-2 cells were not internalizing A β 42 even with 2 h of incubation at 37 °C. These results contradict findings from other groups in which BV-2 cells took up various A β 42 species (Jiang, et al., 2008; Koenigsknecht and Landreth, 2004; Kopec and Carroll, 1998; Mandrekar, et al., 2009; Tahara, et al., 2006; Webster, et al., 2001). The A β 42 conformers used in those studies included monomers, oligomers and fibrils, but were not prepared by SEC. The peptides in the “soluble” A β solutions probably contained some oligomers and protofibrils, while the fibrillar solutions most likely contained oligomers and protofibrils as well.

3.3 Effect of temperature on A β 42 binding to BV-2 cell surfaces

Another possibility for the difference in my results and previous studies is that treatment for 30 min at 4 °C was negatively affecting the BV-2 microglia such that uptake was compromised. With that in mind, I also conducted experiments in which the first 30-minute incubation was conducted at room temperature. The results (not shown) are similar to the images in Figure 3.2, with A β 42 collecting on the outer cell surfaces of the microglia. From the results in Figure 3.2, I realized that BV-2 cells are not internalizing A β 42 even with 2 h of incubation at 37 °C. Therefore, while they are not proficient at internalization, BV-2 microglia are a good model for cell surface binding in

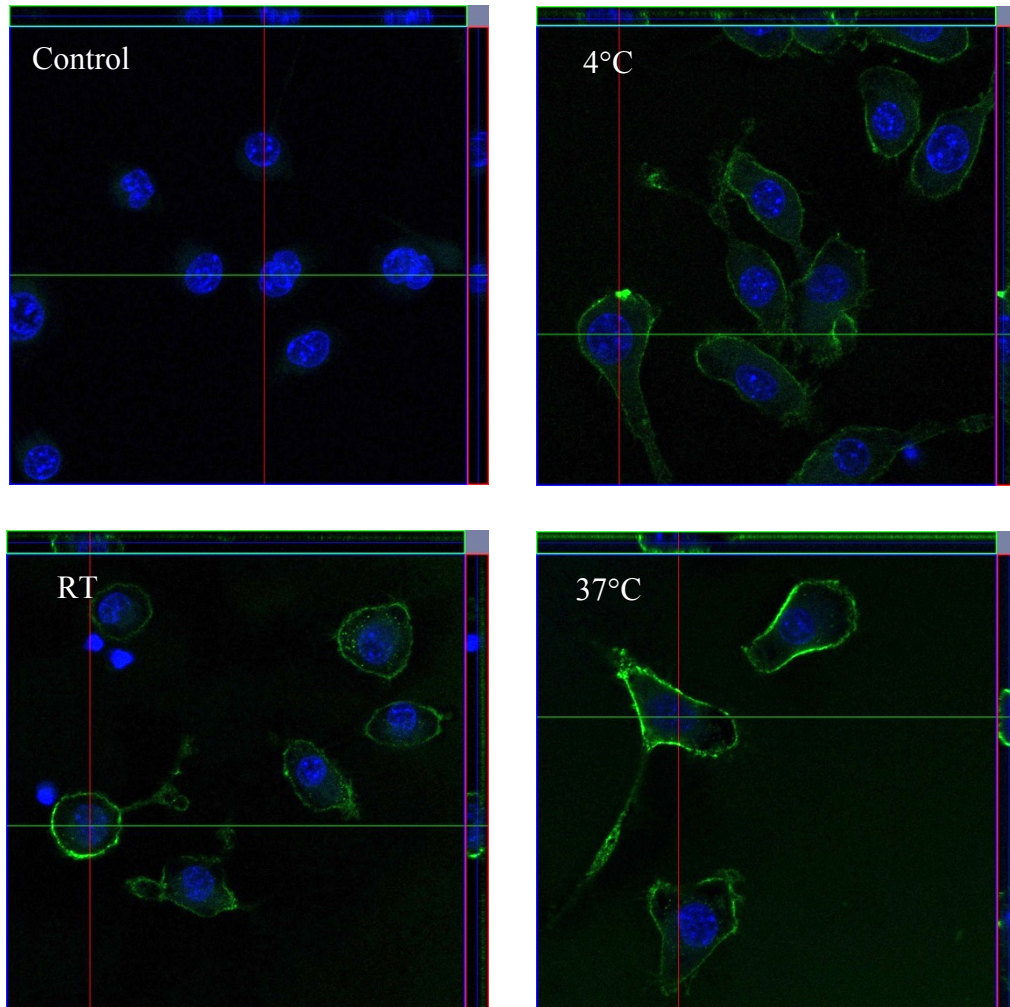


Figure 3.3 Temperature effect on surface binding to BV-2 microglia. Cells were plated in Mat-Tek dishes, 5×10^4 cells/mL. On the following day cells were incubated with $15\mu\text{M}$ $\text{A}\beta_{42}$ protofibrils (green) in assay medium for 30 min at the indicated temperatures. Cells were fixed, underwent an immunofluorescence protocol with Ab9 primary Ab and IgG-NL493 secondary Ab, and were counterstained with DAPI (blue). Images were obtained at 40X magnification on a Zeiss LSM 700 confocal microscope. (37 °C image from Paranjape, Terril, and Gouwens, et al., 2013.)

our culture system. Using immunofluorescence, A β 42 could be visualized on BV-2 microglial surfaces, binding at 4 °C, room temperature (RT), and 37 °C (Figure 3.2). In Mat-Tek dishes, BV-2 cells were incubated for 30 minutes with 15 μ M A β 42 protofibrils, while control cells were untreated but incubated at room temperature in assay medium with aCSF for the same amount of time. After cell fixing, the immunofluorescence assay (Methods 2.6) was conducted and then followed by counterstaining with DAPI, and images were acquired on a Zeiss LSM 700 confocal microscope. Figure 3.3 shows that binding occurs on the outer surface of the cell membrane at each temperature measured, but protofibrils were not taken up by the BV-2 microglia within the 30 minutes of incubation. If A β protofibrils were internalized, green fluorescence would be visible throughout the cells, rather than concentrated on the membrane boundaries. The z-stack views confirm that, for all three temperatures, protofibrils accumulate at BV-2 cell surfaces in our system. While the groups cited above (and shown in Table 3.1) demonstrated uptake at various time points, the species of A β 42 they used varied in size from monomers to fibrils, and none were SEC-purified protofibrils.

3.4 Effect of A β 42 concentration on binding to BV-2 cell surfaces

We reported concentration-dependent production of TNF α by microglia in 2012 (Paranjape, et al., 2012). Both primary and BV-2 microglia showed increased TNF α production upon incubation with increasing concentrations of A β . While the A β treatments reported in 2012 were carried out in F-12 medium (131 mM NaCl, 3 mM KCl, 1 mM NaH₂PO₄, 14 mM NaHCO₃, 0.003 mM MgCl₂, 0.3 mM CaCl₂, 10 mM glucose), the work reported in 2013 utilized artificial cerebrospinal fluid, (aCSF; 130 mM NaCl, 3

Table 3.1 A β internalization in BV-2 microglia and other cell lines

Reference	A β form	A β label	[A β], μ M	Cell type	Incubation time	Uptake (method)
Kopec and Carroll, 1998	“aged” (probably fibrillar)	unlabeled (fluorescent microspheres) or free A β	5	BV-2	1 h	yes (flow cytometry)
Webster, et al., 2001	fibrils	fluorescein	10	BV-2	30 min	yes (FACS, fluorescence microscopy)
Koenigschnect and Landreth, 2004	fibrils (oligomers possibly present)	Cy3	10	BV-2	30 min	yes (confocal microscopy)
Tahara, et al., 2006	polydisperse mixture	none	1	BV-2	24 h	yes (western blot, ELISA, immunofluorescence)
Halle, et al., 2008	fibrils	FITC	10	immortalized mouse line	4 h	yes (confocal microscopy)
	fibrils	HLF488	10	immortalized mouse line	4 h	yes (confocal microscopy)
	fibrils	FITC	10	immortalized mouse line	1h	yes (confocal microscopy)
	fibrils	FITC	10	immortalized mouse line	4 h	yes (confocal microscopy)
Jiang, et al., 2008	monomers and small oligomers	AF488	0.5	BV-2	0-3 h	yes (flow cytometry)
	monomers and small oligomers	AF488	up to 1	BV-2	3 h	yes (ELISA of lysates)
	monomers and small oligomers	Cy3	0.5	BV-2	15 min	yes (confocal microscopy)

continued on next page

Table 3.1 A β internalization in BV-2 microglia and other cell lines, continued

Reference	A β form	A β label	[A β], μ M	Cell type	Incubation time	Uptake (method)
Mandrek, et al., 2009	soluble or fibrillar	Cy3	0.5	BV-2	3 h	yes (confocal microscopy and flow cytometry)
	monomers	AF488	0.5	BV-2	0-180 min	yes (flow cytometry and lysate ELISA)
	monomers	Cy3	0.5	BV-2	3 h	yes (confocal microscopy)
	monomers	Cy3	0.5	BV-2	0-19 min	yes (confocal microscopy, live imaging)
Reed-Geaghan, et al., 2009	fibrils (with oligomers)	none	2.5	BV-2	3-5 min	yes (fluorescence microscopy)
Fu, H, et al., 2012	fibril	AF488	0.5	N9 cell line	1 h	yes (confocal microscopy)
	fibril	AF488	0.5	N9 cell line	0, 15, 30, 60 min	yes (flow cytometry)
	fibril	AF488	0.05, 0.25, 0.5, 1.0, and 2.5	N9	2 h or 5 d	yes (flow cytometry)
	fibril	AF488	0.5	N9	1 h	yes (confocal microscopy)
Baik, et al., 2016	fibril	FITC	1	BV-2	24 h	yes (confocal microscopy)
Paranjape, Terrill, and Gouwens, et al., 2013*	protofibrils	none	15	BV-2	30 min	no (confocal microscopy)
Gouwens, et al., 2016*	protofibrils	AF488	5	BV-2	30 min	no (confocal microscopy)

Abbreviations:

AF488: Alexa Fluor 488

FITC: fluorescein isothiocyanate

HLF488: HiLyte Fluor 488

*results presented herein

mM KCl, 1 mM NaH₂PO₄, 15 mM NaHCO₃). The same concentration-dependent effect on TNF α production was seen with BV-2 cells in aCSF, as shown in Figure 3.4 (Paranjape, Terrill, and Gouwens, et al., 2013). BV-2 cells were treated with A β 42 at various concentrations. ELISAs were conducted on cell medium samples to measure TNF α , a proinflammatory cytokine produced by microglia when activated. Panel A of Figure 3.4 shows a concentration-dependent increase in TNF α production for BV-2 microglia. The location of A β 42 on or in BV-2 microglia was assessed by immunofluorescence and confocal microscopy. Panels B and C of Figure 3.4 show very little fluorescence on the surfaces of BV-2 cells treated with 1 μ M A β 42, while Panel D shows markedly more intense fluorescence on the BV-2 cell membranes. Taken together, these images reveal a concentration-dependent pattern of A β binding to BV-2 cell membranes. These data are in agreement with our research (Paranjape, et al., 2012; Terrill-Usery, et al., 2014) and the findings of other groups (Combs, et al., 2001; Meda, et al., 1995; Stewart, et al., 2010; Yan, et al., 1996) that microglia produce TNF α upon stimulation with A β .

3.5 Correlation of A β 42 binding and BV-2 activation

The surface interaction of A β 42 with BV-2 microglia leads to activation and the production of cytokines. Not all forms of A β 42 can elicit an inflammatory response as measured by cytokines, though. Our lab demonstrated this in 2012 (Paranjape, et al., 2012) and 2013 (Paranjape, Terrill, Gouwens, et al., 2013) via ELISA, but there were no images made at the time. In order to correlate binding with activation, I conducted an experiment that measured TNF α production as BV-2 cells encountered two different

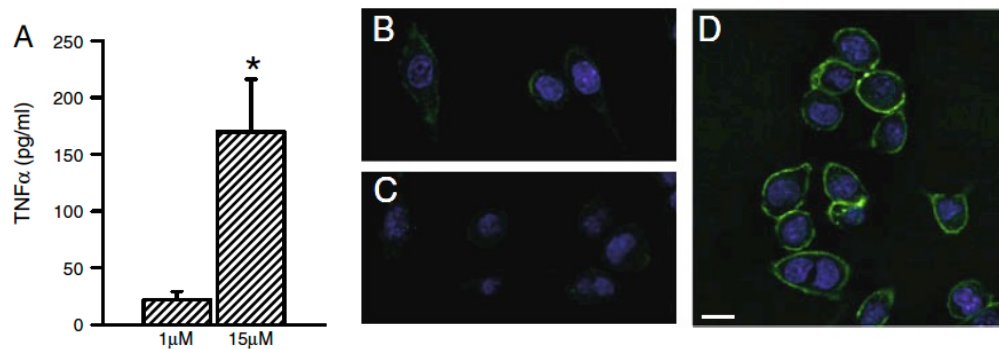


Figure 3.4 Aβ42 concentration dependence of cytokine secretion by BV-2 microglia. BV-2 cells were treated with 1 and 15 μM Aβ42 for 30 min at 37 °C. (A) TNFα ELISA; (B & C) Confocal micrographs of cells incubated with 1 μM Aβ42; (D) Confocal micrograph of cells incubated with 15 μM Aβ42. Green: Aβ42. Blue: nuclei (Paranjape, Terrill, Gouwens, et al. (2013))

A β 42 conformers, and obtained confocal LSM images of BV-2 interactions with the different forms of A β 42 in a parallel experiment. Experiments were carried out on the same day, with microglia seeded from one batch of cells and A β from the same labeled preparation. The only difference was incubation time, because longer time periods were needed for the TNF α part of the experiments in order to generate measurable amounts of the cytokine. The data in Figure 3.5 shows the distinct effects that monomers and protofibrils have on BV-2 microglia. Panel A reveals that BV-2 microglia secrete more TNF α in the presence of protofibrils than monomers, especially at 6 h. The images in Panel B show that the difference in activation is correlated with distinct interaction differences, i.e., BV-2 cells are more prone to interact with protofibrils than monomers. The report by our lab in 2013 was the first to distinguish between monomers, protofibrils and fibrils in the activation of primary murine microglia. To my knowledge, no one has previously shown both images and ELISA data to distinguish between activation due to monomers and protofibrils in BV-2 microglia.

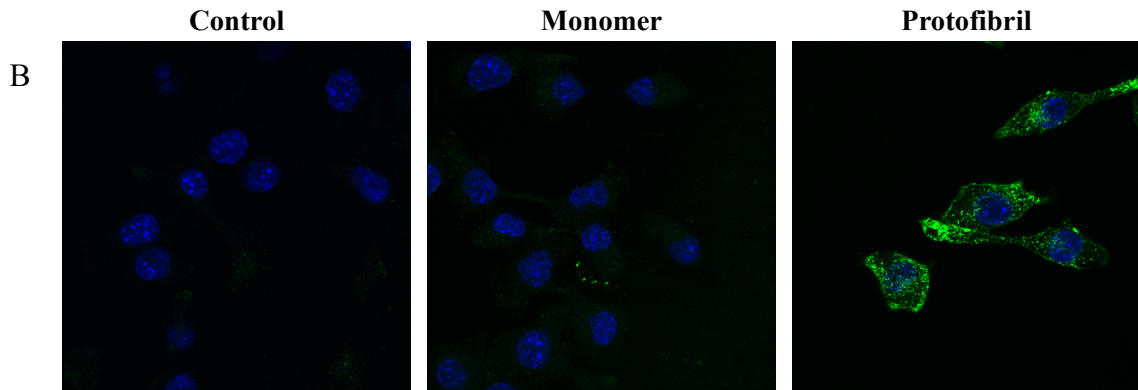
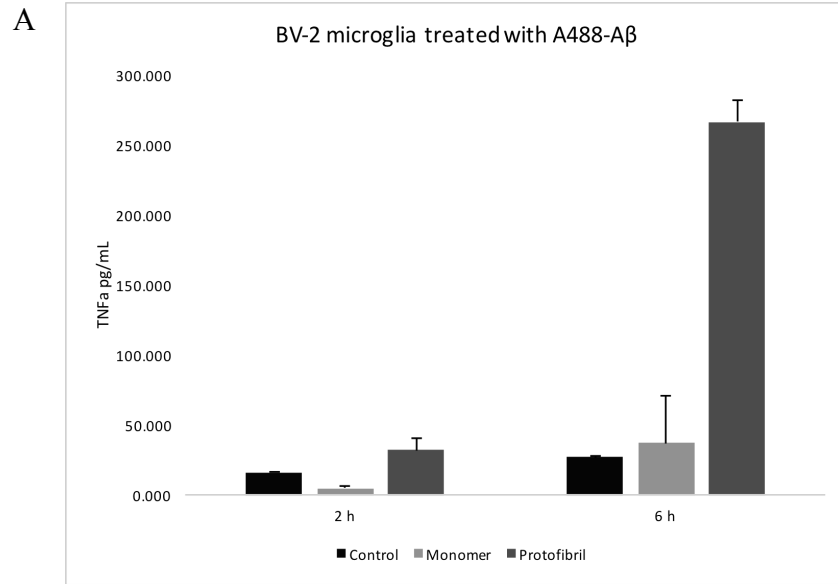


Figure 3.5 Correlation of A β 42 binding and BV-2 cell activation. BV-2 microglia were treated with AF488-A β to correlate conformer binding with activation. (A) At 2 and 6 h time points, TNF α production is greater for protofibril-treated cells than monomer-treated cells. (B) Images show that BV-2 cells associate with protofibrils but not monomers. Green = AF488-A β fluorescence; blue = nuclei (DAPI) fluorescence.

CHAPTER 4: SELECTIVE INTERNALIZATION OF A β BY MICROGLIA

Having demonstrated differential binding of A β 42 species to microglia, and the resulting activation of the cells, I sought to determine the fate of A β 42 once it was internalized by microglia. The Alexa Fluor® 488-TFP (AF488-TFP) fluorophore was used to label A β 42 in solutions containing a mix of monomers and protofibrils. The mixture was labeled before SEC purification based on a report by Jungbauer and coworkers (2009) showing that labeling peptides after the formation of oligomers and fibrils, rather than before, resulted in AF488-A β that was most similar to unlabeled A β . After conjugation of the fluorophore to A β , AF488-monomers and -protofibrils were separated by SEC. The labeling process and characterization of labeled A β 42 is described in the Methods chapter, Section 2.2. It proved advantageous to use fluorophore-labeled A β because direct fluorescence provided higher quality images than immunodetection, required less time to prepare cells for imaging than immunofluorescence assays, and allowed live cell imaging. My objectives were to compare monomer and protofibril uptake, assess the time- and concentration-dependence of uptake, determine if uptake has a limit using mixtures of labeled and unlabeled A β , and confirm colocalization of A β with cellular lysosomes.

4.1 Comparison of unlabeled and fluorescently-labeled A β 42 monomer, protofibril, and fibril interactions with BV-2 and primary microglia

Once the AF488-A β had been characterized (Methods 2.2), I set out to assess and compare the interactions of both BV-2 and primary murine microglia with the labeled peptide. I wanted to be sure the binding of AF488-A β to BV-2 microglia was similar to cell surface binding observed with unlabeled A β . Further, I wanted to be sure that the interactions of primary microglia with AF488-A β were similar to unlabeled A β . In both cases, I found that the fluorophore label was not affecting A β -cell interactions. Unlabeled A β 42 was detected via immunofluorescence, and three comparisons are shown in Figure 4.1. The top two panels compare primary microglia treated with 5 μ M unlabeled (left) and labeled (right) monomers for 30 min, with no significant differences between the images. There is a negligible amount of green fluorescence shown in the images, which indicates that monomers have not been internalized by the primary microglia. Previous data shows that BV-2 microglia do not bind or internalize A β 42 monomers (Paranjape, Terrill, and Gouwens, et al., 2013), and these images confirm that finding for AF488-A β 42 monomers. Primary microglia incubated with 5 μ M protofibrils for 30 min are shown in the middle two panels, unlabeled on the left and labeled on the right. The green fluorescence in the images indicates the location of A β 42. Again, there is virtually no difference in how primary microglia interact with protofibrils either with or without a label. The bottom two panels show a comparison of BV-2 microglial surface interactions

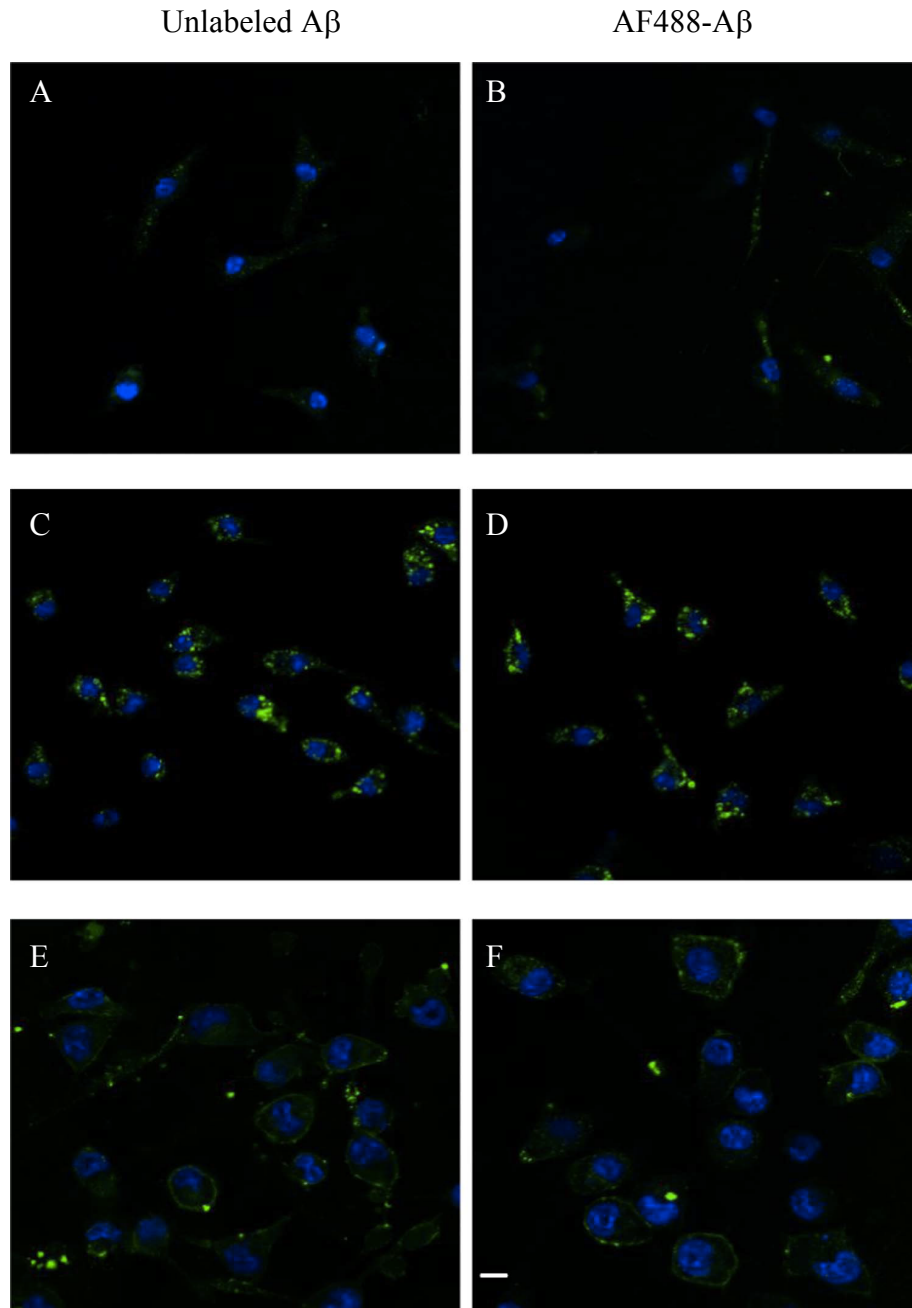


Figure 4.1 The AF488 fluorophore does not affect microglial interactions with A β . A & B: primary microglia with unlabeled and labeled monomers, respectively (10 μ M, 10 min, 37 °C); C & D: primary microglia with unlabeled and labeled protofibrils, respectively (5 μ M, 10 min, 37 °C); E & F: BV-2 microglia with unlabeled and labeled protofibrils, respectively (5 μ M, 30 min, RT). Green – A β ; blue – cell nuclei

with both unlabeled (left) and labeled (right) protofibrils upon incubation for 30 min with 5 μ M A β . Most of the A β 42 (green fluorescence) is located on the surfaces of BV-2 cells. As with the previous comparisons, the two images are similar, indicating that the label does not affect BV-2 microglial interaction with AF488-A β .

Additionally, the proinflammatory responses measured by TNF α production show that primary microglia are activated and produce TNF α when treated with AF488-A β protofibrils, but not monomers. Figure 4.2, panel C, shows ELISA results for primary microglia treated with monomers and protofibrils of labeled A β . Primary microglia were activated and produced high quantities of TNF α only when incubated with AF488-A β protofibrils. These data agree with our previous results from BV-2 microglia treatments and primary cell experiments with unlabeled A β (Paranjape, et al., 2012; Paranjape, Terrill, Gouwens, et al., 2013).

4.2 Time dependent internalization of AF488-A β by primary microglia

We had often conducted cell treatments for 30 min or more, yet macropinocytosis of A β 42 can occur in just a few minutes in microglia (Tables 1.1 and 1.2). To determine how quickly uptake can occur in our primary microglia, AF488-A β treatments were performed as described in Methods 2.4.1. Representative of multiple fields from at least two experiments, Figure 4.2, Panel A, provides visualization of uptake at four time-points (green fluorescence is AF488-A β 42, blue is cell nuclei). Monomer internalization is shown in the top row, and protofibril uptake in the bottom row of Panel A. Compared to monomers, which show a low level of internalization at all four measured time points,

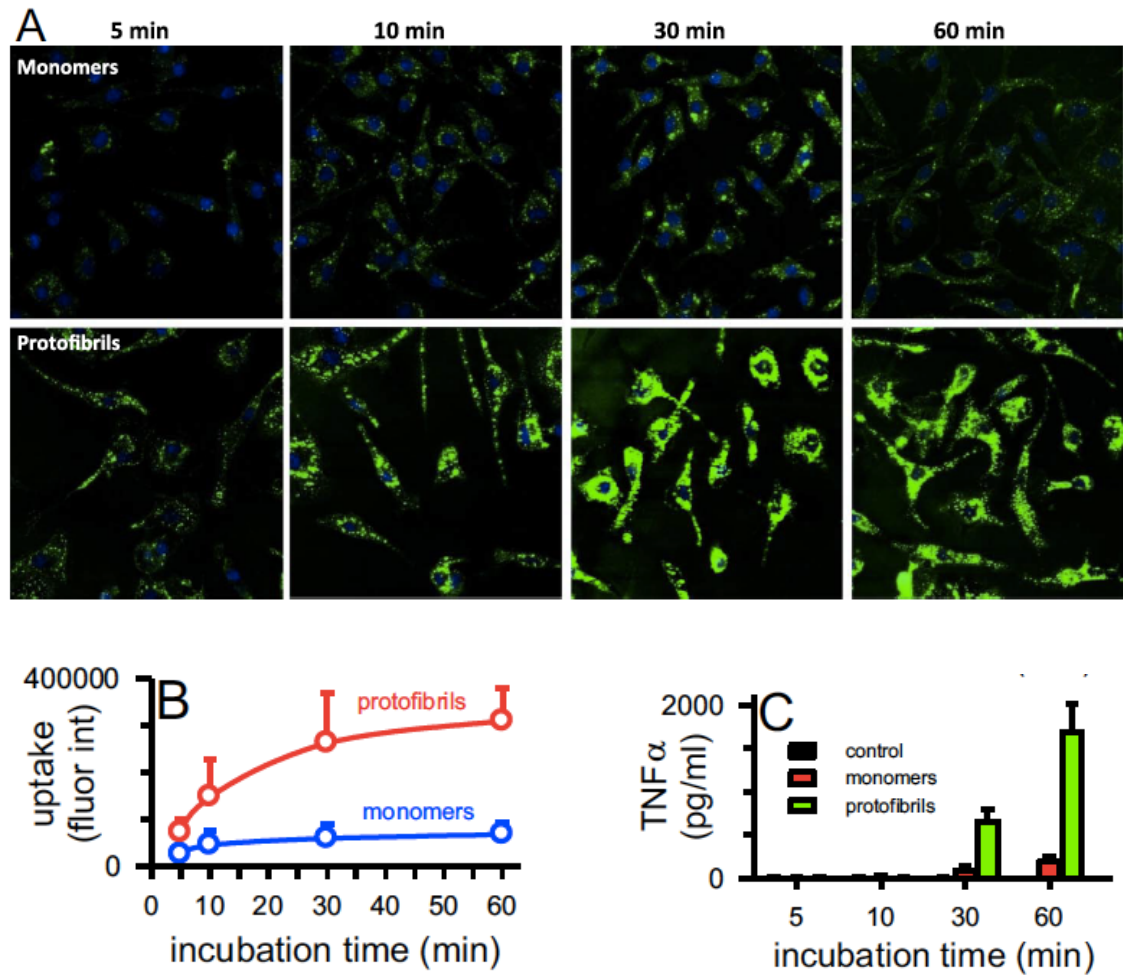


Figure 4.2 Internalization of AF488-A β by primary microglia. Uptake is time dependent for protofibrils but not monomers. (A) Images of time-dependent uptake of monomers (top) and protofibrils (bottom). (B) Quantitation of image fluorescence intensity. (C) TNF α ELISA for the same experiments.

protofibril internalization is much more robust. Recalling that the stoichiometry of labeling was about four times higher for monomers than protofibrils, shown in Table 2.1, it is striking that the fluorescence is so much more intense for protofibrils than monomers. This is an indication of the speed and extent of A β 42 protofibril internalization by primary microglia. While the visual evidence is compelling, quantitation of the images provides more objective evidence of the difference between monomer and protofibril uptake. By measuring fluorescence intensity per cell in multiple fields from two different experiments, the graph shown in Figure 4.2, Panel B, was produced. The data clearly indicate that protofibrils are quickly internalized by primary microglia, and the uptake of AF488-A β 42 protofibrils increases with time. Also, monomers are taken up at much lower amounts than protofibrils, even at longer incubation times.

Monomer uptake (Jiang, et al., 2008; Taneo, et al., 2015) and soluble A β uptake (Chu, et al., 1998; Chung, 1999; Hjorth, et al., 2010; Jiang, et al., 2008; Liu, et al., 2010; Mandrekar, et al., 2009) have been demonstrated by other research groups, and all except Chu (1999) used labeled A β . However important differences are present between their studies and ours. With regard to monomers, Jiang reported a mix of monomers and soluble A β , and the Taneo experiments were carried out for 24 h, which is enough time for monomers to aggregate. In either case, the uptake was most likely of something larger than monomers. As for the groups reporting internalization of “soluble” A β , the uptake was likely not of monomers since soluble species include oligomers and protofibrils. Another difference involves treatment time points. These experiments involved longer time points, hours to even days, allowing plenty of time for oligomers and protofibrils to

form and be taken up. Their data is better compared to our results with SEC-purified protofibrils in Figure 4.2.

As part of the same internalization experiments, microglial activation was measured at these time points by looking at cytokine production. The ELISA results shown in Figure 4.2, Panel C, reveal that the amount of TNF α produced correlated with AF488-A β 42 protofibril internalization by microglia. At 5 and 10 min of treatment, measurable TNF α is not present for AF488-A β 42 monomers or protofibrils, but protofibrils produced a greater amount of TNF α than monomers at 30 min and 6 h.

In another set of experiments, time-dependent uptake of protofibrils and monomers was quantitated with immuno-dot blot assays of primary microglia cell lysates using the procedure described in Methods 2.7. Extensive washing of the cells after incubation with AF488-A β 42, including an acid wash step to remove monomers or protofibrils bound to the cell surface, allowed quantitation of the intracellular AF488-A β 42 at each time point. While there is virtually no uptake of AF488-A β 42 monomers at any of the time points (Figure 4.3 A & B), the quantity of AF488-A β 42 protofibrils taken up by primary microglia increases with time. These cell treatments were done in a 96-well cell culture plate, and, before lysing the microglia, fluorescence measurements were made in a plate reader to determine the relative amounts AF488-A β 42 internalized at each time point (Figure 2.8 and Section 2.5 of Methods). The intracellular fluorescence is reported as a percentage of the fluorescence in the assay medium removed from the cells after incubation so that results from different experiments could be combined. The results, shown in Figure 4.3 Panel C, confirm the findings that protofibrils are more likely

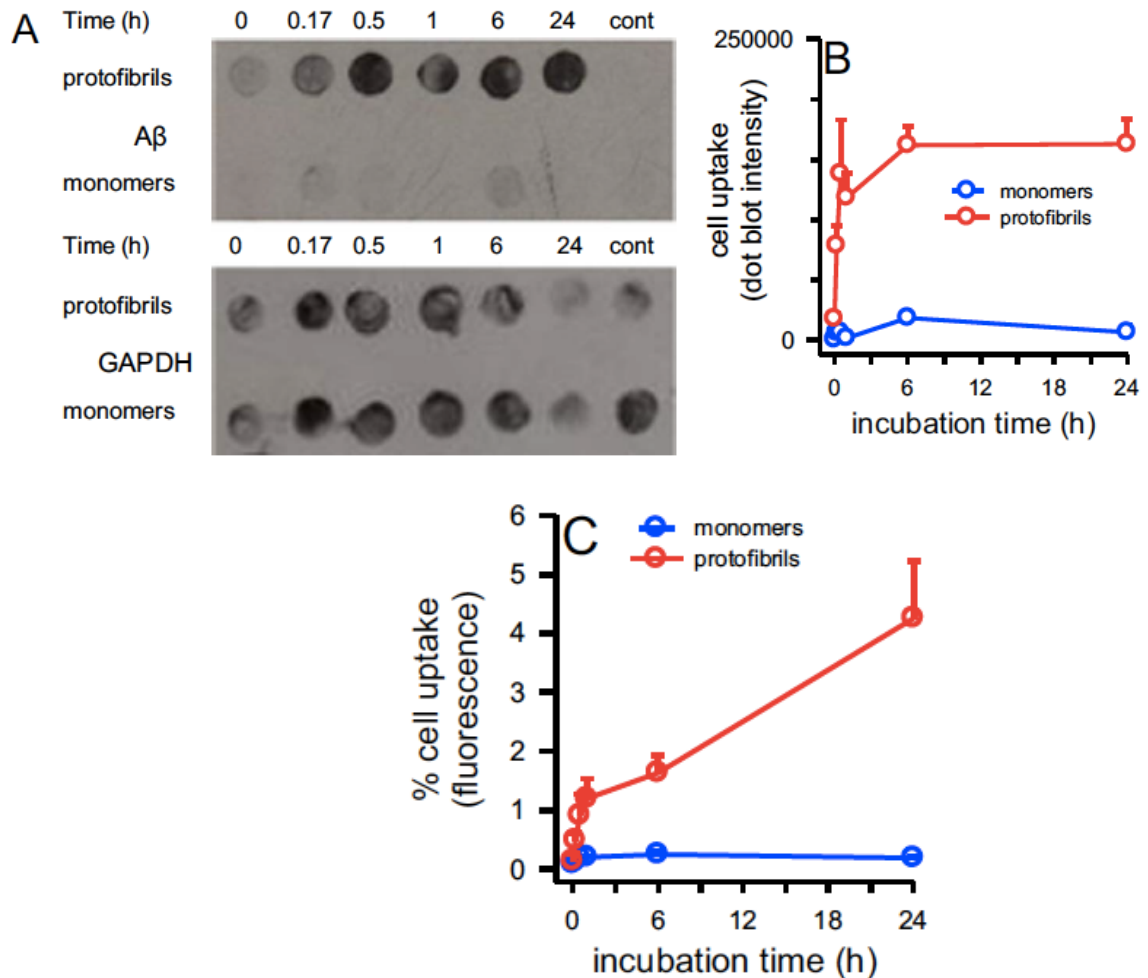


Figure 4.3 Primary microglia take up AF488-A β protofibrils, but not AF488-A β monomers, in a time-dependent manner. (A) Immuno-dot blot of cell lysates showing A β internalization; representative of three different experiments. (B) Densitometry for immuno-dot blot in (A) using ImageJ (pixel intensity) for three experiments. (C) Quantitation of plate reader fluorescence, normalized to fluorescence in cell medium at 0 h for three experiments.

than monomers to be taken up by primary microglia. Primary murine microglia show a clear preference for internalizing protofibrils over monomers. Comparison of SEC-purified monomers and protofibrils is a novel contribution to the literature regarding microglial uptake of A β .

Interestingly, the protofibrils do not appear to be degraded even when microglia are incubated for 24 h with them. The resistance of A β to breakdown confirms findings in the literature. In the late 1990s, Maxfield's group showed that only a portion of what they characterized as "microaggregates" (probably oligomers and/or protofibrils) was degraded by primary murine microglia, most of the A β remained in the cells (Chung, 1999; Paresce, et al., 1997). Cole and colleagues (1999) reported a 50-60% decrease in fibrillar A β in rat microglia after a 24-h treatment. Conducting pulse-chase experiments in which the treatment medium containing excess A β was removed, several groups noted that A β was retained in primary microglia (Jiang, et al., 2016; Majumdar, et al., 2008; Majumdar, et al., 2007; Shibuya, et al., 2014). Yang, et al., (2011) were able to show complete degradation of oligomeric A β after a 30-minute treatment followed by a 30-minute chase, but that is likely due to the fact that they were using oligomers, which have a different structure than protofibrils. There is a constant supply of A β being produced in the brain, so, while a pulse-chase experiment has some value for assessing degradation rates, it does not accurately reflect physiological conditions.

4.3 Effect of AF488-A β concentration on primary microglial uptake

This goal for this set of experiments was to determine the effect of AF488-A β 42 concentration on internalization by microglia, comparing monomers to protofibrils.

Primary microglia were incubated for 10 min (37 °C, 5% CO₂) with varying concentrations of AF488-A β monomers or protofibrils. As seen in the Figure 4.4 confocal images (Panel A) AF488-A β monomer uptake is extremely low at all four concentrations tested, and only slightly visible at 5 and 10 μ M concentrations. On the other hand, AF488-A β protofibrils are visible in the cells even at 0.5 μ M, and fluorescence appears to increase in intensity as the concentration increases. The quantitation results in Panel B of Figure 4.4 confirm these observations. The integrated fluorescence intensity acquired in the AF488 channel for each image was divided by the number of nuclei in the DAPI channel for each image. Results from three different experiments were combined. At all four concentrations examined, protofibrils are internalized at a greater extent than monomers, and internalization of AF488-A β protofibrils increases as concentration increases. Once again, it is important to note that monomers had a higher stoichiometry of labeling, yet the intracellular fluorescence intensity is markedly stronger for protofibrils. Concentration-dependence of A β uptake has been demonstrated in primary murine microglia and in the BV-2 and N9 microglial cell lines (Fu, et al., 2012; Liu, et al., 2005; Mandrekar, et al., 2009; Yang, et al., 2011), but as Table 4.1 summarizes, none of these groups compared monomers and protofibrils purified by SEC as we did. The protofibril uptake findings reported here are novel to the scientific literature.

4.4 Non-saturable A β uptake in primary microglia

If there is a limit to the protofibril quantity that can be ingested by primary microglia, it might be possible to use a mixture of both labeled and unlabeled A β 42 to

Table 4.1 Primary microglia A β uptake experiments

Reference	A β conformation	A β label	[A β], μ M	Cell type	Incubation time	Uptake (method)
Ard, et al., 1996	“not fibrillar”	³⁵ S-Met	0.22, 1.1, 4.4, or 25	rat primary	24 or 48 h	yes (immunofluorescence; lysate immunoblot)
Paresce, et al., 1996	“microaggregates” <400 nm length	Cy3	0.22	mouse primary	10 min	yes (fluorescence microscopy, not confocal)
		Cy3	up to 11	mouse primary	15 min	yes (fluorescence microscopy, not confocal)
		unlabeled	4	mouse primary	30 min	yes (fluorescence microscopy, not confocal)
Paresce et al., 1997	“microaggregates”	Cy3	1	mouse primary	15 min, followed by 3 h to 6 d chase times	yes (confocal LSM)
		Cy3	2	mouse primary	1 h, followed by 1 h or 2 d chase	yes (confocal LSM)
		¹²⁵ I	0.2	mouse primary	1 h, followed by up to 75 min chase	yes (cell associated radioactivity)
		unlabeled	2	mouse primary	1 h, followed by 6 and 24 h chase	yes (immunofluorescence)
Chung, et al., 1999	fibrils	¹²⁵ I	0.2	mouse primary	1 h, various chase times	yes (cell associated radioactivity)
	fibrils	Cy3	0.2	mouse primary	1 h, various chase times	yes (confocal image quantitation)
	soluble	¹²⁵ I	1	mouse primary	2 h, various chase times	yes (cell associated radioactivity)
	soluble	Cy3 and unlabeled	1 + up to 100 unlabeled	mouse primary	15 min	yes (confocal image quantitation)
	soluble	Cy3	0.5	mouse primary	1.5 h, 1 h chase	yes (confocal microscopy)

continued on next page

Table 4.1 Primary microglia A β uptake experiments, *continued*

Reference	A β conformation	A β label	[A β], μ M	Cell type	Incubation time	Uptake (method)
Cole, et al., 1999	fibrils	none	0.2	rat primary	24 h	yes (immunofluorescence)
Webster, et al., 2000	“minimally aggregated”	¹⁴ C	0-50	rat primary	2 h and 6 h	yes (cell-associated radioactivity)
	“minimally aggregated”	fluorescein	5, 50	rat primary	2 h and 6 h	yes (immunofluorescence)
Liu Y, et al., 2005	fibrils/protofibrils	biotin	0.055, 0.55, 5.5	mouse primary	1 h	yes, (quantitation of confocal microscopy, AF488)
	fibrils/protofibrils	biotin	0.55	mouse primary	5, 30, 60, 120 min	yes, (quantitation of confocal microscopy, AF488)
	fibrils/protofibrils	biotin	0.55	mouse primary	5, 30 min; 1, 2 h	yes, (confocal microscopy, Cy3-streptavidin)
Townsend, et al., 2005	fibrils	FITC	0.3	mouse primary	15, 30, 60 min	yes (fluorometry of lysates)
	fibrils	none	0.3	mouse primary	1 h	yes (western blot of lysates)
	fibrils	Cy3	0.05	mouse primary	1 h	yes (confocal microscopy)
Floden and Combs, 2006	fibrils	FITC	0.5	primary mouse, neonatal and aged	6 h	yes (fluorometry)
Tahara, et al., 2006	oligomers	none	0.25	mouse primary	24 h	yes (immunofluorescence microscopy)
Majumdar, et al., 2007	fibrils	Cy3	1	mouse primary	60 min, then 72 h chase	yes (fluorescence image quantitation)
Mandrekar, et al., 2009	soluble (monomers with some small oligomers) or fibrillar	Cy3	0.5	mouse primary	3 h	yes (confocal microscopy and flow cytometry)

continued on next page

Table 4.1 Primary microglia A β uptake experiments, *continued*

Reference	A β conformation	A β label	[A β], μ M	Cell type	Incubation time	Uptake (method)
Liu Z, et al., 2010	soluble	HLF555	2	primary murine	2 h	yes (confocal microscopy)
Majumdar, et al., 2011	fibril	Cy3	0.25	primary murine	1 h, chase times vary	yes (confocal microscopy)
Yang, et al., 2011	oligomer	none	1	primary murine	5 and 30 min; 1 and 4 h	yes (confocal microscopy)
	oligomer	none	0.5, 1.0, 2.5, 5.0	primary murine	30 min	yes (fluorescence intensity quantitation)
	oligomer	FAM	1	primary murine	15 min	yes (confocal microscopy)
Fu, H, et al., 2012	fibril	AF488	0.5	primary murine	1 h	yes (confocal microscopy)
	fibril	AF488	0.5	primary murine	0, 15, 30, 60 min	yes (flow cytometry)
	fibril	AF488	0.5	primary murine	1 h	yes (confocal microscopy)
Lee, CY, et al., 2012	soluble	AF555	0.4	primary murine	18 h	yes (flow cytometry)
	soluble	AF555	0.2	primary murine	7 min, 10 min chase	yes (confocal microscopy)
Taneo, et al., 2015	monomer	none	10	primary murine	24 h	yes (confocal microscopy)
	oligomer	none	10	primary murine	24 h	yes (confocal microscopy)
	fibril	none	10	primary murine	24 h	yes (confocal microscopy)
Baik, et al., 2016	fibril (PF)	FITC	1	primary murine	24 h	yes (confocal microscopy)
Gouwens, et al., 2016*	monomers	AF488	0.5 – 10	primary murine	0-24 h	no (confocal microscopy; immunodot-blot; plate reader)
	protofibrils	AF488	AF488	primary murine	0-24 h	yes (confocal microscopy; immunodot-blot; plate reader)

Abbreviations: AF488: Alexa Fluor 488; AF555: Alexa Fluor 555; Cy3: Cyanine 3; FAM: carboxyfluorescein; FITC: fluorescein isothiocyanate; HLF488: HiLyte Fluor 488

*work presented herein

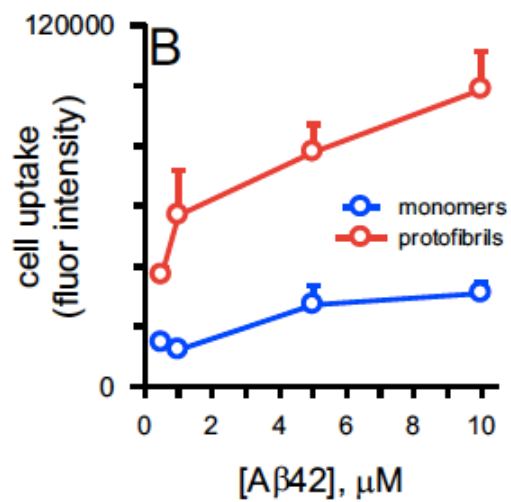
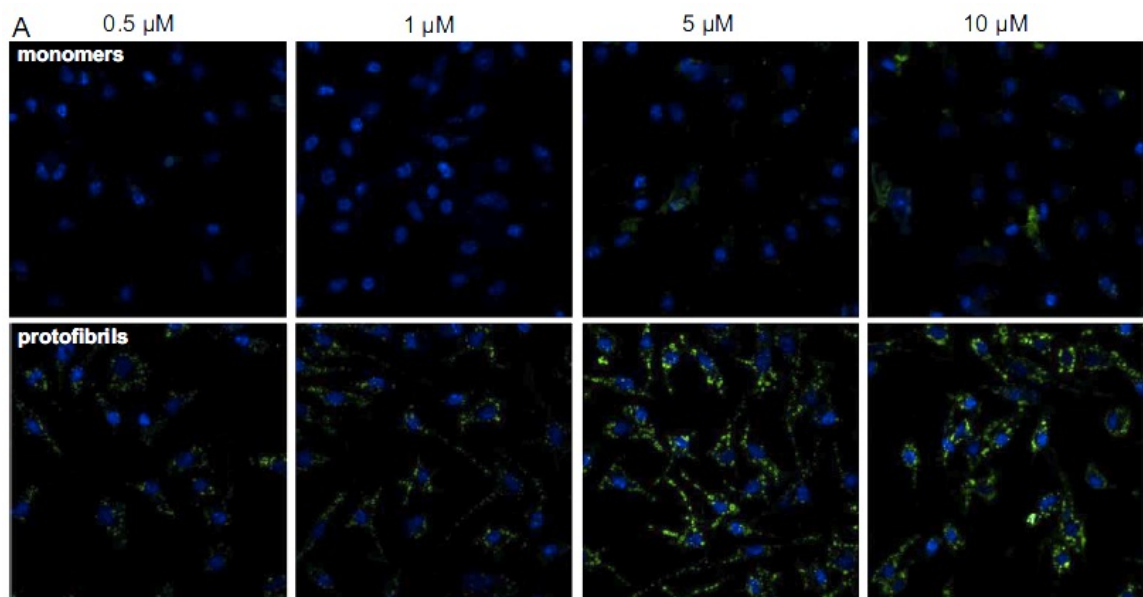


Figure 4.4 Concentration-dependent internalization of AF488-A β by primary microglia. (A) Images of monomer-treated (top) and protofibril-treated (bottom) cells. Concentrations indicated above columns. Green – AF488-A β , blue – nuclei. (B) Quantitation of fluorescence intensity for AF488-A β . Fluorescence intensity for the fields imaged in panel A and two other experiments. ImageJ was used to measure integrated intensity, which was then divided by the number of nuclei in the field.

visualize such a limit. Uptake that is receptor-mediated or regulated by a transport mechanism could prevent the internalization of ever-greater amounts of A β 42. By maintaining a constant AF488-A β 42 concentration while increasing the amount of unlabeled A β 42, a decrease in fluorescence would indicate that cells were saturated with A β and could not internalize any more. If the fluorescence intensity is not diminished by increasing the ratio of unlabeled A β , then the uptake mechanism cannot be saturated (up to the total amount of labeled + unlabeled A β in the experiment). To probe the limits of uptake by primary microglia, unlabeled and AF488-A β 42 were mixed in various ratios before application to and incubation of microglia. As seen in Figure 4.5, Panel A, the first set of experiments did not indicate a saturation of uptake even at 20 μ M total A β 42. All three images show similar green fluorescence intensity, indicating AF488-A β internalization was not saturable. Different AF488-A β :unlabeled A β ratios were used in another set of experiments, and the image fluorescence intensity quantitation is shown in Panel B of Figure 4.5. Again, there is no significant difference in measured fluorescence intensity, even when there is three times as much unlabeled A β 42 mixed with AF488-A β 42. These results confirm the findings of Mandrekar et al. (2009) that A β uptake is not receptor-mediated, and in addition show that there is no limit to internalization up to 20 μ M A β 42. These images show internalized A β , only the fluorescence on the boundaries of the cells could be considered as surface-attached A β . We have shown that the amount of internalized A β increases at 6 and 24 h, an increase that would not be present if the protofibrils were rapidly cycling into and out of the cells. Additionally, it is not likely that the membranes of the cell could support a rapid turnover leading to equilibrium. Other

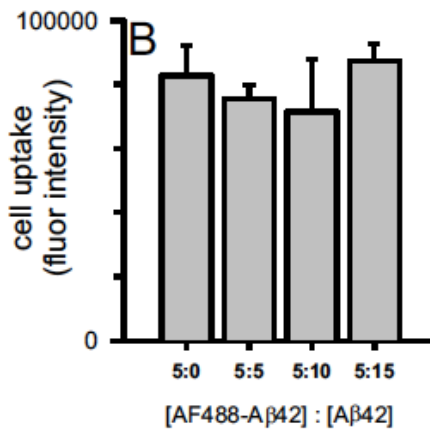
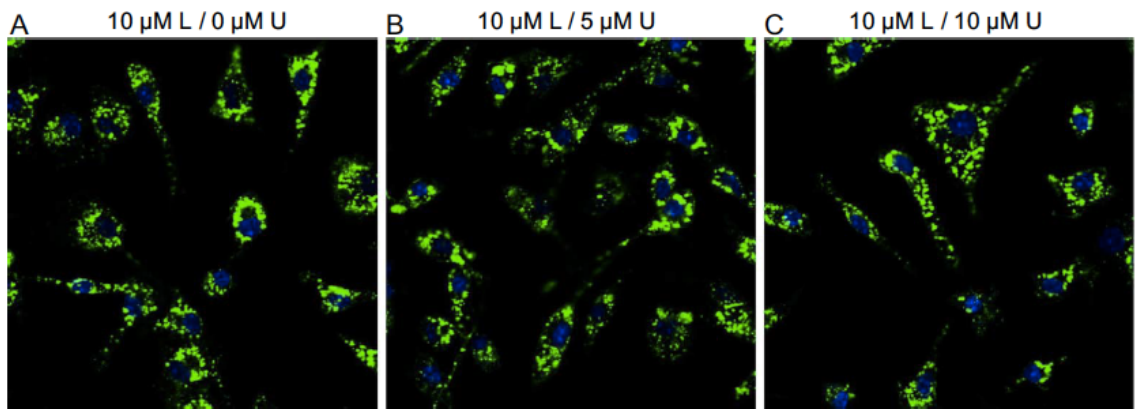


Figure 4.5 Competition/saturation images and quantitation. (A) Representative images of primary microglia treated with the indicated concentrations of labeled and unlabeled Aβ. (B) Quantitation of fluorescence intensity in images of primary microglia treated with the indicated concentrations of labeled and unlabeled Aβ. ImageJ was used to measure integrated intensity for each field, which was divided by the number of nuclei in the field. (n = 2 experiments)

groups have conducted pulse-chase experiments in which the A β -containing medium was removed and the amount of internalized A β was then measured at different time points. but their purpose was to measure degradation, not uptake saturation (Chung, 1999; Lee, et al., 2012; Majumdar, et al., 2011; Majumdar, et al., 2007; Paresce, et al., 1997). While these groups did show some degradation, it was limited. Even if degradation occurred in the experiments reported here, it would not be enough to affect the outcome because the rate of degradation would not be enough to offset uptake, and the rate would be the same for all of the ratios. Two early studies, involving “microaggregates” or fibrillar A β seemed to indicate saturation of uptake, as both groups found that intracellular fluorescence increased with increasing concentration, but leveled off after 10-11 μ M A β (Kopec and Carroll, 1998; Paresce, et al., 1996). These two groups did not use ratios as we did. Other studies used the approach of keeping the amount of labeled A β constant while mixing in increasing concentrations of unlabeled peptide, and those groups did report saturation of uptake (Chung, 1999; Mandrekar, et al., 2009).

4.5 Colocalization analysis of AF488-A β with lysosomes

The question of whether or not A β is degraded by microglia is not settled. Two reports indicated that oligomers are degraded in microglia (Shibuya, et al., 2014; Yang, et al., 2011) but oligomers do not have the same β -sheet structure as protofibrils or fibrils, so it is perhaps not surprising that they are degraded. Several studies showed slow and/or limited breakdown of internalized fibrils (Chung, et al., 1999 ; Majumdar, et al., 2011; Majumdar, et al., 2008; Majumdar, et al., 2007; Paresce, et al., 1997). Monomers and soluble species were also shown to be slowly or incompletely degraded (Ard, et al., 1996; Griciuc, et al., 2013; Jiang, et al., 2008). In these studies, there was no SEC purification

of protofibrils, so it is possible that both the fibril and soluble solutions used contained some protofibrillar A β . Further, the degradation was incomplete when it occurred at all, so more investigation is warranted. In cells, the break down unwanted material occurs in the lysosomes, acidic “digestive” organelles. If A β is being degraded, it would first have to be trafficked to lysosomes. Many studies have shown A β colocalized with lysosomes, and they are summarized in Table 4.1. Various A β conformers were used for cell treatments in those experiments, but no one had reported using SEC-purified protofibrils.

In an effort to show colocalization of protofibrils with lysosomes in our primary microglial system, I had tried using LysoTracker® Red DND-99 (Invitrogen) for labeling lysosomes prior to cell treatment, but did not have good enough results to definitively conclude colocalization or lack thereof. Lysosomal associated membrane protein (LAMP1) is a transmembrane protein that is found on lysosomes in many tissues. To visualize colocalization of A β 42 and lysosomes, I used immunofluorescence to label the LAMP1 protein. The primary antibody was anti-LAMP1 (Novus Biological) and the secondary antibody was anti-mouse IgG-NL637 (R & D Systems). Primary microglia were treated with AF488-A β protofibrils, fixed, immunostained, counterstained with DAPI, and then imaged on a Zeiss LSM 700. The images in Figure 4.6 represent several experiments. Yellow arrows in the images indicate areas of colocalization (yellow) of AF488-A β (green) with lysosomes (red). White arrows in the images show either AF488-A β (green) that is intracellular but not in lysosomes, or empty lysosomes (red). While other groups have shown A β -lysosome colocalization in BV-2 and primary microglia, and some concluded that A β is degraded in lysosomes, my results indicated that trafficking to lysosomes is not necessarily the fate of AF488-A β protofibrils. This is

Table 4.2 Lysosome colocalization experiments.

Reference	A β form	A β label	[A β], μ M	Cell type	Incubation time	Colocalization method
Ard, et al., 1996	“not fibrillar”	³⁵ S-Met	0.22, 1.1, 4.4, or 25	rat primary	24 or 48 h	immunogold, EM
Paresce, et al., 1996	“microaggregates” <400 nm length	Cy3	0.22	mouse primary	10 min	FITC- α 2M
Paresce et al., 1997	“microaggregates”	Cy3	2	mouse primary	1 h, 1 h or 2 d chase	FITC-dextran
Chung, et al., 1999	soluble	Cy3	0.5	mouse primary	1.5 h, 1 h chase	FITC- α 2M
Webster, et al., 2000	“minimally aggregated”	fluorescein	5, 50	rat primary	2 h and 6 h	cathepsin D
Liu Y, et al., 2005	fibrils/protofibrils	biotin	0.55	mouse primary	5, 30 min; 1, 2 h	Lamp2
Bolmont, et al., 2008	plaques	none	endogenous	APP transgenic mouse, in vivo		Lamp1
Halle, et al., 2008	fibrils	FITC	10	immortalized mouse line	4 h	Lamp1
	fibrils	HL488	10	immortalized mouse line	4 h	LysoTracker Red
	fibrils	FITC	10	immortalized mouse line	1h, 4 h	1 h: cathepsin B 4 h: Lamp1 (no colocalization)
Jiang, et al., 2008	monomers and small oligomers	Cy3	0.5	BV-2	15 min	LysoTracker Green
Mandrekar, et al., 2009	monomers	Cy3	0.5	BV-2	3 h	Lamp1, Lamp2, Rab5
	monomers	Cy3	0.5	BV-2	0-19 min	LysoTracker Green

Table 4.2 Lysosome colocalization experiments, continued.

Reference	A β form	A β label	[A β], μ M	Cell type	Incubation time	Colocalization method
Hjorth, et al., 2010	soluble	HL488	0.25	human CHME3 line	4 h	Lamp2
Liu Z, et al., 2010	protofibril	HL555	0.4	in vivo, mouse	up to 4 d	Lamp1
Majumdar, et al., 2011	fibril	Cy3	0.25	primary murine	1 h, chase times vary	Lamp1
Yang, et al., 2011	oligomer	FAM	1	primary murine	15 min	DQ-BSA lysosome label
Fu, H, et al., 2012	fibril	AF488	66 (0.6 μ g total)	mouse in vivo	2 h or 5 d	Lamp1
	fibril	AF488	0.5	N9	1 h	LysoTracker
	fibril	AF488	0.5	primary murine	1 h	LysoTracker
Lee, CY, et al., 2012	soluble	AF555	0.2	primary murine	7 min, 10 min chase	fluorescent microspheres
Taneo, et al., 2015	monomer	none	10	primary murine	24 h	Lamp1 (not colocalized)
	oligomer	none	10	primary murine	24 h	Lamp 1 (not colocalized)
	fibril	none	10	primary murine	24 h	Lamp1 (not colocalized)
Baik, et al., 2016	fibril (PF)	FITC	1	BV-2	24 h	LysoTracker
	fibril (PF)	FITC	1	primary murine	24 h	LysoTracker
Gouwens, et al., 2016	protofibril	AF488	5	primary murine	30 min	Lamp1 (partial colocalization)

Abbreviations: AF488: Alexa Fluor 488; AF555: Alexa Fluor 555; Cy3: Cyanine 3; FAM: carboxyfluorescein; FITC: fluorescein isothiocyanate; HLF488: HiLyte Fluor 488; HL555: HiLyte Fluor 555; ³⁵S-Met: ³⁵S-methionine radioisotope

*work presented herein

evident in the increase of A β protofibril load over a 24-h incubation (Figure 4.3) and in the confocal images of Figure 4.6 which show a significant amount of AF488-A β distributed throughout the cytosol. The stability of intracellular SEC-purified protofibrils in microglia is a novel finding that was reported in *Brain Research* in 2016 (Gouwens, et al., 2016).

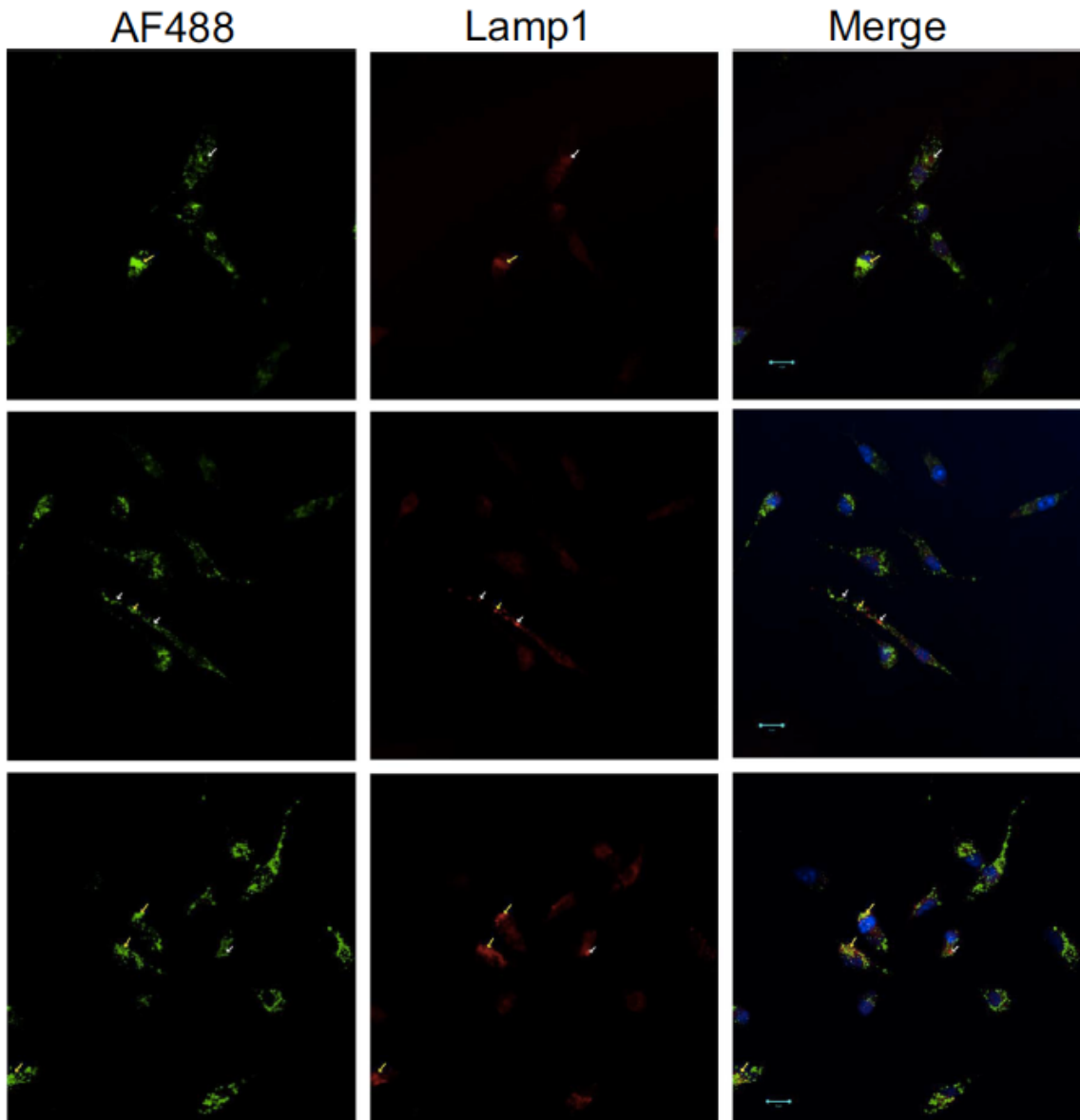


Figure 4.6 Lysosome colocalization. Three fields (top, middle and bottom rows) of primary cells treated with AF488-A β show that much of the AF488-A β remains outside of microglial cells. Yellow arrows indicate lysosome (red, Lamp1) and AF488-A β (green) colocalization. White arrows show lysosomes that have no AF488-A β within them. Nuclei are stained with DAPI (blue).

CHAPTER 5: MICROVESICLES

Having demonstrated that microglia internalize A β protofibrils without necessarily degrading them, we began to wonder if the protofibrils are released from microglial cells. If there is a release of A β , that could partly explain why plaques form in the AD brain. Structures called microvesicles (Section 1.4) are one way microglia could disperse A β . Microvesicles (described in Section 1.4) are released by glial cells when P2X₇ receptors are stimulated by ATP (Bianco, et al., 2005). In their work, Bianco and colleagues used the N9 murine microglial cell line as well as primary mixed cultures (containing astrocytes and microglia) from embryonic rat pups to demonstrate the release of microvesicles from microglial cells. Rat primary microglia (Joshi, et al., 2014), and human THP-1 monocytes and HEK cells (MacKenzie, et al., 2001) have also been used in experiments to produce microvesicles. Further, P2X₇ receptors of microglia have been shown to mediate the inflammatory responses in rat hippocampus (McLarnon, et al., 2006). My goals were to generate and characterize microvesicles from both BV-2 and primary murine microglia.

5.1 Microvesicles from BV-2 microglia

Due to their small size, capturing a substantial amount of microvesicles requires treatment of many cells in an experiment. BV-2 microglia are relatively easy to culture in the amounts needed for microvesicle generation, so I started my experiments with them. Using T-150 flasks (Corning), which have a 150 cm² growing surface, the BV-2 cells

were cultured to confluence. The experiments required two such flasks, a control flask that was incubated with 4 mL artificial cerebrospinal fluid (aCSF) and a second flask that was incubated with 1 mM ATP in 4 mL aCSF to stimulate the production of microvesicles (Methods 2.9). To confirm that microvesicles were produced, we employed a variety of techniques: fluorescently labeled Annexin V, BCA protein measurements, dynamic light scattering (DLS) measurements, transmission electron microscopy (TEM), and NBD C6-HPC fluorescence.

5.1.1. A488-Annexin V visualization of BV-2 microvesicles

Annexin V is an anticoagulant protein that also has a high affinity for phosphatidylserine (PS). Normally PS is found on inner leaflets of the cell membrane, but, in apoptotic cells and microvesicles, PS is externalized (Hugel, et al., 2005). We used Annexin V conjugated to Alexa Fluor® 488 (AF488-AV) to visualize microvesicles generated in the experiments (Figure 5.1). After the cells were treated, the medium was subjected to centrifugation at 2000g for 20 minutes to remove apoptotic cells and cell debris from the medium. Soluble microvesicles are in the supernatant, to which AF488-AV was added. After incubation at room temperature, the solution was then centrifuged at 12,200g for 40 minutes to pellet the microvesicles. The pellet was washed and resuspended, and microvesicles were mounted on slides and imaged using a Zeiss LSM 700. As seen in Figure 5.1 A & B, the microvesicles are produced by both control (A) and ATP-treated (B) cells and are in the expected 100 – 1000 nm size range. Microvesicle production from the control cells (treated with aCSF only) is not necessarily surprising since microvesicles are routinely found in blood and spinal fluid (Budnik, et al., 2016), indicating constitutive generation by cells in the body. Panel C of Figure 5.1 is

a zoomed in view of an area near the center of Panel B which includes a 5 μm scale bar that confirms the size of the microvesicles. The images here are consistent with MacKenzie, et al. (2001), who showed a series of HEK cell images taken at 5 s intervals in which microvesicles are visualized with FITC-conjugated Annexin V bound to externalized PS. They imaged whole cells, and a halo of microvesicles is visible in the same size range as our microvesicles. Wilson, et al. (2004) demonstrated external PS (calling it “PS flip”) in human umbilical vein epithelial cells and murine macrophages. Their images were not of microvesicles, rather, they showed FITC-Annexin V binding to the surfaces of macrophages after treatment with ATP, demonstrating PS externalization. This is the same PS externalization that occurs with microvesicle release. Bianco, et al. (2005) also show FITC-Annexin V in close association with ATP-stimulated N9 microglia, with a few blebs on the cell surface and structures that have the size and morphology of microvesicles. The researchers showed images of microvesicles in a subsequent publication, appearing as dots of fluorescence (Bianco, et al., 2009). One of the methods of microvesicle visualization used by Verderio, et al. (2012) was FITC-Annexin V. Their image, similar to Bianco’s images, does not show the circular fluorescence seen in Figure 5C, which is indicative of hollow spheres. The images in Figure 5 indicate that our protocol for generating microvesicles from ATP-treated BV-2 microglia and separating them from apoptotic bodies via centrifugation is successful.

5.1.2. Bicinchoninic acid protein assay of BV-2 microvesicles

IL-1 β has been found in microvesicles generated from human THP-1 monocytes (MacKenzie, et al., 2001) and dendritic cells (Pizzirani, et al., 2007), as well as murine microglia (Bianco, et al., 2005) treated with ATP. Therefore, we expected to find protein

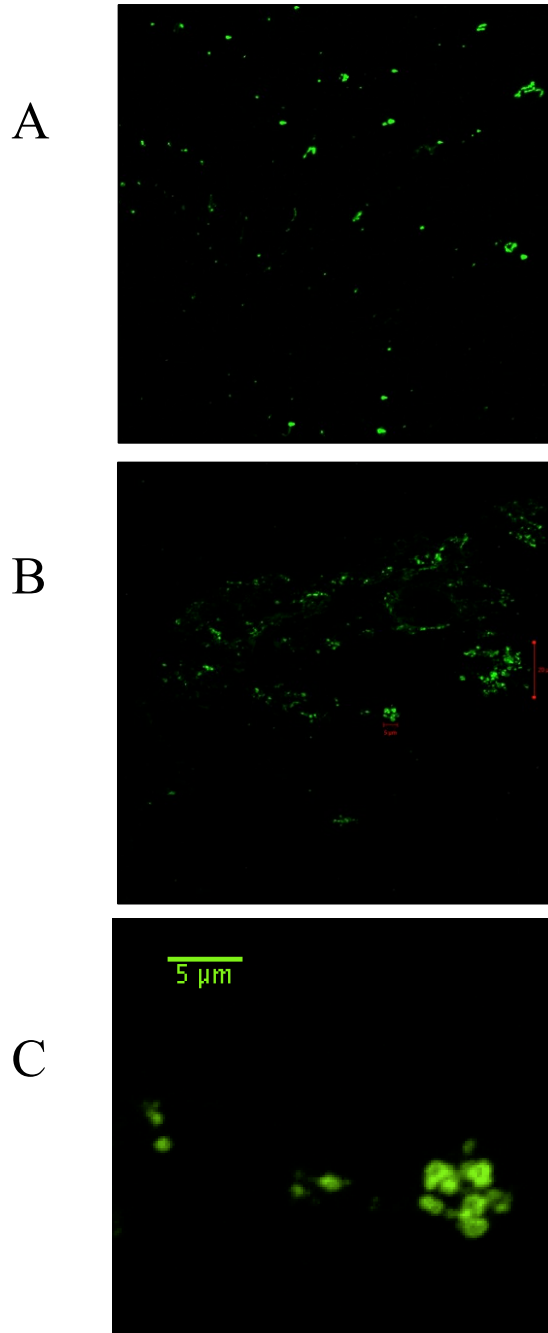


Figure 5.1 AF488-Annexin V visualization of microvesicles from BV-2 cells. Microvesicles were generated from BV-2 microglia with or without ATP treatment. After generation from BV-2 microglia, microvesicles were incubated with AF488-Annexin V and imaged via confocal microscopy. (A) Control: microvesicles generated from microglia incubated in aCSF without ATP; 40X magnification. (B) Microvesicles generated from BV-2 microglia treated with 1 mM ATP. 40X magnification; vertical red scale bar = 20 μm ; horizontal red scale bar = 5 μm . C. Zoomed in view of area near horizontal red scale bar in (B)

in the BV-2 microvesicles. Bicinchoninic acid (BCA) protein assays were employed to provide measurements of overall microvesicle protein content. By measuring absorbance at 562 nm and comparing the samples to a standard curve generated with bovine serum albumin, protein concentration within the microvesicles can be determined. While both control and ATP-treated cells produced microvesicles, the microvesicles from treated cells had much more total protein (Figure 5.2), with virtually no protein in the microvesicles from control cells. The combined data from four preps showed a protein concentration of $\sim 150 \mu\text{g/mL}$ protein in ATP-treated cells compared to virtually none in the control cells. It is likely that the contents of our microvesicles derived from ATP-stimulated BV-2 microglia contain IL-1 β , as was found by the MacKenzie, Pizzirani, and Bianco studies mentioned above. Regarding the control cells, constitutive microvesicle production is not unusual, and the lack of protein is likely a consequence of there being no ATP in the aCSF to activate IL-1 β production and release.

5.1.3. Dynamic light scattering characterization of BV-2 microvesicles

Particles in solution will move randomly as they collide with molecules of the solution, and smaller particles will move faster than relatively larger ones. Light passing into a solution containing microvesicles, for instance, will be scattered upon encountering a sphere crossing its path. Scattered light then encounters other particles, causing wave interference that is either constructive or destructive. As the particles diffuse through the solution, the scattering intensity changes, as does the correlation between the intensities and interferences. The intensity measurements are fitted to an autocorrelation curve, and from the exponential decay a diffusion coefficient can be calculated, which is then used to calculate hydrodynamic radii of microvesicles. We used these principles of dynamic

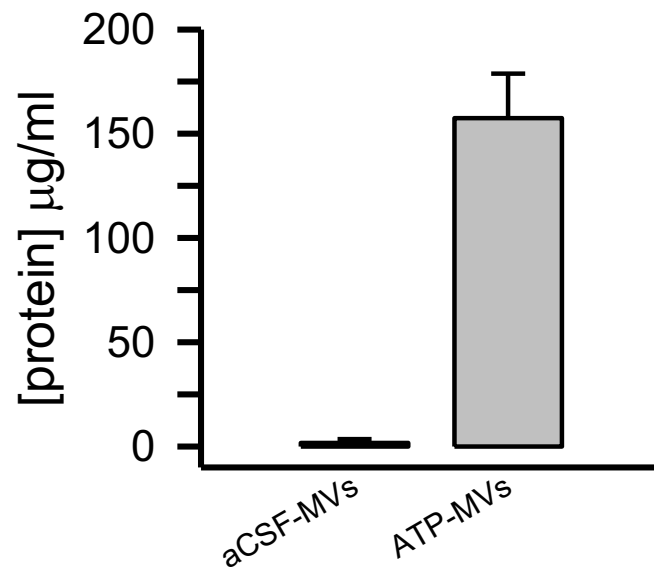
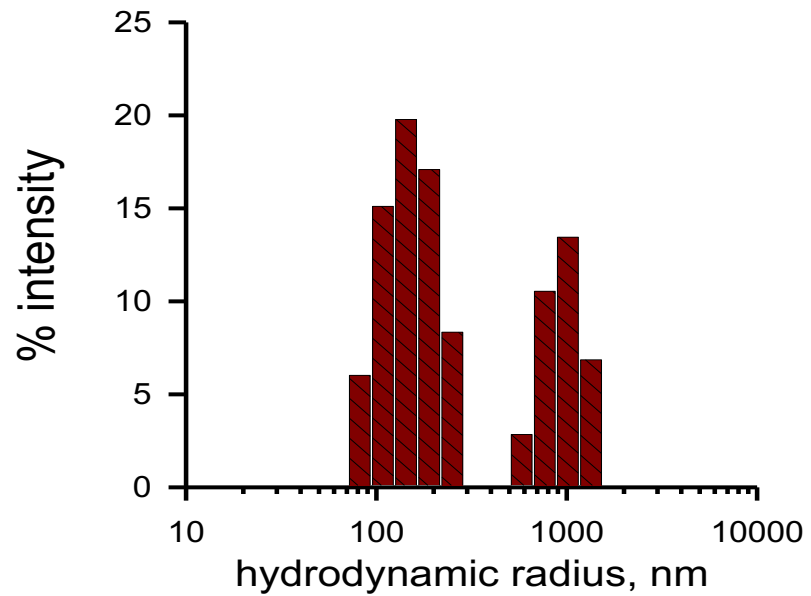
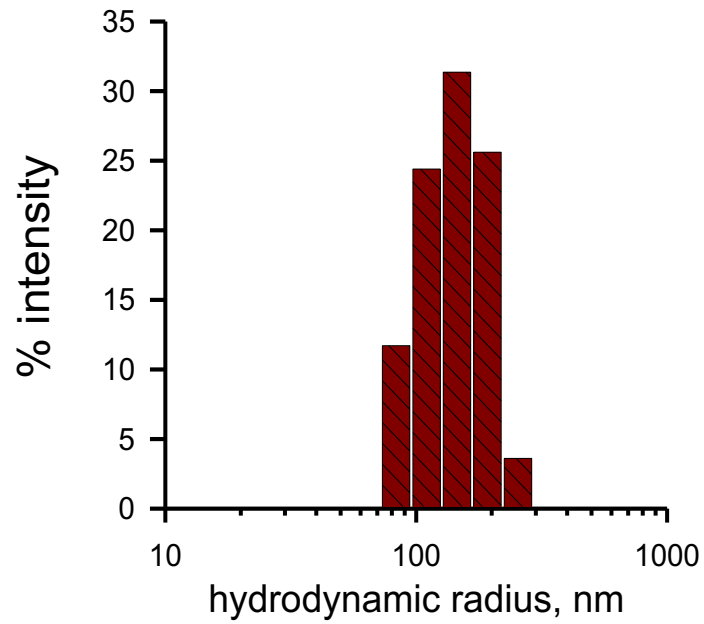


Figure 5.2 BCA assays. There is greater protein production in microvesicles generated from ATP-treated cells than control cells in aCSF. Average of four microvesicle preparations from BV-2 microglia. (BCA assays conducted by Mudar Ismail and Nathan Zeller; figure from Dr. Michael Nichols)

light scattering (DLS) to characterize microvesicle size (Methods 2.2.5). Histograms of percent intensity vs. hydrodynamic radius (R_H) were generated by Dynamics software (Wyatt Technologies) data regularization, and intensity-weighted mean R_H values were derived from regularized histograms. What we found, shown in the representative histograms in Figure 5.3, is that the microvesicles we isolated from BV-2 microglia are approximately 100-1000 nm in size, with an average $R_H = 129$ nm for the ATP-treated BV-2 microvesicles in 5.3A, and an average $R_H = 207$ nm for the microvesicles in 5.3B, which were also from ATP-treated BV-2 cells. Microvesicles generated from control cells in the same experiments had average $R_H = 136$ and 208 nm, respectively. The defined microvesicle size range is 100-1000 nm, described by Budnik, et al. (2016), and these representative DLS data for all of the microvesicle preps show that our microvesicles were within that range

5.1.4. Transmission electron microscopy of resin-embedded BV-2 microvesicles

Microvesicles from BV-2 cells were embedded in resin (Methods 2.11) for imaging via TEM. Dr. Agnes Kittel's gracious help was vital to this endeavor. After reading a paper that featured TEM images of microvesicles (Crescitelli, et al., 2013), I emailed the corresponding authors and they identified Dr. Kittel as the TEM technician responsible for the images. Our correspondence led to the method used for obtaining the images of BV-2 microvesicles in Figure 5.4. The intricate process involved pelleting the microvesicles, fixing with formaldehyde, treatment with osmium tetroxide, multi-step alcohol dehydration using uranyl acetate stain in the first step, and resin polymerization. David Osborn acquired the images shown in Figure 5.4 after slicing the resin-embedded sample with a microtome. The top panel shows BV-2 microvesicles from control



5.3 Dynamic light scattering analysis of microvesicles. Microvesicles were generated from BV-2 microglia. Results from two different experiments are shown. (Figure created by Dr. M.R. Nichols.)

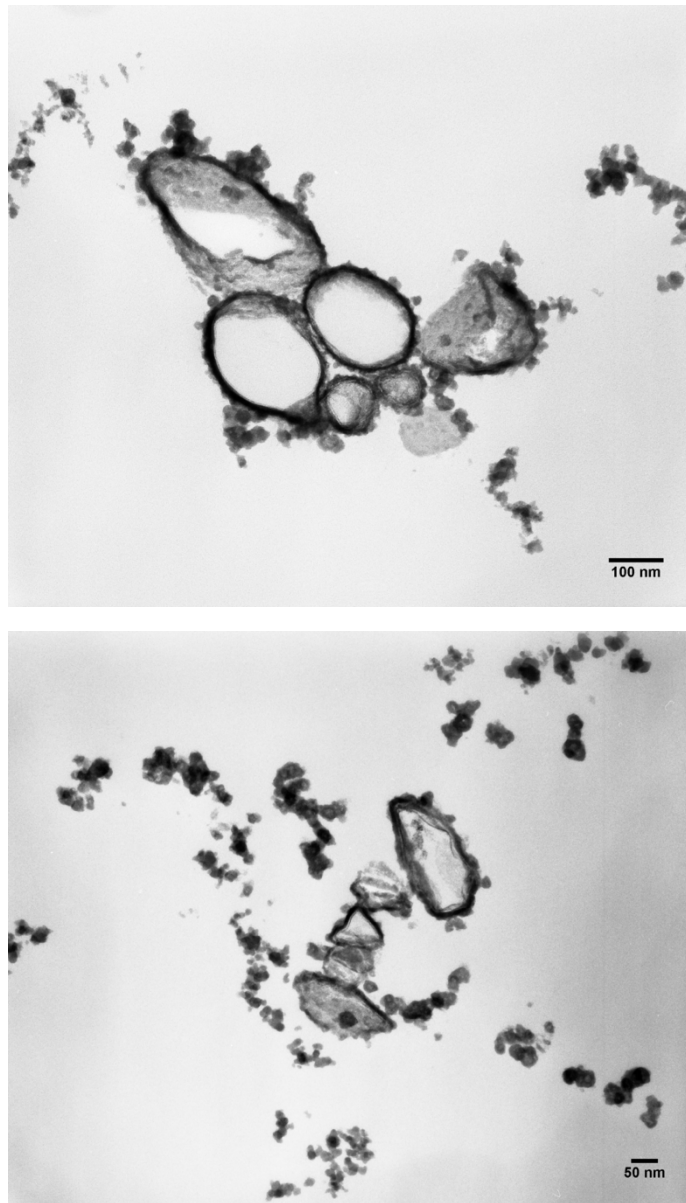


Figure 5.4 TEM of resin-embedded BV-2 microvesicles
Top: control BV-2 MVs (no ATP). Bottom: ATP-treated BV-2 MVs. Both sets of microvesicles are within the size range expected. (Resin embedding done by myself and Mudar Ismail; image by Dr. David Osborn.)

microglia, and the bottom panel shows BV-2 microvesicles from the ATP-treated microglia. The microvesicles are similar in size and appearance, despite the presence or absence of ATP during the experiment. Bianco (2009) and Verderio (2012) presented TEM of vesicles isolated by differential centrifugation, which they refer to as P2 (1200g), P3 (10,000g), and P4 (110,000g). The microvesicles from our experiments (Figure 5.4) correspond to their P3 pellet, and look much like the structures in their images. That is expected, considering the similarities in our isolation protocols; their 1200g and 10,000g centrifugations correspond to our 2000g and 12,200g centrifugations. The lower speed should pellet whole cells, debris, and apoptotic bodies, and the higher speed produces a pellet of microvesicles. In the Crescitelli, et al. (2013) study, three cell types were used: human mast cells, human erythroleukemia cells, and BV-2 murine microglia. They were able to visualize microvesicles from all three, and our BV-2 microvesicles resemble them in size and appearance. These images provide compelling evidence for our ability to generate microvesicles from BV-2 microglia.

5.1.5 Tracking microvesicles with NBD C6-HPC fluorescence

The miniscule pellets presented a challenge when isolating microvesicles. To better track microvesicles, and reassure ourselves that they were indeed present, we took advantage of the NBD fluorophore conjugated to phosphatidylcholine (PC). The NBD C6-HPC (Setareh Biotech; Figure 5.5) molecule inserts into lipid bilayers, and its emission at 536 nm (excitation: 436 nm) can be used to identify membranes. The use of NBD C6-HPC to visualize microvesicles from healthy rat CSF and to quantify microvesicles from rat microglial cell culture was reported by Verderio, et al. (2012). CSF microvesicles isolated from healthy rats were visualized by adding NBD C6-HPC to

pellet fractions, placing drops onto a slide, and imaging the microvesicles with a fluorescence microscope. In their work, microglia were pretreated with NBD C6-HPC before the experiment to label cell membranes, then, after collecting the microvesicles, the researchers quantified NBD C6-HPC fluorescence intensity to make a comparison of microvesicle amounts produced by known stimulants of microglial activation and microvesicle production, such as ATP or LPS. Bianco, et al. (2009) also used NBD C6-HPC to label cell membrane lipids and visualize both real-time microvesicle release from BzATP-treated human glioma cells and microvesicles isolated from cell the culture medium of BzATP-treated astrocytes.

In our experiments, supernatants from microglia treated with ATP or BzATP were processed as described in Methods (2.9 and 2.10). NBD C6-HPC is added to the supernatant collected from the 2000g spin of the cell treatment medium, which pellets cell debris and apoptotic bodies. The supernatant with fluorophore is then incubated at room temperature for 10-15 min, after which the microvesicles are pelleted via centrifugation at 12,200-15,000g and washed with aCSF two to five times to remove excess fluorophore. A fluorimeter is used to measure fluorescence of the washes and resuspended pellets. Fluorescence emission is recorded from 500-600 nm, and integrated from 505-550 nm to produce the values that are graphed. Since most of the unincorporated fluorophore is removed during the washes, greater fluorescence intensity in the resuspended pellet compared to the last wash indicates the presence of microvesicles. Figure 5.5 shows representative data from an experiment in which BV-2 and primary microglia were treated with ATP to stimulate microvesicle production. The bottom panel shows a comparison among two washes and the resuspended microvesicle

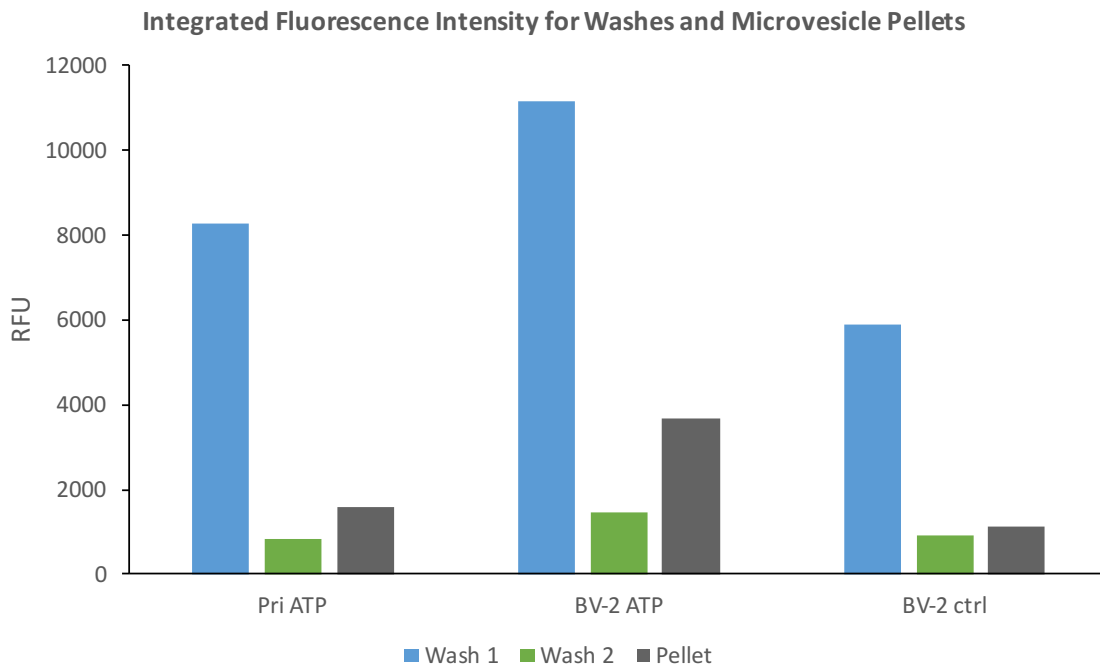
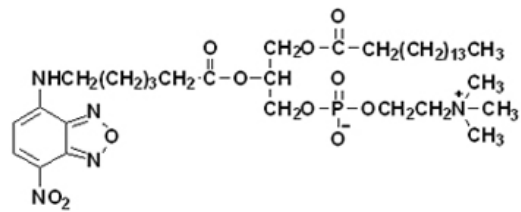


Figure 5.5 NBD C6-HPC fluorescence indicates the presence of microvesicles. Top: NBD PC conjugate. Bottom: representative fluorescence intensity measurements for microvesicles generated from BV-2 and primary microglia. Greater fluorescence intensity in the resuspended pellet than in the final wash confirms the presence of microvesicles.

pellet from ATP-treated primary microglia, and from treated and control BV-2 cells. For the ATP-treated BV-2 cells, the first wash has a fluorescence intensity of 11144, the second wash is 1465 and the pellet is 3658, 2.5-fold greater. This indicates that the NBD C6-HPC is embedded in the membranes of the microvesicles in the pellet. The washes from the control (aCSF-treated) BV-2 microvesicles had intensities of 5984, 899, and the pellet intensity was 1126. In this case, the pellet has only 25% greater intensity, but that is still much lower than the first wash, and it seems there fewer microvesicles in the control pellet than in the pellet from the ATP-treated BV-2 microglia. This representative result is typical of the microvesicle preparations we have done so far.

5.2 Characterization of microvesicles from primary microglia

Generating microvesicles from primary microglia is challenging because it is difficult to culture primary microglia in the amounts needed to produce enough microvesicles to assay. Our primary microglia are in co-culture with astrocytes, so I first tried using a co-culture of microglia and astrocytes to generate MVs. The data were promising in that, after using NBD C6-HPC, I was able to detect greater fluorescence intensity in the microvesicles than in the final wash. However, both the control flask and the treated flask were not able to be used again after that experiment. New co-cultures require isolation from mouse pups, so their availability is limited. It is necessary, then, to use cultures of only primary microglia that are removed from the astrocyte + microglia co-culture. To isolate primary microglia for experiments, co-culture flasks are shaken for 5 h at 250 rpm. From two T150 (Corning) flasks containing primary murine astrocytes and microglia, the yield of primary microglia has ranged from 5×10^4 to 8×10^5 cells/mL, which is not even enough to cover one T75 flask to confluence. An additional consideration was

the viability of the primary microglia seeded in a flask. We had previously plated primary microglia in 96-well plates for experiments, but I had no experience with primary microglia monocultures or experimenting on them in a culture flask.

First, I seeded four 25 cm² flasks with 5×10^4 cells/mL in 5 mL and cultured them for a week, changing the medium twice. The data showed promise, but fluorescence intensity from the microvesicles was only slightly more intense than 4th wash. However, from this I confirmed that the primary microglia could be cultured in a flask for at least one week. Next, 2 T-75 flasks were seeded with 1.6×10^5 cells/mL in 10 mL. After 5 days of culture, with one medium change, these cells were used for a microvesicle generation experiment. Only 2 washes were done, as seen in Figure 5.5. After this, fewer co-culture flasks were available, allowing the seeding of just one T-75 flask at a time. With only one T-75 flask of primary microglia, I did not set up a control (untreated) flask when generating microvesicles from primary microglia.

The data from an early experiment with primary cells is shown in Figure 5.5. For microvesicles generated from primary cells, the first wash had an integrated fluorescence intensity of 8269, the second wash was 842, and the pellet integrated intensity was 1564 – nearly double that of the last wash. Later experiments were done with BzATP, which has been shown to be more effective at stimulating the P2X₇ receptor. Results from those microvesicle experiments are similar, with about 2-fold greater integrated intensity for the resuspended pellet than the last wash, indicating the presence of microvesicles.

Following consistent generation of microvesicles from primary microglia, further investigation would involve experiments in which we treat primary microglia with A β so

they internalize it, use BzATP to stimulate microvesicle production, and probe the microvesicles for A β using immuno-dot blots and/or ELISAs.

5.3 Overall conclusion

We have shown that surface interaction of A β with BV-2 microglia produces a proinflammatory response in the presence of protofibrils, but not monomers or fibrils of A β . The proinflammatory response, as measured by TNF α secretion, correlated with the time of exposure to A β in BV-2 microglia. Primary microglia are much more likely to internalize SEC-purified protofibrils than monomers, as demonstrated by both time- and concentration-dependent treatments. SEC separation of A β monomers and protofibrils is a strategy that we employ which sets apart our work from the literature on microglial uptake of A β and explains differences between our findings and those of other groups. For instance, we reported that much of the A β taken up by primary microglia is not degraded in the lysosomes. We were also able to show that we can generate microvesicles from BV-2 and primary microglia. Further investigation into whether these microvesicles can carry internalized A β back out of microglia is warranted.

The five novel findings from this research include (1) the labeling of a solution of monomers and protofibrils which are then separated by SEC; (2) protofibrils are internalized by primary microglia in greater quantities than monomers in both time- and concentration-dependent experiments; (3) quantitation methods utilizing a plate-reader to measure uptake of labeled A β in cells that were treated in a 96-well culture plate; (4) A β internalization could not be saturated, even when the concentration of unlabeled A β was three-fold greater than labeled A β ; and, (5) contradictory to many reports in the literature,

a significant amount of internalized A β was found in the cytoplasm, outside of lysosomes, and remained stable as protofibrils.

BIBLIOGRAPHY

- Alzheimer's Organization. Fact Sheet March 2015.
<<http://www.alz.org/facts/overview.asp>> Accessed August 22, 2015.
- World Health Organization. Dementia Fact Sheet No. 362.
<<http://www.who.int/mediacentre/factsheets/fs362/en/>> Accessed August 22, 2015.
- Agosta, F., Dalla Libera, D., Spinelli, E. G., Finardi, A., Canu, E., Bergami, A., Bocchio Chiavetto, L., Baronio, M., Comi, G., Martino, G., Matteoli, M., Magnani, G., Verderio, C. and Furlan, R. 2014. Myeloid microvesicles in cerebrospinal fluid are associated with myelin damage and neuronal loss in mild cognitive impairment and alzheimer disease. *Ann Neurol*, 76:813-25.
- Ajit, D., Udan, M. L., Paranjape, G. and Nichols, M. R. 2009. Amyloid-beta(1-42) fibrillar precursors are optimal for inducing tumor necrosis factor-alpha production in the thp-1 human monocytic cell line. *Biochemistry*, 48:9011-21.
- Ansari, N., Muller, S., Stelzer, E. H. and Pampaloni, F. 2013. Quantitative 3d cell-based assay performed with cellular spheroids and fluorescence microscopy. *Methods Cell Biol*, 113:295-309.
- Antonucci, F., Turola, E., Riganti, L., Caleo, M., Gabrielli, M., Perrotta, C., Novellino, L., Clementi, E., Giussani, P., Viani, P., Matteoli, M. and Verderio, C. 2012. Microvesicles released from microglia stimulate synaptic activity via enhanced sphingolipid metabolism. *EMBO J*, 31:1231-40.
- Ard, M. D., Cole, G. M., Wei, J., Mehrle, A. P. and Fratkin, J. D. 1996. Scavenging of alzheimer's amyloid beta-protein by microglia in culture. *J Neurosci Res*, 43:190-202.
- Bamberger, M. E., M.E., H., McDonald, D. R., Husemann, J. and Landreth, G. E. 2003. A cell surface receptor complex for fibrillar beta-amyloid mediates microglial activation. *J Neurosci*, 23:2665-2674.
- Banati, R. B. and Graeber, M. B. 1994. Surveillance, intervention and cytotoxicity: Is there a protective role of microglia? *Developmental Neuroscience*, 16:114-27.

- Bianco, F., Perrotta, C., Novellino, L., Francolini, M., Riganti, L., Menna, E., Saglietti, L., Schuchman, E. H., Furlan, R., Clementi, E., Matteoli, M. and Verderio, C. 2009. Acid sphingomyelinase activity triggers microparticle release from glial cells. *EMBO J*, 28:1043-54.
- Bianco, F., Pravettoni, E., Colombo, A., Schenk, U., Moller, T., Matteoli, M. and Verderio, C. 2005. Astrocyte-derived atp induces vesicle shedding and il-1beta release from microglia. *J Immunol*, 174:7268-7277.
- Bitan, G., Kirkitadze, M. D., Lomakin, A., Vollers, S. S., Benedek, G. B. and Teplow, D. B. 2003. Amyloid β -protein ($a\beta$) assembly: $A\beta_{40}$ and $a\beta_{42}$ oligomerize through distinct pathways. *Proceedings of the National Academy of Sciences*, 100:330-335.
- Blasi, E., Barluzzi, R., Bocchini, V., Mazzolla, R. and Bistoni, F. 1990. immortalization of murine microglial cells by a v-raf/v-myc carrying retrovirus. *J Neuroimmunol*, 27:229-37.
- Brough, D., Le Feuvre, R. A., Iwakura, Y. and Rothwell, N. J. 2002. Purinergic (p2x7) receptor activation of microglia induces cell death via an interleukin-1-independent mechanism. *Mol Cell Neurosci*, 19:272-80.
- Budnik, V., Ruiz-Canada, C. and Wendler, F. 2016. Extracellular vesicles round off communication in the nervous system. *Nat Rev Neurosci*, 17:160-72.
- Burnstock, G. and Knight, G. E. 2004. Cellular distribution and functions of p2 receptor subtypes in different systems. *International Review of Cytology*, 240:31-304.
- Chen, L. and Brosnan, C. F. 2006. Regulation of immune response by p2x7 receptor. *Crit Rev Immunol*, 26:499-513.
- Chu, T., Tran, T., Yang, F., Beech, W., Cole, G. M. and Frautschy, S. A. 1998. Effect of chloroquine and leupeptin on intracellular accumulation of amyloid beta 1-42 peptide in a murine n9 microglial cell line. *FEBS Lett*, 436:439-444.
- Chung, H. B., M.I.; Soe, T.T.; and Maxfield, F.R. 1999. Uptake, degradation, and release of fibrillar and soluble forms of alzheimer's amyloid beta peptide by microglial cells. *Journal of Biological Chemistry*, 274:32301-32308.
- Cole, G. M., Breech, W., Frautschy, S. A., Sigel, J., Glasgow, C. and Ard, M. D. 1999. Lipoprotein effects on amyloid beta accumulation and degradation by microglia in vitro. *J Neurosci Res*, 57:504-520.
- Combs, C. K., Karlo, J. C., Kao, S.-C. and Landreth, G. E. 2001. B-amyloid stimulation of microglia and monocytes results in tnfa-dependent expression of inducible

- nitric oxide synthase and neuronal apoptosis. *The Journal of Neuroscience*, 21:1179-1188.
- Conner, S. D. and Schmid, S. L. 2003. Regulated portals of entry into the cell. *Nature*, 422:
- Crescitelli, R., Lasser, C., Szabo, T. G., Kittel, A., Eldh, M., Diansani, I., Buzas, E. I. and Lotvall, J. 2013. Distinct rna profiles in subpopulations of extracellular vesicles: Apoptotic bodies, microvesicles and exosomes. *J Extracell Vesicles*, 2:
- De Strooper, B. and Karran, E. 2016. The cellular phase of alzheimer's disease. *Cell*, 164:603-15.
- Dickson, D. W., Lee, S. C., Mattiace, L. A., Yen, S. H. and Brosnan, C. 1993. Microglia and cytokines in neurological disease, with special reference to aids and alzheimer's disease. *Glia*, 7:75-83.
- Doens, D. and Fernández, P. L. 2014. Microglia receptors and their implications in the response to amyloid β for alzheimer's disease pathogenesis. *J Neuroinflammation*, 11:48.
- El Khoury, J. B., Moore, K. J., Means, T. K., Leung, J., Terada, K., Toft, M., Freeman, M. W. and Luster, A. D. 2003. Cd36 mediates the innate host response to beta-amyloid. *J Exp Med*, 197:1657-66.
- Esen, N. and Kielian, T. 2007. Effects of low dose gm-csf on microglial inflammatory profiles to diverse pathogen-associated molecular patterns (pamps). *J Neuroinflammation*, 4:10.
- Fassbender, K., Walter, S., Kuhl, S., Landmann, R., Ishii, K., Bertsch, T., Stalder, A. K., Muehlhauser, F., Liu, Y., Ulmer, A. J., Rivest, S., Lentschat, A., Gulbins, E., Jucker, M., Staufenbiel, M., Brechtel, K., Walter, J., Multhaup, G., Penke, B., Adachi, Y., Hartmann, T. and Beyreuther, K. 2004. The lps receptor (cd14) links innate immunity with alzheimer's disease. *FASEB J*, 18:203-5.
- Ferrari, D., Chiozzi, P., Falzoni, S., Dal Susino, M., Collo, G., Buell, G. and Di Virgilio, F. 1997. Atp-mediated cytotoxicity in microglial cells. *Neuropharmacology*, 36:1295-301.
- Frankola, K. A., Greig, N. H., Luo, W. and Tweedie, D. 2011. Targeting tnf-alpha to elucidate and ameliorate neuroinflammation in neurodegenerative diseases. *CNS Neurol Disord Drug Targets*, 10:391-403.
- Frost, J. L. and Schafer, D. P. 2016. Microglia: Architects of the developing nervous system. *Trends Cell Biol*,

- Fu, H., Liu, B., Frost, J. L., Hong, S., Jin, M., Ostaszewski, B., Shankar, G. M., Costantino, I. M., Carroll, M. C., Mayadas, T. N. and Lemere, C. A. 2012. Complement component c3 and complement receptor type 3 contribute to the phagocytosis and clearance of fibrillar abeta by microglia. *Glia*, 60:993-1003.
- Gaikwad, S., Larionov, S., Wang, Y., Dannenberg, H., Matozaki, T., Monsonego, A., Thal, D. R. and Neumann, H. 2009. Signal regulatory protein-beta1: A microglial modulator of phagocytosis in alzheimer's disease. *Am J Pathol*, 175:2528-39.
- Gouwens, L. K., Makoni, N. J., Rogers, V. A. and Nichols, M. R. 2016. Amyloid-beta42 protofibrils are internalized by microglia more extensively than monomers. *Brain Res*,
- Griciuc, A., Serrano-Pozo, A., Parrado, A. R., Lesinski, A. N., Asselin, C. N., Mullin, K., Hooli, B., Choi, S. H., Hyman, B. T. and Tanzi, R. E. 2013. Alzheimer's disease risk gene cd33 inhibits microglial uptake of amyloid beta. *Neuron*, 78:631-43.
- Halle, A., Hornung, V., Petzold, G. C., Stewart, C. R., Monks, B. G., Reinheckel, T., Fitzgerald, K. A., Latz, E., Moore, K. J. and Golenbock, D. T. 2008. The nalp3 inflammasome is involved in the innate immune response to amyloid-beta. *Nat Immunol*, 9:857-65.
- Harper, J. D., Wong, S. S., Lieber, C. M. and Lansbury, P. T. 1997. Observation of metastable abeta amyloid protofibrils by atomic force microscopy. *Chem Biol*, 4:119-25.
- Harper, J. D., Wong, S. S., Lieber, C. M. and Lansbury, P. T. 1999. Assembly of abeta amyloid protofibrils: An in vitro model for a possible early event in alzheimer's disease. *Biochemistry*, 38:8972-8980.
- Hide, I., Tanaka, M., Inoue, A., Nakajima, K., Kohsaka, S., Inoue, K. and Nakata, Y. 2000. Extracellular atp triggers tumor necrosis factor-alpha release from rat microglia. *J Neurochem*, 75:965-72.
- Hjorth, E., Frenkel, D., Weiner, H. and Schultzberg, M. 2010. Effects of immunomodulatory substances on phagocytosis of abeta(1-42) by human microglia. *Int J Alzheimers Dis*, 2010:
- Hugel, B., Martinez, M. C., Kunzelmann, C. and Freyssinet, J. M. 2005. Membrane microparticles: Two sides of the coin. *Physiology (Bethesda)*, 20:22-7.
- Jarrett, J. T., Berger, E. P. and Lansbury, P. T., Jr. 1993. The carboxy terminus of the beta amyloid protein is critical for the seeding of amyloid formation: Implications for the pathogenesis of alzheimer's disease. *Biochemistry*, 32:4693-7.

- Jarrett, J. T. and Lansbury, P. T. 1992. Amyloid fibril formation requires a chemically discriminating nucleation event: Studies of an amyloidogenic sequence from the bacterial protein osmb. *Biochemistry*, 31:12345-12352.
- Jarrett, J. T. and Lansbury, P. T., Jr. 1993. Seeding "one-dimensional crystallization" of amyloid: A pathogenic mechanism in alzheimer's disease and scrapie? *Cell*, 73:1055-8.
- Ji, K., Miyauchi, J. and Tsirka, S. E. 2013. Microglia: An active player in the regulation of synaptic activity. *Neural Plast*, 2013:627325.
- Jiang, Q., Lee, C. Y., Mandrekar, S., Wilkinson, B., Cramer, P., Zelcer, N., Mann, K., Lamb, B., Willson, T. M., Collins, J. L., Richardson, J. C., Smith, J. D., Comery, T. A., Riddell, D., Holtzman, D. M., Tontonoz, P. and Landreth, G. E. 2008. ApoE promotes the proteolytic degradation of abeta. *Neuron*, 58:681-93.
- Jiang, T., Zhang, Y. D., Gao, Q., Zhou, J. S., Zhu, X. C., Lu, H., Shi, J. Q., Tan, L., Chen, Q. and Yu, J. T. 2016. Trem1 facilitates microglial phagocytosis of amyloid beta. *Acta Neuropathol*, 132:667-683.
- Joshi, P., Turola, E., Ruiz, A., Bergami, A., Libera, D. D., Benussi, L., Giussani, P., Magnani, G., Comi, G., Legname, G., Ghidoni, R., Furlan, R., Matteoli, M. and Verderio, C. 2014. Microglia convert aggregated amyloid- β into neurotoxic forms through the shedding of microvesicles. *Cell Death Differ*,
- Jungbauer, L. M., Yu, C., Laxton, K. J. and LaDu, M. J. 2009. Preparation of fluorescently-labeled amyloid-beta peptide assemblies: The effect of fluorophore conjugation on structure and function. *J Mol Recognit*, 22:403-13.
- Kayed, R., Head, E., Thompson, J. L., McIntire, T. M., Milton, S. C., Cotman, C. W. and Glabe, C. G. 2003. Common structure of soluble amyloid oligomers implies common mechanism of pathogenesis. *Science*, 300:486-9.
- Kettenmann, H., Hanisch, U. K., Noda, M. and Verkhratsky, A. 2011. Physiology of microglia. *Physiol Rev*, 91:461-553.
- Kheterpal, I., Lashuel, H. A., Hartley, D. M., Walz, T., Lansbury, P. T., Jr. and Wetzel, R. 2003. Abeta protofibrils possess a stable core structure resistant to hydrogen exchange. *Biochemistry*, 42:14092-8.
- Koenigsknecht, J. and Landreth, G. 2004. Microglial phagocytosis of fibrillar beta-amyloid through a beta1 integrin-dependent mechanism. *J Neurosci*, 24:9838-46.
- Koffie, R. M., Meyer-Luehmann, M., Hashimoto, T., Adams, K. W., Mielke, M. L., Garcia-Alloza, M., Micheva, K. D., Smith, S. J., Kim, M. L., Lee, V. M., Hyman, B. T. and Spire-Jones, T. L. 2009. Oligomeric amyloid β associates with

postsynaptic densities and correlates with excitatory synapse loss near senile plaques. *Proceedings of the National Academy of Sciences*, 106:4012-4017.

- Kopec, K. K. and Carroll, R. T. 1998. Alzheimer's beta-amyloid peptide 1-42 induces a phagocytic response in murine microglia. *J Neurochem*, 71:2123-31.
- Lee, C. Y., Tse, W., Smith, J. D. and Landreth, G. E. 2012. Apolipoprotein e promotes beta-amyloid trafficking and degradation by modulating microglial cholesterol levels. *J Biol Chem*, 287:2032-44.
- Li, H. Q., Chen, C., Dou, Y., Wu, H. J., Liu, Y. J., Lou, H. F., Zhang, J. M., Li, X. M., Wang, H. and Duan, S. 2013. P2y4 receptor-mediated pinocytosis contributes to amyloid beta-induced self-uptake by microglia. *Mol Cell Biol*, 33:4282-93.
- Li, J., Kanekiyo, T., Shinohara, M., Zhang, Y., LaDu, M. J., Xu, H. and Bu, G. 2012. Differential regulation of amyloid-beta endocytic trafficking and lysosomal degradation by apolipoprotein e isoforms. *J Biol Chem*, 287:44593-601.
- Liu, G., Dou, S., Yin, D., Squires, S., Liu, X., Wang, Y., Rusckowski, M. and Hnatowich, D. J. 2007. A novel pretargeting method for measuring antibody internalization in tumor cells. *Cancer Biotherapy & Radiopharmaceuticals*, 22:33-39.
- Liu, S., Liu, Y., Hao, W., Wolf, L., Kiliaan, A. J., Penke, B., Rube, C. E., Walter, J., Heneka, M. T., Hartmann, T., Menger, M. D. and Fassbender, K. 2012. Tlr2 is a primary receptor for alzheimer's amyloid beta peptide to trigger neuroinflammatory activation. *J Immunol*, 188:1098-107.
- Liu, Y., Walter, S., Stagi, M., Cherny, D., Letiembre, M., Schulz-Schaeffer, W., Heine, H., Penke, B., Neumann, H. and Fassbender, K. 2005. Lps receptor (cd14): A receptor for phagocytosis of alzheimer's amyloid peptide. *Brain*, 128:1778-89.
- Liu, Z., Condello, C., Schain, A., Harb, R. and Grutzendler, J. 2010. Cx3cr1 in microglia regulates brain amyloid deposition through selective protofibrillar amyloid-beta phagocytosis. *J Neurosci*, 30:17091-101.
- Luzio, J. P., Hackmann, Y., Dieckmann, N. M. and Griffiths, G. M. 2014. The biogenesis of lysosomes and lysosome-related organelles. *Cold Spring Harb Perspect Biol*, 6:a016840.
- MacKenzie, A., Wilson, H. L., Kiss-Toth, E., Dower, S. K., North, R. A. and Surprenant, A. 2001. Rapid secretion of interleukin-1beta by microvesicle shedding. *Immunity*, 8:825-835.
- Majumdar, A., Capetillo-Zarate, E., Cruz, D., Gouras, G. K. and Maxfield, F. R. 2011. Degradation of alzheimer's amyloid fibrils by microglia requires delivery of clc-7 to lysosomes. *Mol Biol Cell*, 22:1664-76.

- Majumdar, A., Chung, H., Dolios, G., Wang, R., Asamoah, N., Lobel, P. and Maxfield, F. R. 2008. Degradation of fibrillar forms of alzheimer's amyloid beta-peptide by macrophages. *Neurobiol Aging*, 29:707-15.
- Majumdar, A., Cruz, D., Asamoah, N., Buxbaum, A., Sohar, I., Lobel, P. and Maxfield, F. R. 2007. Activation of microglia acidifies lysosomes and leads to degradation of alzheimer amyloid fibrils. *Mol Biol Cell*, 18:1490-6.
- Mandrekar, S., Jiang, Q., Lee, C. Y., Koenigsnecht-Talboo, J., Holtzman, D. M. and Landreth, G. E. 2009. Microglia mediate the clearance of soluble abeta through fluid phase macropinocytosis. *J Neurosci*, 29:4252-62.
- McGeer, E. G. and McGeer, P. L. 1998. The importance of inflammatory mechanisms in alzheimer disease. *Exp Gerontol*, 33:371-8.
- McGeer, P. L., Itagaki, S., Tago, H. and McGeer, E. G. 1987. Reactive microglia in patients with senile dementia of the alzheimer type are positive for the histocompatibility glycoprotein hla-dr. *Neurosci Lett*, 79:195-200.
- McLarnon, J. G., Ryu, J. K., Walker, D. G. and Choi, H. B. 2006. Upregulated expression of purinergic p2x(7) receptor in alzheimer disease and amyloid-beta peptide-treated microglia and in peptide-injected rat hippocampus. *J Neuropathol Exp Neurol*, 65:1090-7.
- Meda, L., Cassatella, M. A., Szendrei, G. I., Otvos, L., Jr., Baron, P., Villalba, M., Ferrari, D. and Rossi, F. 1995. Activation of microglial cells by beta-amyloid protein and interferon-gamma. *Nature*, 374:647-50.
- Meyer-Luehmann, M., Spires-Jones, T. L., Prada, C., Garcia-Alloza, M., de Calignon, A., Rozkalne, A., Koenigsnecht-Talboo, J., Holtzman, D. M., Bacsikai, B. J. and Hyman, B. T. 2008. Rapid appearance and local toxicity of amyloid-beta plaques in a mouse model of alzheimer's disease. *Nature*, 451:720-4.
- Mittag, J. J., Milani, S., Walsh, D. M., Rädler, J. O. and McManus, J. J. 2014. Simultaneous measurement of a range of particle sizes during a β 1-42 fibrillogenesis quantified using fluorescence correlation spectroscopy. *Biochem Biophys Res Commun*,
- Moore, K. J., El Khoury, J., Medeiros, L. A., Terada, K., Geula, C., Luster, A. D. and Freeman, M. W. 2002. A cd36-initiated signaling cascade mediates inflammatory effects of beta-amyloid. *J Biol Chem*, 277:47373-9.
- Nichols, M. R., Colvin, B. A., Hood, E. A., Paranjape, G. S., Osborn, D. C. and Terrill-Uery, S. E. 2015. Biophysical comparison of soluble amyloid-beta(1-42) protofibrils, oligomers, and protofilaments. *Biochemistry*,

- Nichols, M. R., Moss, M. A., Reed, D. K., Lin, W. L., Mukhopadhyay, R., Hoh, J. H. and Rosenberry, T. L. 2002. Growth of beta-amyloid(1-40) protofibrils by monomer elongation and lateral association. Characterization of distinct products by light scattering and atomic force microscopy. *Biochemistry*, 41:6115-27.
- O'Nuallain, B., Freir, D. B., Nicoll, A. J., Risse, E., Ferguson, N., Herron, C. E., Collinge, J. and Walsh, D. M. 2010. Amyloid beta-protein dimers rapidly form stable synaptotoxic protofibrils. *J Neurosci*, 30:14411-9.
- Paranjape, G. S., Gouwens, L. K., Osborn, D. C. and Nichols, M. R. 2012. Isolated amyloid-beta(1-42) protofibrils, but not isolated fibrils, are robust stimulators of microglia. *ACS Chem Neurosci*, 3:302-11.
- Paranjape, G. S., Terrill, S. E., Gouwens, L. K., Ruck, B. M. and Nichols, M. R. 2013. Amyloid-beta(1-42) protofibrils formed in modified artificial cerebrospinal fluid bind and activate microglia. *J Neuroimmune Pharmacol*, 8:312-22.
- Paresce, D. M., Chung, H. and Maxfield, F. R. 1997. Slow degradation of aggregates of the alzheimer's disease amyloid β -protein by microglial cells. *Journal of Biological Chemistry*, 272:29390-29397.
- Paresce, D. M., Ghosh, R. N. and Maxfield, F. R. 1996. Microglial cells internalize aggregates of the alzheimer's disease amyloid β protein via a scavenger receptor. *Neuron*, 17:553-565.
- Parvathenani, L. K., Tertyshnikova, S., Greco, C. R., Roberts, S. B., Robertson, B. and Posmantur, R. 2003. P2x7 mediates superoxide production in primary microglia and is up-regulated in a transgenic mouse model of alzheimer's disease. *J Biol Chem*, 278:13309-17.
- Patel, N. S., Paris, D., Mathura, V., Quadros, A. N., Crawford, F. C. and Mullan, M. J. 2005. Inflammatory cytokine levels correlate with amyloid load in transgenic mouse models of alzheimer's disease. *J Neuroinflammation*, 2:9.
- Pizzirani, C., Ferrari, D., Chiozzi, P., Adinolfi, E., Sandona, D., Savaglio, E. and Di Virgilio, F. 2007. Stimulation of p2 receptors causes release of il-1 β -loaded microvesicles from human dendritic cells. *Blood*, 109:3856-64.
- Rampe, D., Wang, L. and Ringheim, G. E. 2004. P2x7 receptor modulation of beta-amyloid- and lps-induced cytokine secretion from human macrophages and microglia. *J Neuroimmunol*, 147:56-61.
- Ransohoff, R. M. and Cardona, A. E. 2010. The myeloid cells of the central nervous system parenchyma. *Nature*, 468:253-62.

- Reed-Geaghan, E. G., Savage, J. C., Hise, A. G. and Landreth, G. E. 2009. Cd14 and toll-like receptors 2 and 4 are required for fibrillar β -stimulated microglial activation. *J Neurosci*, 29:11982-92.
- Roychaudhuri, R., Yang, M., Hoshi, M. M. and Teplow, D. B. 2009. Amyloid-beta protein assembly and alzheimer disease. *J Biol Chem*, 284:4749-4753.
- Selkoe, D. J. 2011. Alzheimer's disease. *Cold Spring Harb Perspect Biol*, 3:1-16.
- Selkoe, D. J. and Hardy, J. 2016. The amyloid hypothesis of alzheimer's disease at 25 years. *EMBO Mol Med*,
- Shibuya, Y., Chang, C. C., Huang, L. H., Bryleva, E. Y. and Chang, T. Y. 2014. Inhibiting *acat1/soat1* in microglia stimulates autophagy-mediated lysosomal proteolysis and increases β 1-42 clearance. *J Neurosci*, 34:14484-501.
- Stelzmann, R. A., Schnitzlein, H. N. and Murtagh, F. R. 1995. An english translation of alzheimer's 1907 paper, "uber eine eigenartige erkankung der hirnrinde". *Cilical Anatomy*, 8:429-431.
- Stewart, C. R., Stuart, L. M., Wilkinson, K., van Gils, J. M., Deng, J., Halle, A., Rayner, K. J., Boyer, L., Zhong, R., Frazier, W. A., Lacy-Hulbert, A., El Khoury, J., Golenbock, D. T. and Moore, K. J. 2010. Cd36 ligands promote sterile inflammation through assembly of a toll-like receptor 4 and 6 heterodimer. *Nat Immunol*, 11:155-61.
- Su, F., Bai, F., Zhou, H. and Zhang, Z. 2015. Microglial toll-like receptors and alzheimer's disease. *Brain Behav Immun*,
- Surprenant, A., Rassendren, F., Kawashima, E., North, R. A. and Buell, G. 1996. The cytolytic p2z receptor for extracellular atp identified as a p2x receptor (p2x7). *Science*, 272:735-8.
- Tahara, K., Kim, H. D., Jin, J. J., Maxwell, J. A., Li, L. and Fukuchi, K. 2006. Role of toll-like receptor signalling in β uptake and clearance. *Brain*, 129:3006-19.
- Takenouchi, T., Sekiyama, K., Sekigawa, A., Fujita, M., Waragai, M., Sugama, S., Iwamaru, Y., Kitani, H. and Hashimoto, M. 2010. P2x7 receptor signaling pathway as a therapeutic target for neurodegenerative diseases. *Archivum Immunologiae et Therapiae Experimentalis*, 58:91-6.
- Taneo, J., Adachi, T., Yoshida, A., Takayasu, K., Takahara, K. and Inaba, K. 2015. Amyloid beta oligomers induce interleukin-1 β production in primary microglia in a cathepsin b- and reactive oxygen species-dependent manner. *Biochem Biophys Res Commun*,

- Tang, D., Kang, R., Coyne, C. B., Zeh, H. J. and Lotze, M. T. 2012. Pamps and damp: Signal 0s that spur autophagy and immunity. *Immunological Reviews*, 249:158-75.
- Terrill-Usery, S. E., Mohan, M. J. and Nichols, M. R. 2014. Amyloid-beta(1-42) protofibrils stimulate a quantum of secreted il-1beta despite significant intracellular il-1beta accumulation in microglia. *Biochim Biophys Acta*,
- Terry, R. D., Gonatas, N. K. and Weiss, M. 1964. Ultrastructural studies in alzheimer's presenile dementia. *Am J Pathol*, 44:269-297.
- Turola, E., Furlan, R., Bianco, F., Matteoli, M. and Verderio, C. 2012. Microglial microvesicle secretion and intercellular signaling. *Front Physiol*, 3:149.
- van der Kant, R. and Goldstein, L. S. 2015. Cellular functions of the amyloid precursor protein from development to dementia. *Dev Cell*, 32:502-15.
- Verderio, C., Muzio, L., Turola, E., Bergami, A., Novellino, L., Ruffini, F., Riganti, L., Corradini, I., Francolini, M., Garzetti, L., Maiorino, C., Servida, F., Vercelli, A., Rocca, M., Dalla Libera, D., Martinelli, V., Comi, G., Martino, G., Matteoli, M. and Furlan, R. 2012. Myeloid microvesicles are a marker and therapeutic target for neuroinflammation. *Ann Neurol*, 72:610-24.
- Walsh, D. M., Hartley, D. M., Kusomoto, Y., Fezoui, Y., Condron, M. M., Lomakin, A., Benedek, G. B., Selkoe, D. J. and Teplow, D. B. 1999. Amyloid-beta protein fibrillogenesis: Structure and biological activity of protofibrillar intermediates. *J Biol Chem*, 36:25945-25-952.
- Walsh, D. M., Lomakin, A., Benedek, G. B., Condron, M. M. and Teplow, D. B. 1997. Amyloid-beta protein fibrillogenesis. *J Biol Chem*, 272:22364-22372.
- Webster, S. D., Galvan, M. D., Ferran, E., Garzon-Rodriguez, W., Glabe, C. G. and Tenner, A. J. 2001. Antibody-mediated phagocytosis of the amyloid beta-peptide in microglia is differentially modulated by c1q. *J Immunol*, 166:7496-503.
- Wilkins, H. M. and Swerdlow, R. H. 2016. Amyloid precursor protein processing and bioenergetics. *Brain Res Bull*,
- Wilson, H. L., Francis, S. E., Dower, S. K. and Crossman, D. C. 2004. Secretion of intracellular il-1 receptor antagonist (type 1) is dependent on p2x7 receptor activation. *J Immunol*, 173:1202-8.
- Yan, S. D., Chen, X., Fu, J., Chen, M., Zhu, H., Roher, A., Slattery, T., Zhao, L., Nagashima, M., Morser, J., Migheli, A., Nawroth, P., Stern, D. and Schmidt, A. M. 1996. Rage and amyloid-beta peptide neurotoxicity in alzheimer's disease. *Nature*, 382:685-91.

Yang, C. N., Shiao, Y. J., Shie, F. S., Guo, B. S., Chen, P. H., Cho, C. Y., Chen, Y. J., Huang, F. L. and Tsay, H. J. 2011. Mechanism mediating oligomeric abeta clearance by naive primary microglia. *Neurobiol Dis*, 42:221-30.

Ye, C. P., Selkoe, D. J. and Hartley, D. M. 2003. Protofibrils of amyloid beta-protein inhibit specific k⁺ currents in neocortical cultures. *Neurobiol Dis*, 13:177-90.

Yu, Y. and Ye, R. D. 2014. Microglial a β receptors in alzheimer's disease. *Cellular and Molecular Neurobiology*, 35:71-83.

VITA

Lisa (Picard) Gouwens is originally from Linwood, Michigan. After earning a B.S. in biology with a chemistry minor, and a M.Ed. in secondary education from the University of Arkansas-Monticello, Lisa taught high school science in the St. Louis, Missouri, area for eight years. She returned to college in 2009 and completed a M.S. in biochemistry and biotechnology in 2011. Lisa was accepted into the chemistry doctorate program at University of Missouri-St. Louis in 2012. Now that the Ph.D. is complete, she plans to teach chemistry and continue to pursue research, ideally at a small liberal arts university. Lisa lives in the St. Louis metro area with her husband, Don. She has two sons, Jaeson and Kyle. Jaeson is married to Jess, and they are the parents of Lisa's splendid granddaughter, Luise.